

1979

A new series of chelated organochromium (III) complexes

George Joseph Samuels
Iowa State University

Follow this and additional works at: <https://lib.dr.iastate.edu/rtd>

 Part of the [Inorganic Chemistry Commons](#)

Recommended Citation

Samuels, George Joseph, "A new series of chelated organochromium (III) complexes " (1979). *Retrospective Theses and Dissertations*. 6621.
<https://lib.dr.iastate.edu/rtd/6621>

This Dissertation is brought to you for free and open access by the Iowa State University Capstones, Theses and Dissertations at Iowa State University Digital Repository. It has been accepted for inclusion in Retrospective Theses and Dissertations by an authorized administrator of Iowa State University Digital Repository. For more information, please contact digirep@iastate.edu.

INFORMATION TO USERS

This was produced from a copy of a document sent to us for microfilming. While the most advanced technological means to photograph and reproduce this document have been used, the quality is heavily dependent upon the quality of the material submitted.

The following explanation of techniques is provided to help you understand markings or notations which may appear on this reproduction.

1. The sign or "target" for pages apparently lacking from the document photographed is "Missing Page(s)". If it was possible to obtain the missing page(s) or section, they are spliced into the film along with adjacent pages. This may have necessitated cutting through an image and duplicating adjacent pages to assure you of complete continuity.
2. When an image on the film is obliterated with a round black mark it is an indication that the film inspector noticed either blurred copy because of movement during exposure, or duplicate copy. Unless we meant to delete copyrighted materials that should not have been filmed, you will find a good image of the page in the adjacent frame.
3. When a map, drawing or chart, etc., is part of the material being photographed the photographer has followed a definite method in "sectioning" the material. It is customary to begin filming at the upper left hand corner of a large sheet and to continue from left to right in equal sections with small overlaps. If necessary, sectioning is continued again—beginning below the first row and continuing on until complete.
4. For any illustrations that cannot be reproduced satisfactorily by xerography, photographic prints can be purchased at additional cost and tipped into your xerographic copy. Requests can be made to our Dissertations Customer Services Department.
5. Some pages in any document may have indistinct print. In all cases we have filmed the best available copy.

University
Microfilms
International

300 N. ZEEB ROAD, ANN ARBOR, MI 48106
18 BEDFORD ROW, LONDON WC1R 4EJ, ENGLAND

7916213

SAMUELS, GEORGE JOSEPH
A NEW SERIES OF CHELATED ORGANOCROMIUM(III)
COMPLEXES.

IOWA STATE UNIVERSITY, PH.D., 1979

University
Microfilms
International

300 N. ZEEB ROAD, ANN ARBOR, MI 48106

A new series of chelated organochromium(III) complexes

by

George Joseph Samuels

A Dissertation Submitted to the
Graduate Faculty in Partial Fulfillment of
The Requirements for the Degree of
DOCTOR OF PHILOSOPHY

Department: Chemistry
Major: Chemistry (Inorganic-Organic)

Approved:

Signature was redacted for privacy.

In Charge of Major Work

Signature was redacted for privacy.

For the Major Department

Signature was redacted for privacy.

For the Graduate College

Iowa State University
Ames, Iowa

1979

TABLE OF CONTENTS

	Page
PART I. THE KINETICS AND MECHANISM OF FORMATION OF ORGANOCHROMIUM(III) CHELATES FROM CHROMIUM(II) CHELATE AND ORGANIC HALIDES	1
INTRODUCTION	2
HISTORICAL DEVELOPMENT	4
EXPERIMENTAL SECTION	24
Materials	24
Preparation of $\text{CrCl}_2 \cdot 4\text{H}_2\text{O}$	24
Preparation of [15]ane N_4 -1,4,8,12-tetraaza- cyclopentadecane	25
Halides	26
Solvent preparation	26
$\text{Cr}([\text{15}] \text{aneN}_4)^{2+}$	27
Other materials	28
Methods	28
Analyses	28
Separation and purification of reaction mixtures	29
Isolation of organochromium salts	30
Spectra	31
Gas Chromatography	32
Electrochemistry	33
Stoichiometry	34
Kinetics	35
Results	38
Characterization of $\text{Cr}([\text{15}] \text{aneN}_4)^{2+}$	38
Characterization of the Products of Reaction of $\text{Cr}([\text{15}] \text{aneN}_4)$ with Organic Halides	39
General description	39

Characterization of the Inorganic Reaction Products	42
Characterization of the Organochromium Species	49
Characterization of the Reaction of Organic Halides with $\text{Cr}([\text{15}] \text{aneN}_4)^{2+}$	60
Geminal Halides and their Reaction with $\text{Cr}([\text{15}] \text{aneN}_4)^{2+}$	63
Radical Intermediates and the Rate of Radical Capture	64
Kinetics	66
Activation Parameters	77
DISCUSSION	85
PART II. REACTIONS OF SIGMA BONDED ORGANOCROMIUM(III) CHELATE COMPLEXES WITH MERCURY(II) ELECTROPHILES	97
INTRODUCTION	98
EXPERIMENTAL	101
Preparation of Organochromium Compounds	101
n-Alkyl($[\text{15}] \text{aneN}_4$)chromium(III) complexes	101
Secondary and benzyl $\text{Cr}(\text{L})^{2+}$ complexes	102
1-Adamantylchromium($[\text{15}] \text{aneN}_4$) $^{2+}$	103
Mercury compounds	103
Other materials	104
Methods	104
Analyses	104
Spectra	106
Stoichiometry	106
Kinetics	107

RESULTS	110
Characterization	110
$\text{RCr}([\text{15}] \text{aneN}_4)^{2+}$	110
Organomercury(II) products	110
Characterization of Reactions	110
Kinetics	111
Preliminary experiments	111
Kinetics of Hg^{2+} reactions	116
Kinetics of CH_3Hg^+ reactions	124
Activation Parameters - Isokinetic Relationships	128
DISCUSSION	145
PART III. THE CRYSTAL STRUCTURE OF [trans- CHLOROQUO(1,4,8,12-TETRAAZACYCLO- PENTADECANE)CHROMIUM(III)DIIODIDE- DIHYDRATE	158
INTRODUCTION	159
EXPERIMENTAL	160
Preparations	160
$[\underline{\text{t}}\text{-ClCr}([\text{15}] \text{aneN}_4)\text{H}_2\text{O}]\text{I}_2 \cdot 2\text{H}_2\text{O}$	160
Crystal data	160
Collection and Reduction of X-ray Intensity Data	162
Solution and Refinement	164
DESCRIPTION AND DISCUSSION	169
LITERATURE CITED	175
ACKNOWLEDGEMENTS	182

LIST OF TABLES

	Page
Table I-1. Relative rates of reduction of alkyl halides by the $\text{Cr}^{\text{II}}(\text{en})$ reagent at 25°	13
Table I-2. Perfluoroalkylchromium chelate complexes	19
Table I-3. Rate constants for reduction of alkyl iodides by $\text{Co}(\text{CN})_5^{3-}$ at 25° , ref. 40	22
Table I-4. Spectral parameters for the various <u>trans</u> - $\text{XCr}([\text{15}] \text{aneN}_4)\text{H}_2\text{O}^{n=+2,3}$ complexes	48
Table I-5. Spectral parameters for various <u>trans</u> - $\text{RCr}([\text{15}] \text{aneN}_4)^{2+}$ complexes	59
Table I-6. Kinetic data for the reactions of $\text{Cr}([\text{15}] \text{aneN}_4)^{2+}$ with organic mono-halides. Conditions 1:1 v/v t-butanol/water, $\mu = 0.20 \text{ M}$ (Li^+), $T = 25^\circ$	70
Table I-7. Summary of the kinetic data for the reactions of $\text{Cr}([\text{15}] \text{aneN}_4)^{2+}$ with geminal dihalides and pseudo halide. Conditions: Solvent 1:1 v/v t-butanol/water, $\mu = 0.20 \text{ M}$, $T = 25^\circ$	74
Table I-8. Temperature dependence of the reaction rate of EtBr with $\text{Cr}([\text{15}] \text{aneN}_4)^{2+}$	78
Table I-9. Temperature dependence of the reaction rate of EtI with $\text{Cr}([\text{15}] \text{aneN}_4)^{2+}$	80

Table I-10.	Temperature dependence of the reaction rate of PhCH_2Cl with $\text{Cr}([\text{15}] \text{aneN}_4)^{2+}$	82
Table I-11.	Summary of the kinetic data for the reactions of $\text{Cr}([\text{15}] \text{aneN}_4)^{2+}$ with organic monohalides. Conditions: Solvent 1:1 v/v <i>t</i> -butanol/water, $\mu = 0.20 \text{ M}$, $T = 25.0^\circ$	88
Table I-12.	A comparison of reaction rates of RX with reduced metal species ($\text{dm}^3 \text{ mol}^{-1} \text{ s}^{-1}$)	91
Table I-13.	Summary of activation parameters for the reaction of organic halides with reducing metal complexes	95
Table II-1.	Kinetic data for the reactions of Hg^{2+} with $\text{RCr}([\text{15}] \text{aneN}_4)^{2+}$ complexes, R = primary alkyls. Conditions: $[\text{H}^+] = 0.25 \text{ M}$, $\mu = 0.50 \text{ M}$, $T = 25.0^\circ$	125
Table II-2.	Kinetic data for the reactions of Hg^{2+} with $\text{RCr}([\text{15}] \text{aneN}_4)^{2+}$ complexes, R = secondary and tertiary alkyls. Conditions: $[\text{H}^+] \cong 0.17 \text{ M}$, $\mu \cong 1.46 \text{ M}$, $T = 25.0^\circ$	127
Table II-3.	Kinetic data for the reaction of CH_3Hg^+ with $\text{RCr}([\text{15}] \text{aneN}_4)^{2+}$. Conditions: $[\text{H}^+] = 0.25 \text{ M}$, $\mu = 0.50 \text{ M}$, $T = 25.0^\circ$	130

- Table II-4. Temperature dependence of the rate of reaction of Hg^{2+} with ethylCr(L)^{2+} .
Conditions: $[\text{H}^+] = 0.25 \text{ M}$,
 $\mu = 0.50 \text{ M}$ 135
- Table II-5. Temperature dependence of the rate of reaction of Hg^{2+} with $\text{n-propylCr(L)}^{2+}$.
Conditions: $[\text{H}^+] = 0.25 \text{ M}$,
 $\mu = 0.50 \text{ M}$ 136
- Table II-6. Temperature dependence of the rate of reaction of Hg^{2+} with n-butylCr(L)^{2+} .
Conditions: $[\text{H}^+] = 0.25 \text{ M}$,
 $\mu = 0.50 \text{ M}$ 137
- Table II-7. Temperature dependence of the rate of reaction of Hg^{2+} with $\text{n-pentylCr(L)}^{2+}$.
Conditions: $[\text{H}^+] = 0.25 \text{ M}$,
 $\mu = 0.50 \text{ M}$ 138
- Table II-8. Temperature dependence of the rate of reaction of Hg^{2+} with benzylCr(L)^{2+} .
Conditions: $[\text{H}^+] = 0.25 \text{ M}$,
 $\mu = 0.25 \text{ M}$ 139
- Table II-9. Activation parameters for the reaction of Hg^{2+} with $\text{R-Cr}([15]\text{aneN}_4)^{2+}$ 142
- Table II-10. Summary of reaction rates for Hg^{2+} with RCr(L)^{2+} . Conditions:
 $[\text{H}^+] = 0.25 \text{ M}$, $\mu = 0.50 \text{ M}$,
 $T = 25.0^\circ$ 147

Table II-11.	Summary of reaction rates for CH_3Hg^+ with RCr(L)^{2+} . Conditions: $[\text{H}^+] = 0.25 \text{ M}$, $\mu = 0.50 \text{ M}$, $T = 25.0^\circ$	148
Table II-12.	Summary of reaction rates of Hg(II) with organochromium cations, $k/\text{dm}^3\text{mol}^{-1}\text{s}^{-1}$. Conditions: $[\text{H}^+] = 0.25 \text{ M}$, $\mu = 0.50 \text{ M}$, $T = 25.0^\circ$	149
Table II-13.	Relative rate trends, $k_{\text{R}}/k_{\text{Et}}$, for various $\text{S}_{\text{E}}2(\text{open})$ reactions of metal alkyls, $\text{R} = \text{aliphatic}$	153
Table II-14.	Summary of the activation parameters for the reaction of Hg(II) with organochromium cations. Conditions: $[\text{H}^+] = 0.25 \text{ M}$, $\mu = 0.50 \text{ M}$	156
Table III-1.	Final atomic positions	166
Table III-2.	Anisotropic thermal parameters ($\times 10^4$)	168
Table III-3.	Bond lengths (\AA) for $\text{ClCr(L)H}_2\text{O}^{2+}$	171
Table III-4.	Bond angles (degrees)	172
Table III-5.	Comparison of bond distances	173

LIST OF FIGURES

	Page
Figure I-1. The cyclic voltammogram for the $\text{Cr(L)}^{3+}/\text{Cr(L)}^{2+}$ couple	40
Figure I-2. The electronic spectrum of $\text{Cr}([\text{15}] \text{aneN}_4)^{2+}$ in 1:1 $t\text{-BuOH}/\text{H}_2\text{O}$	41
Figure I-3. The electronic spectrum of <u>trans</u> - $\text{ClCr(L)H}_2\text{O}^{2+}$	44
Figure I-4. The electronic spectrum of <u>trans</u> - $\text{BrCr(L)H}_2\text{O}^{2+}$	45
Figure I-5. The electronic spectrum of <u>trans</u> - $\text{ICr(L)H}_2\text{O}^{2+}$	46
Figure I-6. The electronic spectrum of <u>trans</u> - $(\text{H}_2\text{O})_2\text{Cr(L)}^{3+}$	47
Figure I-7. Electronic Spectra (a) The electronic spectrum of $\text{CH}_3\text{Cr(L)}^{2+}$ (b) The electronic spectrum of the same solution after the addition of excess Hg^{2+}	50
Figure I-8. The electronic spectrum of methylCr(L)^{2+}	52
Figure I-9. The electronic spectrum of ethylCr(L)^{2+}	52
Figure I-10. The electronic spectrum of <u>n</u> - propylCr(L)^{2+}	53

Figure I-11.	The electronic spectrum of <u>n</u> -butylCr(L) ²⁺	53
Figure I-11a.	The electronic spectrum of <u>n</u> -butylCr(L) ²⁺ -non log scale	54
Figure I-12.	The electronic spectrum of isopropylCr(L) ²⁺	55
Figure I-13.	The electronic spectrum of cyclohexylCr(L) ²⁺	55
Figure I-12a.	The electronic spectrum of isopropylCr(L) ²⁺ -non log scale	56
Figure I-14.	The electronic spectrum of 1-adamantylCr(L) ²⁺	57
Figure I-15.	The electronic spectrum of benzylCr(L) ²⁺	57
Figure I-15a.	The electronic spectrum of benzylCr(L) ²⁺ . Note scale change, the break applies only to the maxima	58
Figure I-16.	Spectrophotometric titration of Cr(L) ²⁺ by C ₆ H ₅ CH ₂ Br	62
Figure I-17.	A standard method plot for the reaction of isopropylbromide with Cr(L) ²⁺	69
Figure I-18.	A standard method plot for the reaction of <u>n</u> -butylbromide with Cr(L) ²⁺	69

Figure I-19.	Plot of k_{obs} vs $[\text{c-C}_6\text{H}_{11}\text{Br}]$	76
Figure I-20.	Plot of k_{obs} vs $[\text{ClCH}_2\text{CN}]$	76
Figure I-21.	Eyring plot for the reaction of EtBr with $\text{Cr}(\text{L})^{2+}$	79
Figure I-22.	Eyring plot for the reaction of EtI with $\text{Cr}(\text{L})^{2+}$	81
Figure I-23.	Eyring plot for the reaction of PhCH_2Cl with $\text{Cr}(\text{L})^{2+}$	83
Figure II-1.	Spectrophotometric titration of $\text{CH}_3\text{Cr}(\text{L})^{2+}$ by Hg^{2+}	112
Figure II-2.	Spectrophotometric titration of $\text{CH}_3\text{Cr}(\text{L})^{2+}$ by CH_3Hg^+	113
Figure II-3.	Standard method plot for the reaction of n -propyl $\text{Cr}(\text{L})^{2+}$ with Hg^{2+}	117
Figure II-4.	Standard method plot for the reaction of 1-adamantyl $\text{Cr}(\text{L})^{2+}$ with Hg^{2+}	118
Figure II-5.	Standard method plot for the reaction of isopropyl $\text{Cr}(\text{L})^{2+}$ with Hg^{2+} using a Swinbourne determined A_∞	119
Figure II-6.	Swinbourne plot for the reaction of cyclohexyl $\text{Cr}(\text{L})^{2+}$ with Hg^{2+}	120
Figure II-7.	Plot of k_{obs} vs $[\text{Hg}^{2+}]$ for the reaction of ethyl $\text{Cr}(\text{L})^{2+}$ with Hg^{2+}	121
Figure II-8.	Plot of k_{obs} vs $[\text{Hg}^{2+}]$ for the reaction of n -propyl $\text{Cr}(\text{L})^{2+}$ with Hg^{2+}	122

Figure II-9.	Plot of k_{obs} vs $[\text{Hg}^{2+}]$ for the reaction of $n\text{-butylCr(L)}^{2+}$ with Hg^{2+}	122
Figure II-10.	Plot of k_{obs} vs $[\text{Hg}^{2+}]$ for the reaction of benzylCr(L)^{2+} with Hg^{2+}	123
Figure II-11.	Standard method plot for the reaction of ethylCr(L)^{2+} with CH_3Hg^+	129
Figure II-12.	Standard method plot for the reaction of benzylCr(L)^{2+} with CH_3Hg^+	129
Figure II-13.	Plot of k_{obs} vs $[\text{CH}_3\text{Hg}^+]$ for the reaction of methylCr(L)^{2+} with CH_3Hg^+	131
Figure II-14.	Plot of k_{obs} vs $[\text{CH}_3\text{Hg}^+]$ for the reaction of ethylCr(L)^{2+} with CH_3Hg^+	132
Figure II-15.	Plot of k_{obs} vs $[\text{CH}_3\text{Hg}^+]$ for the reaction of benzylCr(L)^{2+} with CH_3Hg^+	133
Figure II-16.	Eyring plot for the reaction of ethylCr(L)^{2+} with Hg^{2+}	140
Figure II-17.	Eyring plot for the reaction of $n\text{-propylCr(L)}^{2+}$ with Hg^{2+}	140
Figure II-18.	Eyring plot for the reaction of $n\text{-butylCr(L)}^{2+}$ with Hg^{2+}	141

- Figure II-19. Eyring plot for the reaction of
benzylCr(L)²⁺ with Hg²⁺ 141
- Figure II-20. Plot of $\Delta\bar{H}^\ddagger$ vs $-\Delta\bar{S}^\ddagger$. The numbers
correspond to the data in
Table II-9 143
- Figure III-1. X-ray emission from electron
microprobe analysis of
[trans-ClCr(L)H₂O](I)₂·H₂O 161
- Figure III-2. Perspective drawing of
[trans-ClCr([15]aneN₄)H₂O]²⁺
cation showing 50% probability
thermal ellipsoid 170

PART I. THE KINETICS AND MECHANISM OF FORMATION OF
ORGANOCHROMIUM(III) CHELATES FROM CHROMIUM(II)
CHELATE AND ORGANIC HALIDES

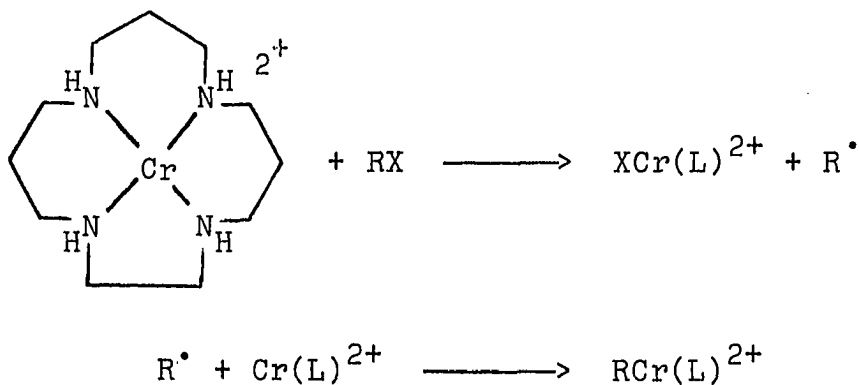
INTRODUCTION

The first part of this work describes the mechanistic characterization of a general synthetic route for the preparation of a new series of chelated organochromium compounds.

All the previously prepared organochromium chelate complexes, discussed below, have been based upon the initial formation of the carbon chromium bond followed by the subsequent addition of the desired ligand to the complex. This required that the carbon-chromium bond survive the chelation step. As a result, only relatively stable carbon-metal bonds could be present. This severely limited the utility of these approaches.

In this work the chromium-macrocycle was synthesized first, allowing a wider range of organochromium species to be prepared. The macrocycle which was chosen for this work was 1,4,8,12-tetraazacyclopentadecane (1), a saturated cyclic tetraamine, which forms only the trans isomer in these complexes.

The proposed reaction sequence involves the initial abstraction of the halogen atom from an organic halide by Cr(L)^{2+} followed by combination of the resulting organic free radical with another Cr(L)^{2+} moiety, Scheme 1. Precedent for this reaction mechanism will be presented in the next section.



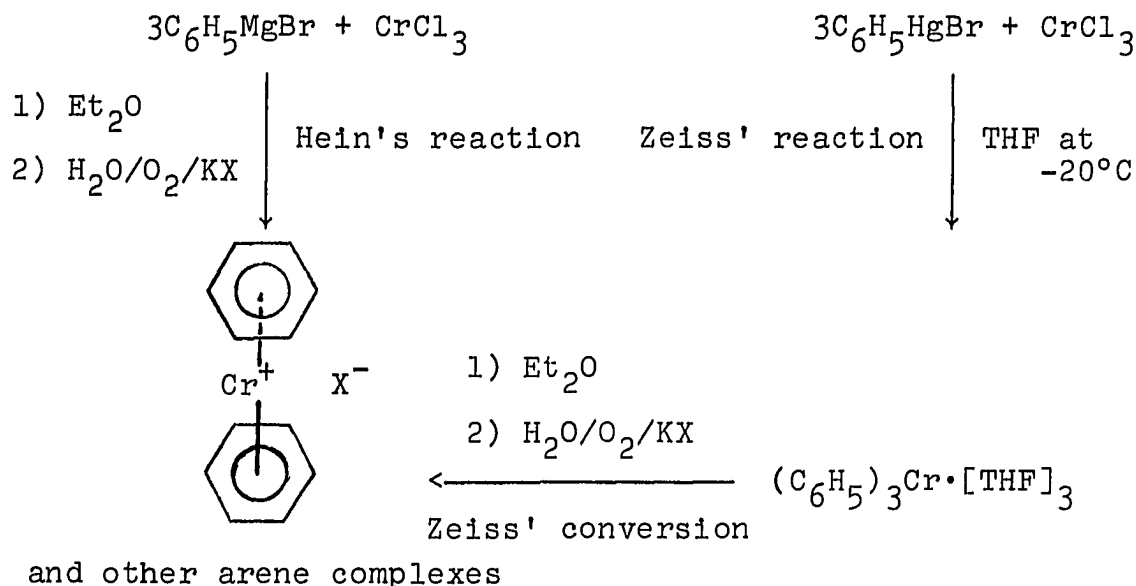
Scheme 1

Because of the increased reduction potential of Cr(L)^{2+} when compared to Cr^{2+} , the choice of organic halides was not as limited. Simple primary, secondary and tertiary organic halides resulted in the formation of the corresponding organochromium complexes, allowing the preparation of a much broader range of compounds than had previously been possible by the other approaches.

The results obtained from a systematic kinetic and mechanistic investigation of this apparently general mechanism for the formation of organometallic complexes will be discussed in light of the precedent presented below.

HISTORICAL DEVELOPMENT

Organochromium compounds represent some of the first organic chemistry of the transition metals. In 1903, Sand and Singer (2) observed the formation of an unstable organochromium species. G. M. Bennett and E. E. Turner (1914) (3), in an attempt to synthesize organochromium species, discovered that the reaction of anhydrous chromium(III) chloride with arylmagnesium halides leads to the formation of biaryls instead of their desired product. It had to wait until 1919 when Hein (4), following up on the Grignard reaction, found that by properly controlling the conditions it was possible to isolate a series of water soluble "phenylchromium" compounds from the reaction of phenylmagnesium bromide and chromium(III) chloride in anhydrous ether. These compounds were quite perplexing for nearly four decades. The aura of mystery which surrounded these compounds was not completely resolved until 1957 when Herwig and Zeiss (5) performed a series of experiments clearing the way for the synthesis of many σ -bonded organochromium(II) and (III) complexes. This was rapidly followed by the revelation that the resultant σ -tris(aryl) chromium(III) formed by the Grignard reaction could be decomposed to bis(arene) chromium π -complexes (Scheme 2) (6,7).



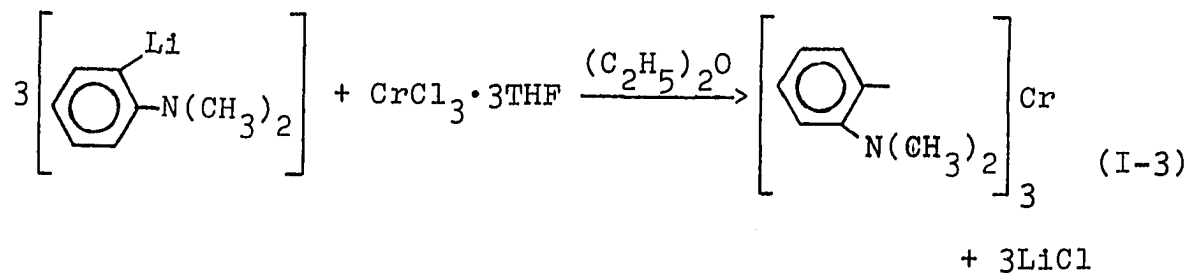
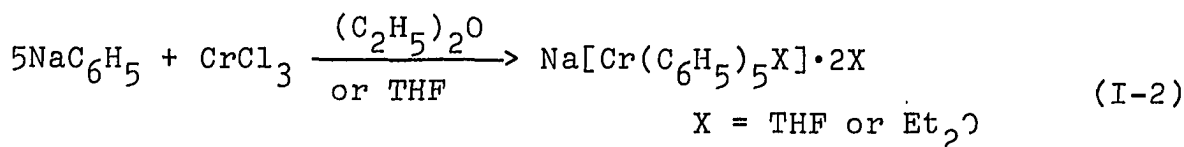
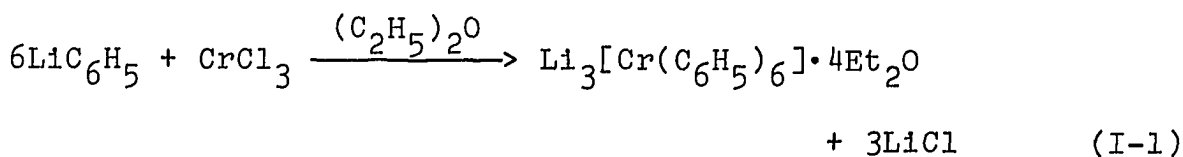
Scheme 2

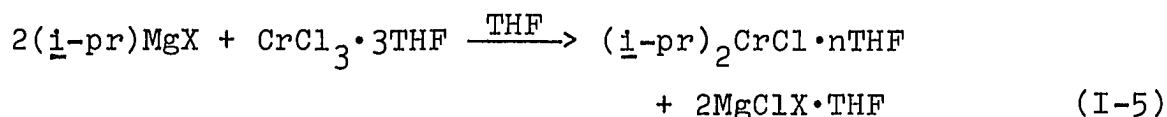
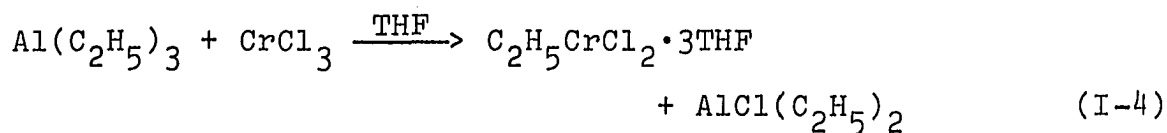
There are several major classes of σ -bonded organochromium compounds. These may be prepared using a variety of methods depending upon the particular category desired.

Solvated σ -bonded organochromium compounds are usually prepared from the reaction of organometallic compounds with chromium halides. This is usually possible only if careful attention is paid to solvent, temperature and reaction stoichiometry.

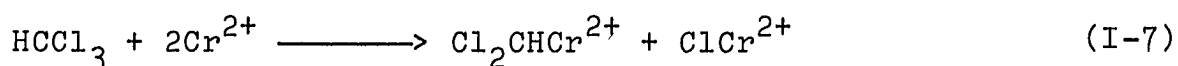
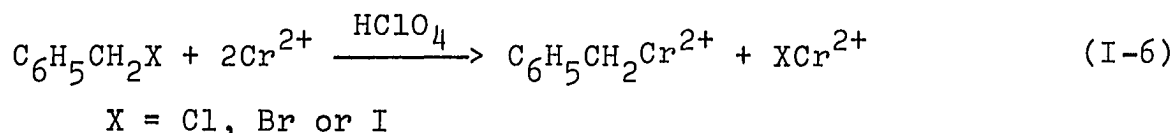
Chromium(III) chloride reacts with phenyl-lithium or sodium to give organochromium complexes containing the alkali metal in several compositions (eqs. I-1 and I-2) (8,9).

In some cases, organolithium reagents have produced lithium free complexes (eq. I-3) (10). Only one organic group is transferred when organoaluminum compounds react with chromium(III) chloride in tetrahydrofuran forming the corresponding monoalkylchromium dichloride complexes (eq. I-4) (11). The most versatile and convenient route to σ -bonded organochromium compounds is the use of Grignard reagents on $\text{CrCl}_3 \cdot 3\text{THF}$ in tetrahydrofuran or in diethyl ether. By varying the stoichiometric ratios of reactants, organochromium compounds of the type $\text{R}_n\text{CrCl}_{3-n} \cdot \text{X}$ sol. ($n = 1, 2$ or 3) have been prepared with R being simple alkyl, aryl or benzyl groups (eq. I-5) (12,13).

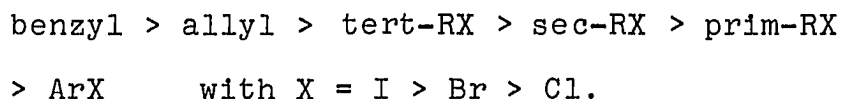




Aqueous solutions containing a pure σ -bonded organochromium species were not known until Anet and LeBlanc (1957) (14) prepared benzylpentaquo chromium(III). They made it and substituted analogs from various benzyl halides and chromium(II) perchlorate (eq. I-6). Additional evidence which helped to confirm the identity of their compound was its reaction with mercuric chloride. This resulted in the formation of benzylmercuric chloride. The stabilities of these compounds were undoubtedly related to the kinetic inertness of the d^3 chromium(III) ion toward ligand substitution. Again in 1959, Anet (15) prepared the first air and water stable σ -bonded organochromium cation from the reaction of chloroform and Cr(II) (eq. I-7).

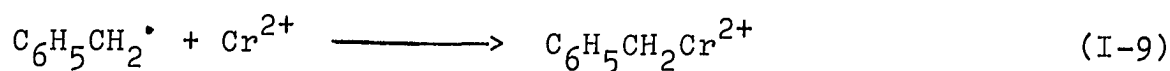
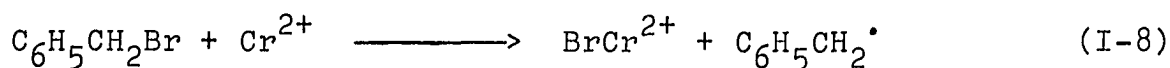


Several years later Castro and Kray (16) mapped out the general reaction sequence of chromous sulfate with alkyl halides in DMF. They presented direct evidence for the generation of a free radical intermediate in the initial and rate determining step of halogen abstraction from the halide substrate. The reactivity of monohalides toward Cr^{2+} fell in the order expected for a radical process:



They failed to isolate any organochromium compound. This was likely due to the conditions they employed.

In 1964, Kochi and Davis (17) thoroughly investigated the mechanism of the formation of the benzylchromium ion (eqs. I-8 and I-9). The relative rate of reaction for $\text{X} = \text{I} > \text{Br} > \text{Cl}$ is 555:124:1 with a second order rate constant for benzyl chloride in 71.5% ethanol-water of $4.0 \times 10^{-3} \text{ dm}^3 \text{ m}^{-1} \text{ s}^{-1}$ at $T = 25^\circ$. They also reported for the first time



the use of a hydroperoxide, dimethylphenethyl hydroperoxide, to generate an organochromium compound, the benzylchromium cation.

The benzylchromium ion undergoes a series of decomposition reactions resulting in the formation of bibenzyl and toluene (18).

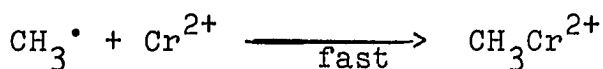
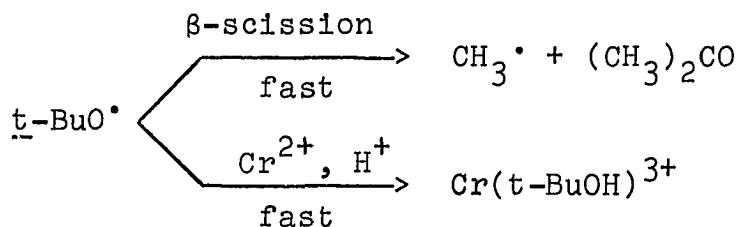
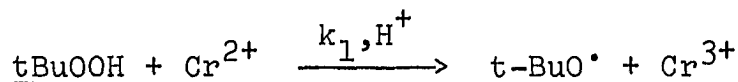
Toluene comes from the protonolysis of the carbon chromium bond. Bibenzyl was shown to result from further reaction with the benzyl halide used to form the complex. A mechanism put forth to explain the formation of various bibenzyl products required the homolytic cleavage of the carbon chromium bond.

This homolytic process has been further investigated by Schmidt and Swaddle (19) and Espenson and Leslie (20) using the 4-pyridinomethylchromium(III) ion (21) and Nohr and Espenson (22) using various substituted benzyl chromium ions. Their results indicate that benzylchromium ions can undergo homolytic scission of the carbon metal bond.

The range of halomethylchromium(III) cations was extended in 1968 by Dodd and Johnson (23) to include mono- and dihalomethyl complexes. $\text{CF}_3\text{Cr}^{2+}$ is the only trihalomethylchromium(III) species stable enough to be isolated (24). It is one of the most water and air stable σ -bonded organochromium complexes known. It was synthesized from CF_3I in a manner analogous to all the other substituted

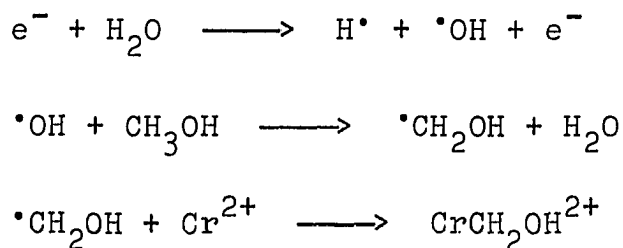
methylpentaquochromium compounds (24). The $\text{CrCH}_2\text{COOH}^{2+}$ complex was similarly synthesized from the haloacetic acids (25).

Simple water and air stable alkylchromium(III) compounds were unknown until 1971 when methylpentaquochromium(III) was independently synthesized and characterized (26). Both groups made use of tert-butyl hydroperoxide as previously suggested by Kochi and Davis (17). This reaction has been expanded by others to generate a wide range of unsubstituted primary, secondary and tertiary alkyls (27). The kinetics and mechanism of the reaction of hydroperoxides and peroxides with Cr^{2+} have been thoroughly studied (Scheme 3) (28).

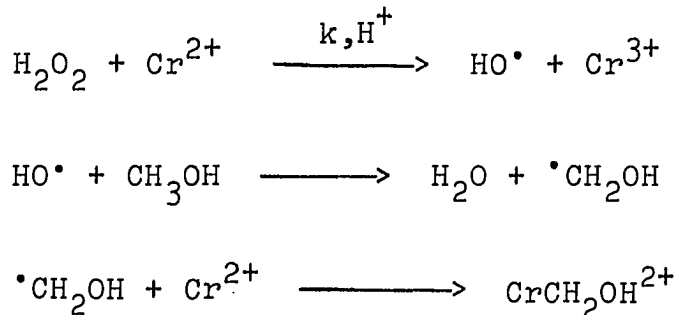


Scheme 3

The rates of reaction of organic radicals with Cr^{2+} have been reported by Cohen and Meyerstein (29). They used pulse radiolysis to generate the free radicals. This method initially produces hydroxyl radical which rapidly attacks saturated hydrocarbons and through hydrogen atom abstraction generates a carbon centered radical as shown below. A



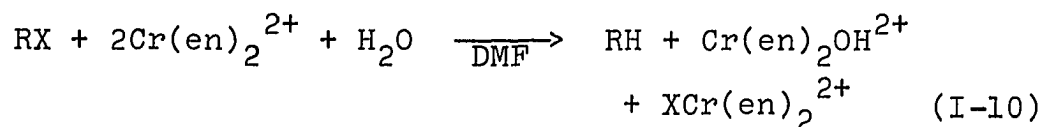
variation of this method was used by Schmidt et al. (26) to generate a series of organochromium compounds. The reaction between Cr^{2+} and H_2O_2 was used to initiate the formation of hydroxyl radical in solution which then carried out subsequent chemistry with the hydrocarbon present (Scheme 4).



Scheme 4

In an attempt to develop a chromium(II) reagent (30) with increased reactivity and enhanced synthetic utility, Kochi and Mocadlo (31) communicated the initial results obtained with a chromium(II) ethylenediamine complex. The ethylenediamine (en) ligand and other nitrogenous ligands (i.e., triethanolamine) greatly enhanced the reductive capacity of chromium(II) toward alkyl halides. It was possible to detect probable alkylchromium compounds as transient intermediates. This report was followed up by Kochi and Powers (32) with a complete discussion of the mechanism of reduction of alkyl halides by the ethylenediamine-chromium(II) complex. This report also established the role of alkylchromium compounds as intermediates (32).

The purple chromous reagent was prepared by the addition of various ratios of ethylenediamine in aqueous DMF to solutions of Cr(II) perchlorate. A 3:1 ratio of (en)/Cr(II) was generally optimal. The stoichiometry of the reduction is given by eq. I-10 (32), assuming the reactive species is the bis(en) complex:



X = Cl, Br or I

The kinetics of reduction of the alkyl halides by Cr(en)_2^{2+} were second order, first order each in halide and complex.

Only relative rates of reduction were determined using n-butyl chloride and isopropyl chloride for calibration standards. These values are presented in Table I-1. At a (en)/Cr(II) ratio of 3:1 the second order rate constants are $1.66 \times 10^{-3} \text{ dm}^3 \text{ mol}^{-1} \text{ s}^{-1}$ and $1.07 \times 10^{-2} \text{ dm}^3 \text{ mol}^{-1} \text{ s}^{-1}$ for the standards, respectively (32).

Table I-1. Relative rates of reduction of alkyl halides by the $\text{Cr}^{\text{II}}(\text{en})$ reagent at 25°

RX/ $1^\circ, 2^\circ, 3^\circ$	Cl	Br	I
n-Pr	0.9	130	11,000
n-Bu	1.0 ^a	140	10,000
i-Bu	0.7	100	7,700
i-Pr	6.3 ^b	1,100	63,000
<u>sec</u> -Bu	---	1,400	110,000
t-Bu	29	5,800	---

$$^a k = 1.66 \times 10^{-3} \text{ dm}^3 \text{ mol}^{-1} \text{ s}^{-1}.$$

$$^b k = 1.07 \times 10^{-2} \text{ dm}^3 \text{ mol}^{-1} \text{ s}^{-1}.$$

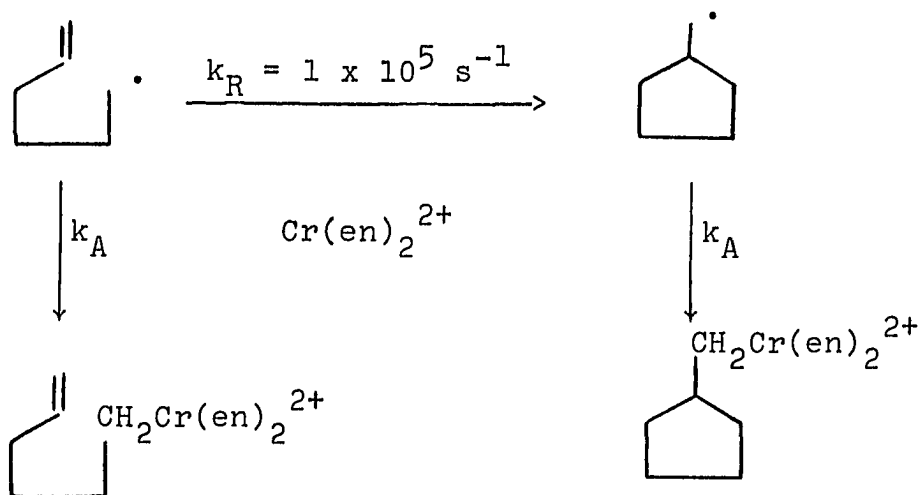
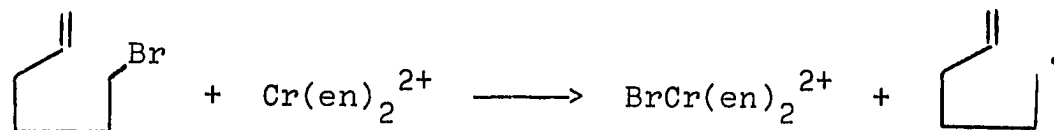
There appears to be an error in the original table for the entry of isopropyl chloride. It should be 6.3 instead of 3.6 as originally presented.

From Table I-1 it is quite apparent that tertiary halides are faster than secondary which are in turn faster than

primary halides. The halide reactivity follows the order $I > Br > Cl$. This pattern of reactivity is what would be expected from a process which generated a radical intermediate.

Several substrates were used with the expressed purpose of demonstrating the existence of organic free radicals as reaction intermediates. The halide which provided the most information was 5-hexenyl bromide (32). The 5-hexenyl radical if formed would cyclize at a known rate, $k_R = 1 \times 10^5 \text{ s}^{-1}$, to the cyclopentylmethyl radical (33). These radicals are both captured by Cr(en)_2^{2+} . The ratio of hydrocarbons resulting from hydrolysis of the alkylchromium intermediates could be measured. This would prove the existence of radical intermediates and give a measure of the rate of radical capture by Cr(en)_2^{2+} (Scheme 5). The rate of radical capture by Cr(en)_2^{2+} is $k_A = 4 \times 10^7 \text{ dm}^3 \text{ m}^{-1} \text{ s}^{-1}$ (32,34).

The presence of an alkyl(ethylenediamine)chromium species as an intermediate was verified by the visible absorption spectrum of the solutions which were quite similar to the visible spectrum of known organopentaaquochromium(III) species. In addition, the rate of disappearance of a major absorption band, $\lambda \approx 380 \text{ nm}$, coincided with the rate of formation of alkane (32).

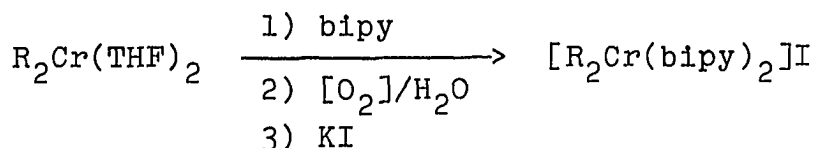
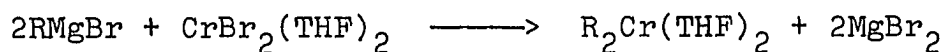


Scheme 5

These organochromium complexes are formed in two steps. The first is the rate determining step of halogen abstraction. The second very fast step is that of radical capture by a second Cr(II) complex (32). These intermediates can be considered the first known case of a chelated organochromium compound, although the disposition of the en ligand is unknown.

In 1972, an attempt was made to isolate as a solid 2- and 3-pyridinomethylbis(ethylenediamine)chromium(III) perchlorate. Loo et al. (35) succeeded in only producing solids of "40% and 27.4% purity, respectively".

Simultaneously, another group (36) prepared the first member (36a) of a new class of solid air and water stable σ -bonded organochromium(III) species, cis-bis(aryl)-bis(2,2'-bipyridine)chromium(III) iodides. These compounds, plus an alkyl complex reported later (36e), were conveniently synthesized by the scheme outlined in Scheme 6.



R = 2-anisyl, 3-anisyl, 4-anisyl, phenyl,
4-methylphenyl and trimethylsilylmethyl

Scheme 6

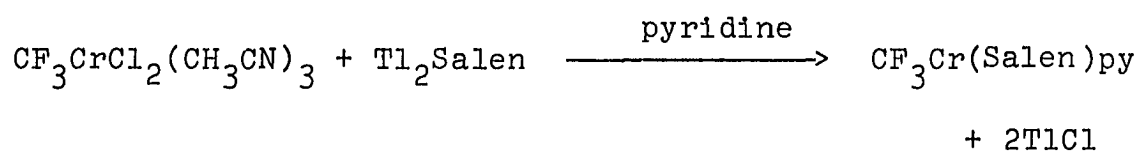
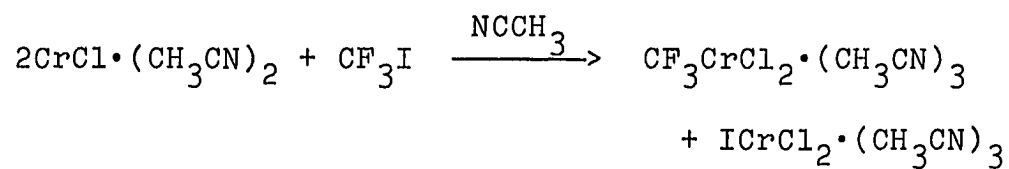
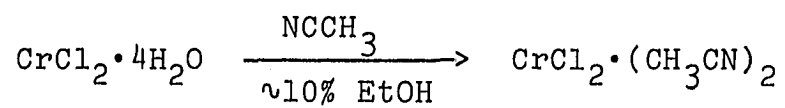
The magnetic moments of the aryl complexes were found to lie in the range of 3.72-3.82 B.M. (36c) whereas for the alkyl species $\mu_{\text{eff}} = 3.64$ B.M. (36e). These values correspond to three unpaired electrons.

Crystal structures have been reported for R = phenyl (36d), 2-anisyl (36a,b) and trimethylsilylmethyl (36e). There is no significant difference in the carbon-chromium bond length. They are 2.087, 2.101 and 2.107 Å, respectively.

These species react rapidly with aqueous HgCl_2 where this reaction was tried (36c).

The second broad class of chelated organochromium complexes consist of perfluoroalkyl species. This restriction is due to their mode of synthesis. Van den Berger et al. (37) prepared these complexes in a manner that drew on the previously discussed synthesis.

First a perfluoroalkylchromium dichloride is formed by attack of $\text{CrCl}_2 \cdot 2\text{NCCH}_3$ on the corresponding perfluoroalkyl iodide. This species is then reacted with a salt of the appropriate ligand. The complexes were purified by successive recrystallization. A specific reaction sequence is shown in Scheme 7 with the compounds listed in Table I-2.



Scheme 7

Table I-2. Perfluoroalkylchromium chelate complexes^a

R-Cr(Salen)·py	R = CF ₃ , C ₂ F ₅ and C ₃ F ₇
R-Cr(Salphen)·py	R = C ₂ F ₅ and C ₃ F ₇
R-Cr(Acen)·py	R = C ₂ F ₅ and C ₃ F ₇
R-Cr(Sal-N-p-tol) ₂ ·py	R = C ₂ F ₅ and C ₃ F ₇
R-Cr(L) ₂ ·py	R = C ₃ F ₇

L = (Sal-N-n-C₄H₉), (Sal), (Acac), (Bzac) (36a) and (R'₂NCS₂) and R' = methyl, ethyl, iso-propyl and phenyl (36b)

^aSalen = N,N'-ethylenebis(salicylaldiminato)(2-);
 Salphen = N,N'-o-phenylenebis(salicylaldiminato)(2-);
 Acen = N,N'-ethylenebis(acetylacetonato)(2-);
 Sal-N-p-tol = N-p-tolylsalicylaldiminato(1-);
 Sal-N-n-C₄H₉ = N-n-butylsalicylaldiminato(1-);
 Sal = Salicylaldehydato(1-); Acac = Acetylacetonato(1-);
 Bzac = Benzoylacetonato(1-); SalenH₂, etc. represent the neutral ligands.

One of the goals of their research was to prepare chromium complexes analogous to known cobalt compounds. But one of the problems associated with their synthetic procedure is that no simple alkylchromium chelate complexes, such as ethyl-, can be prepared by their approach. The analogous perfluorocobalt chelates are not known (38) except for one compound, $C_3F_7Co(Et_2NCS_2)_2py$, prepared by them (37b).

Yet, organocobalt complexes have been prepared by the same mechanism invoked for most σ -bonded organochromium compounds, halogen abstraction followed by subsequent radical capture to yield the organocobalt complex.

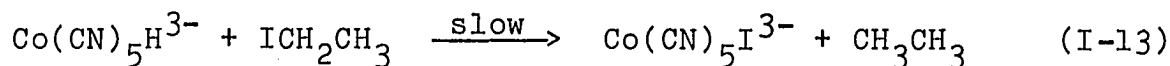
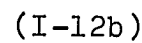
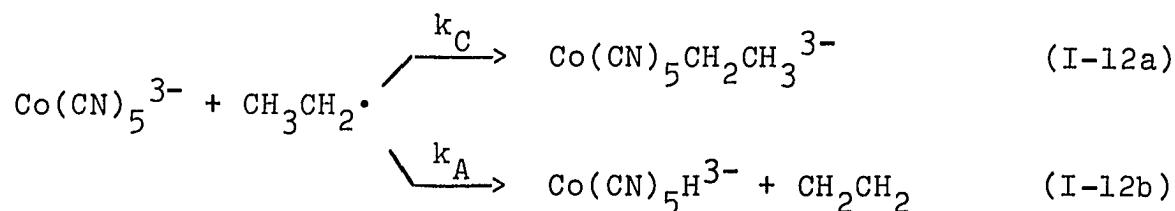
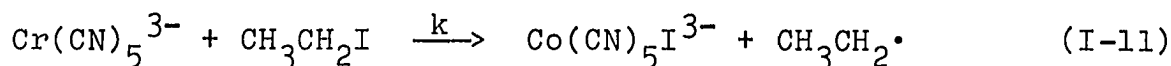
In 1965 Halpern and Maher (39) described the reaction of $Co(CN)_5^{3-}$ with water soluble organic halides. The kinetics were examined and found to be first order both in organic halide and pentacyanocobaltate(II). The results could be interpreted in an analogous manner to that of most of the solvated σ -bonded organochromium complexes as previously shown in eqs. I-7,8, first radical generation formed from halogen abstraction followed by radical capture with the metal complex.

The kinetic data presented by Kochi and Powers (32) are complicated by the fact that only relative rates were determined. This in itself is not crucial but the observed rate of reaction was directly dependent upon ethylenediamine

concentration (32). This implies that the nature of one of their reactants was not well-defined. They did note that various Cr(II)-ethylenediamine equilibria were possible (32).

Halpern's data, on the other hand, were obtained by direct rate measurement using a rather well-defined complex, $\text{Co}(\text{CN})_5^{3-}$ (39).

The range of organic halides used was extended by Chock and Halpern in 1969 (40). This work focused on water insoluble compounds, i.e., ethyl iodide. Equations I-11-13 illustrate the mechanism of reaction for $\text{CH}_3\text{CH}_2\text{I}$.



The rate law, $-\frac{d[\text{Co}(\text{CN})_5^{3-}]}{dt} = 2k[\text{Co}(\text{CN})_5^{3-}][\text{CH}_3\text{CH}_2\text{I}]$, has the same form found for the chromium(II) reductions. Path k_C may be viewed as a radical combination step and k_A an analogous disproportionation. In chromium(II) reductions

path k_A is not seen owing to the instability of aqueous chromium hydride (41).

The reactivity sequence, $C_6H_5CH_2X > (CH_3)_3CX > (CH_3)_2CHX > \text{prim-RX}$ (i.e., CH_3CH_2X) $> CH_3X$, is again seen for this system (40). These values are listed in Table I-3.

Table I-3. Rate constants for reduction of alkyl iodides by $Co(CN)_5^{3-}$ at 25°, ref. 40

R	$k/dm^3 \text{ mol}^{-1} \text{ s}^{-1}$
CH_3	9.5×10^{-3}
CH_3CH_2	5.9×10^{-2}
$CH_3CH_2CH_2$	4.3×10^{-2}
$(CH_3)_2CH$	1.20
$(CH_3)_3C$	9.1
$C_6H_5CH_2$	3.8×10^3

The stabilities of these complexes, $RCo(CN)_5^{3-}$, are clearly demonstrated by the isolation of the sodium salt of $Co(CN)_5CH_2CH_3^{3-}$ (42).

Halpern and others (43) extended this synthetic approach to the formation of organocobalt(III) chelates from the reaction of the corresponding cobalt(II) chelate and either a benzyl iodide or bromide.

Several organometallic chelate complexes are known where the chelate is a completely saturated macrocycle. The first compound of this type reported, trans-aquomethyl (1,4,8,11-tetraazacyclotetradecane)cobalt(III), methyl $\text{Co}([\text{14}] \text{aneN}_4)^{2+}$, was prepared by Roche and Endicott in 1974 (44). The concept of radical capture by a low valent metal complex was used to synthesize this molecule. The methyl radical was generated by the photodecomposition of acetato-pentaminecobalt(III) in the presence of $\text{Co}([\text{14}] \text{-aneN}_4)^{2+}$. This idea was developed one step further by Espenson and Martin (45). The alkyl radicals were generated by the reductive cleavage of an alkyl hydroperoxide with cobalt(II) chelates, i. e., $\text{Me}_6[\text{14}] \text{aneN}_4$ (46). The subsequent radical was captured by another complex. Even a relatively stable methylnickel(II) chelate is known (47).

Though it has been shown that organochromium compounds result, albeit as intermediates (31,32), with saturated amine ligands (ethylenediamine) around chromium no one has yet tried any variations of the above approach for chromium(II) chelates in an attempt to synthesize similar organochromium complexes.

EXPERIMENTAL SECTION

Materials

Preparation of $\text{CrCl}_2 \cdot 4\text{H}_2\text{O}$

This is a variation of an Inorganic Synthesis procedure (48) with the differences delineated below. Two pellets (~ 2 g) of electrolytic chromium metal are placed in a 24/40 S.T. 6" t.t.¹ fitted with a gas lead to deoxygenate the system. The t.t. (with the metal in it) and 30 ml of $\sim 20\%$ HCl ($\sim 1:1$ dilution of conc. HCl) are separately deaerated for ~ 1 hour. Then ~ 15 ml of acid is transferred by Teflon syringe into the reaction vessel through the gas exit. It may be necessary to warm the system to get the reaction going. Gentle heat speeds up the reaction. The t.t. is now heated to remove the excess H_2O with a Bunsen burner. Heating is stopped when the volume has been reduced to ~ 5 ml. The system is allowed to cool. The solid sky blue $\text{CrCl}_2 \cdot 4\text{H}_2\text{O}$ is then rinsed, with agitation, with 3 x 15 ml of deaerated acetone to remove traces of HCl and chromium(III) salts. After the acetone is decanted, deaerated solvent is syringed in. The solution may be transferred to a storage vessel using a Teflon needle. Since these solutions are ~ 0.4 M, $[\text{Cr}^{2+}]$ is most conveniently determined by its absorption spectrum, $\lambda = 713$ nm ($\epsilon = 5.0$).

¹ t.t. test tube.

Preparation of [15]aneN₄-1,4,8,12-tetraazacyclopentadecane

Synthesis of 1,5,9,12-tetraazatridecane This linear tetramine, which is the required starting material, is synthesized in a manner similar to that in ref. 49. The following changes are noted. First, 1,3-dibromopropane (~25 ml for 1/4 scale) is used instead of 1,2-dibromoethane. The preparation is conveniently run on 1/4 - 1/2 scale using a 1-liter 3-neck 24/40 flask. The reaction mixture is heated for ~4 hours in a hot water bath. The 1,3-diaminopropane solvent is stripped off and the resulting viscous oil is distilled using bantam ware. Yield: typically 40% or greater (20 g for 1/4 scale or enough for two [15]aneN₄ preps); boiling point, 147-152°/1 torr.

[15]aneN₄ The procedure is that of ref. 50a with several critical changes suggested by Dr. Frank Wagner (50b). Only a stoichiometric amount of glyoxal is used in the preparation. This must be fresh material, with no white particulate matter at the bottom of the bottle. Use ~5.7 ml of a 40% solution for the literature scale. The reaction is heated, 50-60°, for 4-6 hours after the addition of glyoxal. At this stage, the reaction solution should be deep burgundy in color. The solution is then transferred to a Parr Hydrogenation bottle. Now ~10 g of Ra/Ni catalyst is added. The mixture is exposed to ~70 psi of hydrogen for

2-3 days. At this point, the solution should be blue or purple in color for a good yield, 30% or greater. The solution will be greenish in color if the reaction is a failure. The aqueous solution is made slightly basic by the addition of NaOH. Ten grams of NaCN is then added to decompose the resultant nickel complex of [15]aneN₄. After the yellow color of Ni(CN)₄²⁻ has formed, ~3 hr at 80°, the solution is brought to pH ≥ 12 and extracted with 6 x 50 ml of HCCl₃. The HCCl₃ is stripped off. The yellowish white solid is then recrystallized from either a hot 1:1 THF:hexane solution or hot Et₂O by placing the solution in the freezer. Always obtain a second batch of crystals. The yield from a typical literature scale preparation is ~40% or 3.5 grams of material (blue solution). [15]aneN₄ retains a fair amount of solvent and is hygroscopic, so it should be dried and stored in a desiccator, m.p. 98-99° (lit. m.p. 98-99°) (11).

Halides

All the organic halides were commercially available. They were all distilled before use, under appropriate conditions. 1-Adamantyl bromide was recrystallized twice from methanol.

Solvent preparation

1:1 v/v tert-butanol water was prepared from reagent grade tert-butanol and water containing the appropriate

amount of LiClO_4 to bring the final solution to 0.20 M LiClO_4 . To 473 ml of tert-butanol (one bottle) is added 411.4 ml of distilled water plus 61.6 ml of 3.07 M LiClO_4 . This solution was then stored in a well-sealed bottle, opened only when needed.

$\text{Cr}([\text{15}] \text{aneN}_4)^{2+}$

Solutions of Cr(L)^{2+} were prepared in several ways. For all the kinetics, various aliquots of stock solution of the ligand (0.00466 M) prepared by the addition of 0.100 g of $[\text{15}] \text{aneN}_4$ to a 100 ml vol. flask and bringing to mark with solvent (t-BuOH/ H_2O), were added to 2.00 cm Cary cells. The cells were serum capped and deaerated for a minimum or 20 min with $\text{Cr}_{(\text{aq})}^{2+}$ scrubbed N_2 . After this, a slight deficiency, usually 95-97%, of the required amount of $\text{Cr}_{(\text{solvent})}^{2+}$ was added. Upon appearance of the purple color (~ 2 min), the solutions were ready to use.

Solutions used for product analysis were prepared as follows: 0.100 grams of $[\text{15}] \text{aneN}_4$ was added to 6-10 ml of solvent. In this case the solvent was usually water, though in several cases $\sim 85\%$ aqueous THF and 90% aqueous MeOH were used. The solution was deaerated for ~ 40 min with $\text{Cr}_{(\text{aq})}^{2+}$ scrubbed N_2 , at which time $\sim 95\%$ of the required amount of $\text{Cr}_{(\text{solvent})}^{2+}$ was added. With the formation of the purple color, ~ 3 min, the desired deaerated halide could be added.

Other materials

In some cases solutions of chromium(II) ion were prepared from $\text{Cr}(\text{ClO}_4)_3 \cdot 6\text{H}_2\text{O}$, in which Cr^{3+} is reduced by amalgamated zinc. LiClO_4 was prepared from Li_2CO_3 and perchloric acid then recrystallized twice.

Mercuric perchlorate solutions were prepared by boiling HgO powder in a slight excess of HClO_4 . The solution was then filtered by gravity through high retention filter paper. [Caution: this may deposit an explosive residue upon standing.] Mercuric perchlorate was also purchased from G. F. Smith. In the initial phases of this work $[\text{15}]_4\text{aneN}_4$ was purchased from Strem Chemicals, Inc. All other reagents were used as received.

Methods

Analyses

For all of the chromium(chelate) complexes, the molar absorptivity was determined from a freshly prepared solution. The u.v.-visible spectrum was recorded and then the solution was analyzed for total chromium spectrophotometrically after oxidation with alkaline peroxide, $\lambda = 372 \text{ nm}$ (ϵ , 4830).

The mercury(II) perchlorate stock solutions were analyzed by Volhard titration (51).

Lithium perchlorate solutions were analyzed in the following manner. An aliquot of the Li^+ solution was placed

on a column of Dowex 50W-X8 cation exchange resin in the hydrogen ion form. The column was then washed with H_2O . The liberated H^+ was titrated with standard NaOH to the phenolphthalein endpoint.

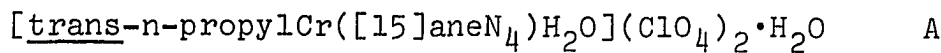
Separation and purification of reaction mixtures

Initial attempts at chromatographic separation of products using Dowex 50W-X8, 100-200 mesh, cation exchange resin proved difficult. Because of this, all product separations and purifications were performed using Sephadex C-25 cation exchange resin. Typically, ~10 ml of product solution was placed upon a 12 x 1.5 cm column of resin after passing the solution through filter paper to remove a small amount of green gel-like material, presumably $Cr(OH)_3(aq)(s)$ or oxidation products of the $Cr([15]aneN_4)^{2+}$. The amount varied with each preparation, from next-to-nothing to several percent while being independent of [RX]. After the solution had been absorbed onto the column, a few milliliters of water was passed through the column. The eluting solution which was found to best effect separation was 0.20 M $NaClO_4$ acidified to $pH \approx 5.0$. After separation had been achieved, the ionic strength in some cases was increased to speed elution of the desired organochromium species. If the acid was raised, the halo- and organochromium complexes were difficult to separate for the

advantage of charge reduction due to the hydrolysis of the halochromium species (52) at $\text{pH} \approx 5$ was lost.

These compounds were air and temperature sensitive, $R = \text{isopropyl, benzyl, cyclopentyl, cyclohexyl and methyl}$. The cation exchange column was deaerated by passing ~ 100 ml of eluent through the column before addition of the reaction solution. To cool the column, ice-water was circulated through a condenser-like jacket surrounding the column. The solutions off the column were collected in a manner appropriate to their respective sensitivity.

Isolation of organochromium salts



solution of the above species was prepared and purified as previously mentioned. This solution, $\sim 3 \times 10^{-3}$ M in RCr(L)^{2+} and 0.40 M in NaClO_4 , $\text{pH} \approx 2$ (added HClO_4 after elution) was placed in the freezer. After a period of weeks, reddish-orange needle-like crystals formed at the flask bottom and in the ice matrix. They may be removed from the ice by physical separation or by letting the ice slowly melt removing the water as it is formed. These crystals are very soluble in H_2O and CH_3CN , soluble in THF, EtOH and MeOH, and insoluble in ether.

[trans-ethylCr([15]aneN₄)NCS]ClO₄ A solution of EtCr([15]aneN₄)H₂O²⁺ was prepared and purified as before. This usually results in approximately 20-30 ml of $\sim 3 \times 10^{-3}$ M solution of the organochromium ion. This species was eluted with only 0.20 M NaClO₄, pH \approx 4.5. To this solution, several tenths of a gram of NaSCN is added, enough to make the solution \sim 0.20 M in NaSCN. This solution is allowed to set, preferably in the refrigerator, and over a period of days orange crystals will form. They may be isolated by decanting off the liquid. They are very soluble in CH₃CN, soluble in EtOH and THF and insoluble in ether.

Spectra

Mass spectrum Gaseous reaction products were detected mass spectrally with an apparatus that allowed reagent mixing and product monitoring while attached to the mass spectrometer. The apparatus was a Y-shaped tube with reagent vessels for either arm. The reaction was initiated by rotating the arms to deposit the reagent into the reactant solution at the bottom of the Y tube. The mass spectra were continuously monitored. If the identity of an ion source was in doubt, its appearance potential was determined by an ionization voltage scan, hence confirming the ion's origin (i.e., CH₂CH₂ vs. N₂).

The mass spectra of the organomercurial chlorides, used for characterization of the new organochromium species, were obtained by slight heating of the solid RHgCl at $\sim 10^{-6}$ torr.

Ethyl bromide was the only volatile organic detected when a purified solution of EtCr(L)^{2+} (~ 20 ml of 0.0026 M) was exposed to saturated Br_2 water. This was done using a Y tube apparatus attached directly to the mass spectrometer.

The organic products resulting from the reaction of $\text{Cr}([\text{15]aneN}_4)^{2+}$ with BrCH_2Cl and BrCCl_3 were determined in a similar manner. Ion origins were verified by their characteristic appearance potential.

I would like to thank Mr. G. D. Flesch for assistance in the mass spectral determinations.

U.V. and visible spectra All absorbance measurements and U.V. visible spectra were recorded using a Cary 14 Spectrophotometer.

Gas Chromatography

All analyses of hydrocarbon mixtures for the competition experiment were performed using a Traycor 550 G.C. at ambient temperature equipped with a 6' x 1/4" (4 mm i.d.) column packed with 10% S.E. 30 on Chromosorb W with a flow rate of 4.8 cm/sec.

A 20.0 ml solution containing different amounts of $\text{Cr}(\text{15-aneN}_4)^{2+}$ in 90% aqueous methanol were reacted with a deficiency of 6-bromohexene. These solutions were allowed to stand between 3 and 14 hours. The excess $\text{Cr}(\text{L})^{2+}$ was destroyed by exposure to air. Next, NaOH in MeOH was added to decompose the organochromium species and then the solutions were acidified with HCl.

The samples of the reaction mixture were injected directly onto the G.C. column. The retention times of 1-hexene and methylcyclopentane were compared with authentic samples. The relative amounts of each were determined by cutting the peaks out and weighing them. The detector was calibrated with a 1:1 mixture of the hydrocarbons.

I wish to acknowledge Larry Kissinger and Terry Marshall for their assistance.

Electrochemistry

The reduction potential of $\text{Cr}([\text{15}]\text{aneN}_4)^{2+}$ was determined by cyclic voltammetry monitoring the reduction of trans- $(\text{H}_2\text{O})_2\text{Cr}([\text{15}]\text{aneN}_4)^{3+}$ in acidic solution ($\text{H}^+ = 0.40 \text{ M}$) at 25°C.

The solution of the diaquo species was prepared by base catalyzed aquation of trans- $\text{I}(\text{H}_2\text{O})\text{Cr}([\text{15}]\text{aneN}_4)^{2+}$ produced from the reaction of ethyl iodide and $\text{Cr}([\text{15}]\text{aneN}_4)^{2+}$. The solution was reacidified and passed through a cation exchange column.

The reference electrode was isolated by a Teflon fritted tube filled with electrolyte solution (0.4 M HClO_4) separated by a KNO_3 salt bridge. The counter electrode was isolated by a ground glass frit. The reduction potential, peak separation, did not vary with scan rate.

The cyclic voltammograms were recorded using a Princeton Applied Research 173 Potentiostat/Galvanostat equipped with a P.A.R. 175 universal programmer. The voltammograms were either photographed from a storage oscilloscope or reproduced by chart recorder.

Stoichiometry

Two experiments were performed to prove that one mole of organic halide reacts with two moles of $\text{Cr}([\text{15}] \text{aneN}_4)^{2+}$.

In the first experiment, four identical 2 cm path length spectrophotometer cells containing a solution of $[\text{15}] \text{aneN}_4$ were deaerated followed by the addition of 95% of the stoichiometric amount of Cr^{2+} . Then, a 4.00 ml aliquot from one cell was removed and total Cr^{2+} determined by the cobalt method (53). Then, several aliquots of PhCH_2Br solution, 0.0841 M , were added to one of the cells with the absorbance measured at λ 390 nm ($\epsilon \approx 2000$) after each addition. Then, the total Cr^{2+} was again determined in another cell in which no RX had been added. This procedure was again repeated. The average Cr^{2+} concentration was then used to

construct a plot of absorbance vs mole ratio, $\text{PhCH}_2\text{Br}/\text{Cr}([\text{15}] \text{aneN}_4)^{2+}$. The point at which this plot breaks yields the value of the mole ratio which indicates the number of moles of PhCH_2Br that react per mole of $\text{Cr}([\text{15}] \text{aneN}_4)^{2+}$.

A kinetic method was also used to determine the stoichiometry. In these kinetic experiments the reagent in pseudo-first order excess was $\text{Cr}([\text{15}] \text{aneN}_4)^{2+}$ and benzyl bromide was the limiting reagent. In all the other kinetic experiments the organic halide was in excess. The absolute rate of reaction is determined with respect to the excess reagent. The ratio of these rates then yields the stoichiometry of reaction with respect to the different excess reagents.

Kinetics

Kinetic runs on slow reactions ($t_{1/2} \geq 10\text{s}$) were monitored at an appropriate wavelength, usually $\lambda \cong 390 \text{ nm}$, using a Cary 14 spectrophotometer equipped with a thermostatted cell compartment. A stock solution, 1:1 tert-butanol:water, $\mu = 0.20$, Li^+ , of $[\text{15}] \text{aneN}_4$ was added to a Cary cell with the volume and concentration adjusted with more solvent. The cell was then stoppered with a rubber serum cap. The solution in the cell was then deaerated for at least 20 minutes. The chromous scrubbed N_2 was passed

through a solvent solution before reaching the cell to minimize solvent evaporation. A slight deficiency of the required amount of $\text{Cr}_{(\text{aq})}^{2+}$ was added, then the cell was thermostatted for ~ 20 min before the reaction was initiated by the addition of neat deaerated organic halide via micro-syringe.

Kinetic runs on faster reactions ($t_{1/2} \leq 20\text{s}$) were performed using a Gibson-Durrum D-110 stopped-flow spectrophotometer using Kel-F components. The spectrophotometer is equipped with a storage oscilloscope for use with reactions having a total life, 90% completion, greater than 20 seconds. For faster reactions the instrument is interfaced with a PDP-15 computer for data acquisition and analysis. The computer calculates the observed rate constant and prints this out via teletype for the user. The raw data for each run could be photographed at the experimenter's discretion.

Pseudo-first-order conditions, with the organic halide in excess, were used in all experiments except for several runs with benzyl bromide where $\text{Cr}([\text{15}]\text{aneN}_4)^{2+}$ was, at times, in excess.

The pseudo-first-order rate constants, k_{obs} , were either obtained from computer analysis of the data or from the standard method.

In the standard method, $A_\infty > A_0$, $-\ln(A_\infty - A_t)$ is plotted against time according to $\ln(A_\infty - A_t) = \ln(A_\infty - A_0) - k_{\text{obs}} t$ and the slope = k_{obs} . The second order rate constant was usually determined from a plot of k_{obs} vs [organic halide]. The slope of such a plot is the second-order rate constant. Where there were a limited number of kinetic runs the second-order rate constant was determined by the quotient of $k_{\text{obs}}/[\text{RX}]$.

In the case of two of the halides, t-butyl bromide and 1-adamantyl bromide, different solvent systems were used. For t-butyl bromide, 85% aqueous THF was used. The solutions of t-butyl bromide were made up in reagent grade THF. With the solutions of Cr(L)^{2+} prepared in 70% aqueous THF. This was done to prevent solvolysis of t-BuBr. The rate measurements were performed on the stopped-flow apparatus. These reactions were calibrated to the t-butanol/water solvent by measuring the reaction rate of ethyl bromide, $k = 0.164 \text{ dm}^3 \text{ mol}^{-1} \text{ s}^{-1}$ (t-BuOH/H₂O) vs $k = 0.116 \text{ dm}^3 \text{ mol}^{-1} \text{ s}^{-1}$ (85% THF/H₂O). This results in a rate ratio of 1.4 for these solvents, respectively.

1-Adamantyl bromide was just not sufficiently soluble in the above solvent system. Its rate of reaction with Cr(L)^{2+} was determined in 99% methanol. This again was done on the stopped-flow. The adamantyl bromide was dissolved in reagent grade methanol. The water was introduced

when $\text{Cr}_{(\text{aq})}^{2+}$ was added to the deaerated solution of [15]aneN₄ in methanol. These reaction rates were scaled in a similar manner using *n*-propyl bromide, $k = 0.166 \text{ dm}^3 \text{ mol}^{-1} \text{ s}^{-1}$ (*t*-BuOH/H₂O) vs $k = 3.3 \text{ dm}^3 \text{ mol}^{-1} \text{ s}^{-1}$ (99% MeOH) with a rate ratio of 0.05.

Results

Characterization of $\text{Cr}([\text{15]aneN}_4)^{2+}$

Chromium(II) complexes are quite rare owing to their extreme air sensitivity. Yet, several types have been isolated. In 1969, several bis and tris ethylenediamine species were characterized (54). Of more relevant interest were the compounds characterized by Dei and Mani (55), $\text{Cr}(\text{Me}_6[\text{14]aneN}_4)\text{X}_2$; X = Cl, Br and I; and $\text{Cr}(\text{Me}_2[\text{14]aneN}_4)\text{X}_2$; X = Cl and Br (56). These species are directly analogous to $\text{Cr}([\text{15]aneN}_4)^{2+}$.

When $\text{Cr}_{(\text{aq})}^{2+}$ is added to a deaerated solution of [15]aneN₄, pronounced color changes take place. The solution is first a brown color which over a period of minutes changes to a deep royal purple. This transformation has been ascribed to the *cis-trans* interconversion of the ligand (55) though the initial formation of the complex must go through several steps.

The Cr^{2+} ion is a potent reducing agent, $E^\circ = 0.408$ volts. A more precise measure of the reduction potential of

the $\text{Cr}([\text{15}] \text{aneN}_4)^{2+}$ was needed since it was known that the coordination of amines appeared to increase the reducing nature of the metal center (57). The reduction potential of $\text{Cr}([\text{15}] \text{aneN}_4)^{2+}$, $E_{1/2} = 0.82 \pm 0.01$ volts vs SCE, $E_{1/2} = 0.58 \pm 0.01$ volts vs SHE, was determined by cyclic voltammetry, Figure I-1.

The spectrum of $\text{Cr}([\text{15}] \text{aneN}_4)^{2+}$ was measured in the reaction solvent, 1:1, v/v, tert-butanol:water. The extinction coefficient was determined by total chromium analysis and this value was in excellent agreement with the extinction coefficient determined by the total amount of Cr^{2+} added ($\lambda_{\text{max}} = 540$ nm (28.7 ± 1), $\lambda_{\text{min}} \approx 430$ nm ($4.7 \pm .2$), Figure I-2. The extinction coefficient and band maximum are in excellent agreement with those of $\text{Cr}(\text{en})_2^{2+}$ (31).

Characterization of the Products of Reaction of $\text{Cr}([\text{15}] \text{aneN}_4)$ with Organic Halides

General description

$\text{Cr}([\text{15}] \text{aneN}_4)^{2+}$ reacted with all organic halides tried except the halobenzenes. The purple solution of $\text{Cr}(\text{L})^{2+}$ will turn to yellow through reddish brown depending upon the halide used.

When the product solution is placed on a column of Sephadex C-25 cation exchange resin in the Na^+ form and slowly eluted with 0.20 M NaClO_4 (pH ≈ 5.0), the following

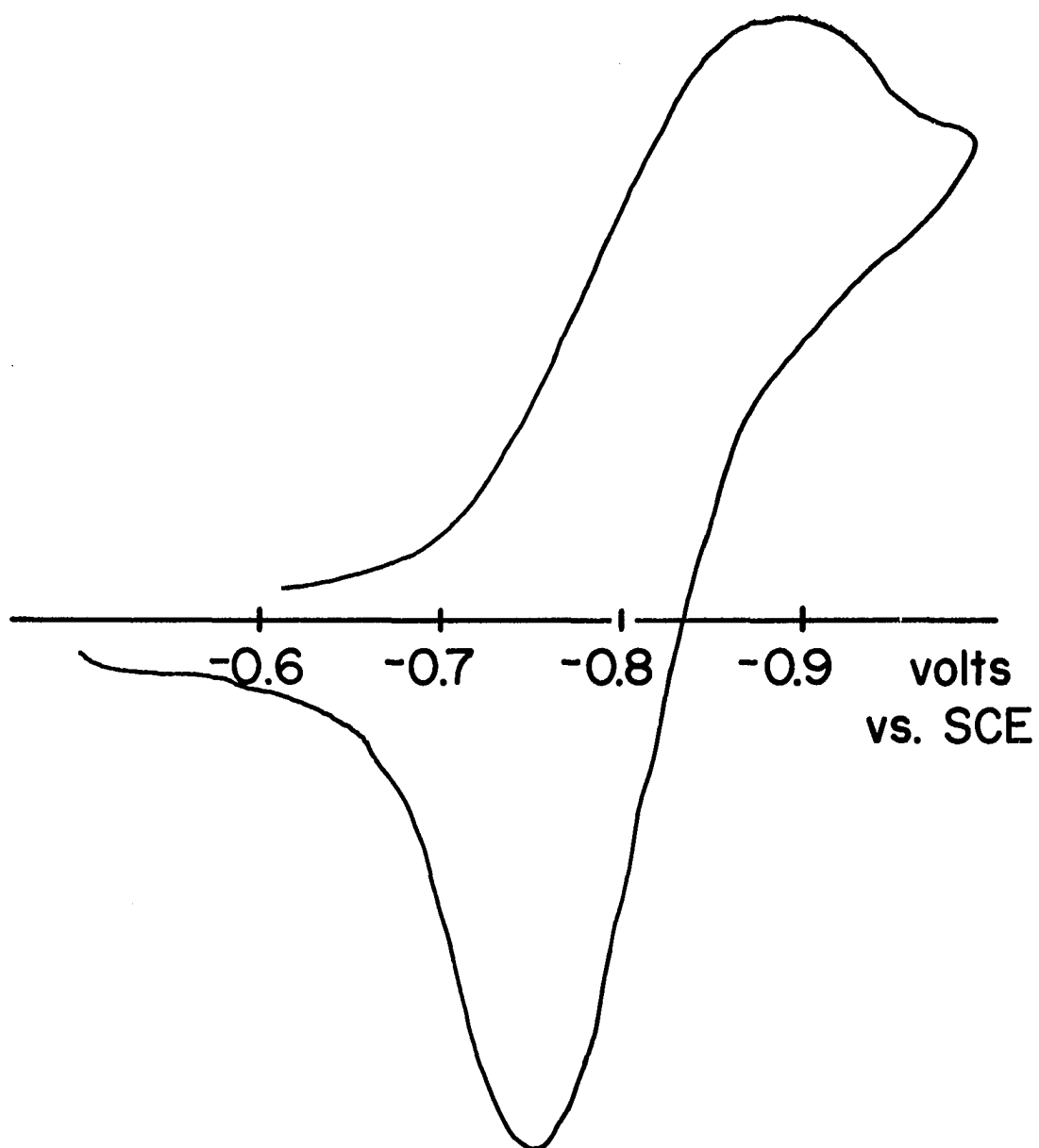


Figure I-1. The cyclic voltammogram for the $\text{Cr(L)}^{3+}/\text{Cr(L)}^{2+}$ couple

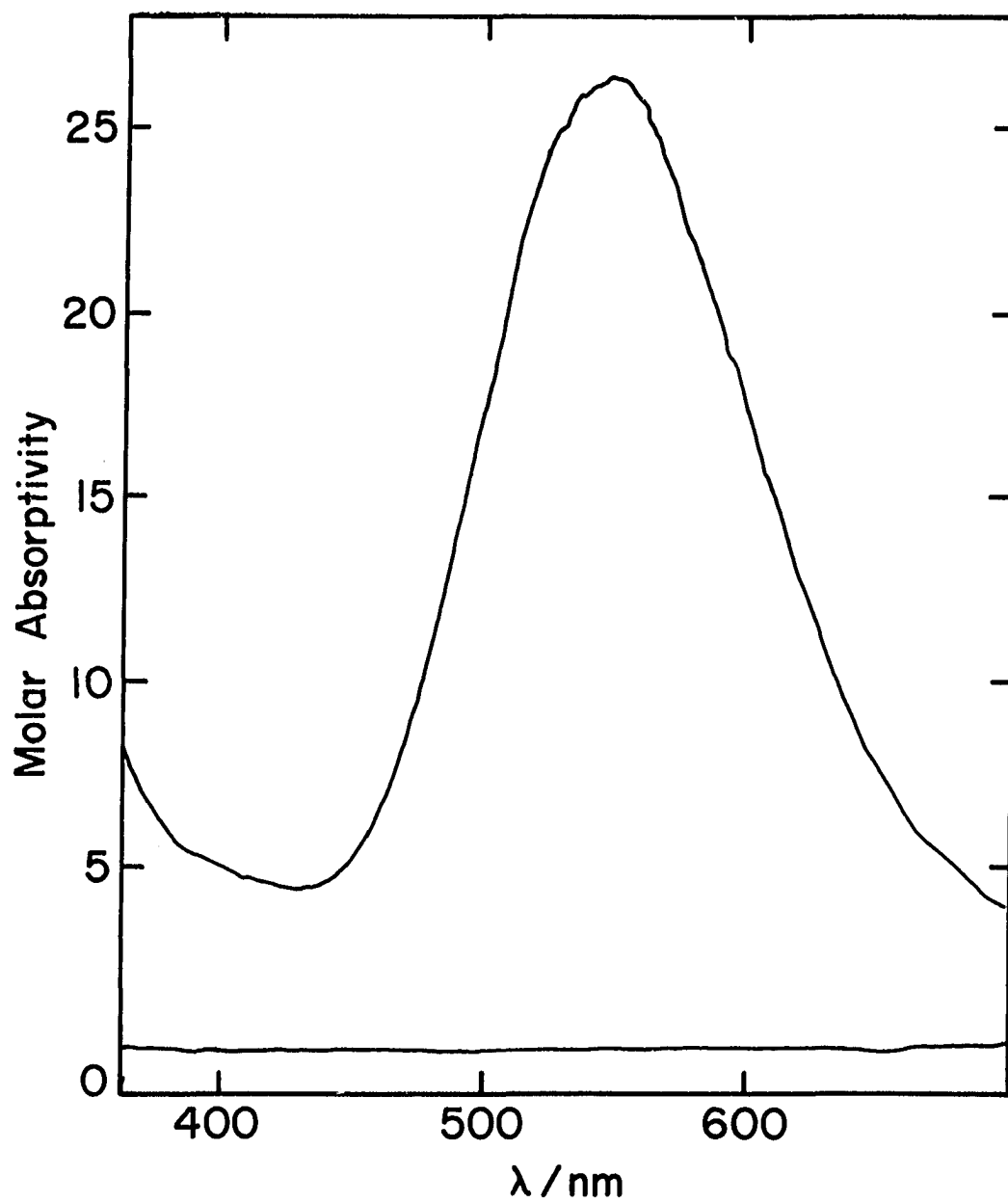


Figure I-2. The electronic spectrum of $\text{Cr}([\text{15}] \text{aneN}_4)^{2+}$ in 1:1 $\text{t-BuOH}/\text{H}_2\text{O}$

characteristic pattern emerges. The first band off the column is dull red in color which turns greenish-brown instantaneously upon the addition of acid. The second band is yellow to orange in color and at times air sensitive, depending upon the organic halide. The last band from the column is reddish-brown. This band also displays a pH dependence (pH 1-6) in its color.

The solutions of first band react with Hg^{2+} to give a cloudy suspension whereas solutions of the second band lose depth of color. Solutions of the third band show no reaction.

Only solutions of the second band react with Br_2 .

Only two bands are observed for the reaction of Cr(L)^{2+} with geminal and vicinal halides (i.e., CH_2Br_2 and $\text{BrCH}_2\text{CH}_2\text{Br}$, respectively).

Characterization of the Inorganic Reaction Products

Upon separation of the reaction products of $\text{Cr}([\text{15}] \text{aneN}_4)^{2+}$ with organic halides, the first band off a neutral (pH \approx 5.0) Sephadex C-25 cation exchange column in the Na^+ form behaves as a 1^+ species. The expected inorganic products $\text{XCr(L)H}_2\text{O}^{2+}$, X = Cl, Br and I, are doubly charged. At first, this was puzzling, so was their rapid reaction with acid (HClO_4). This was easily explained by assuming

that the complex off the column was hydrolyzed, $XCr(L)OH^+$, and all that was accomplished by the addition of H^+ was to shift the protonation equilibria to that of the aquo species.

This explanation appears justified because the previously determined pKa's for trans- $(H_2O)_2Cr(en)_2^{3+}$ and trans- $(SCN)_2(H_2O)_2Cr(en)^+$ were determined to be 4.1 and ~ 6 , respectively (52).

The spectra of the species first off the column, after acidification, for the different halides are shown in Figures I-3 - I-5. The spectrum of the trans-diaquo $Cr([15]aneN_4)^{3+}$ species is shown in Figure I-6. The spectra compare very well in general appearance to those of the trans- $Cr(NH_3)_4AB^{n+}$ cations reported by Glerup and Schaffer (58) and to the spectra reported for the trans- $X_2Cr([14]aneN_4)^{n+}$ ions (59). The major difference is the higher extinction coefficients for the $Cr([15]aneN_4)^{n+}$ complexes. These are listed in Table I-4. The reported values for $ICr(L)^{2+}$ might be in error due to the rapid aquation of this species. As implied above, the trans geometry is assigned by the similarity of the various spectra.

Upon base catalyzed aquation and subsequent reacidification, the same spectrum is obtained (Figure I-6) regardless of the starting halochromium complex. Thermal

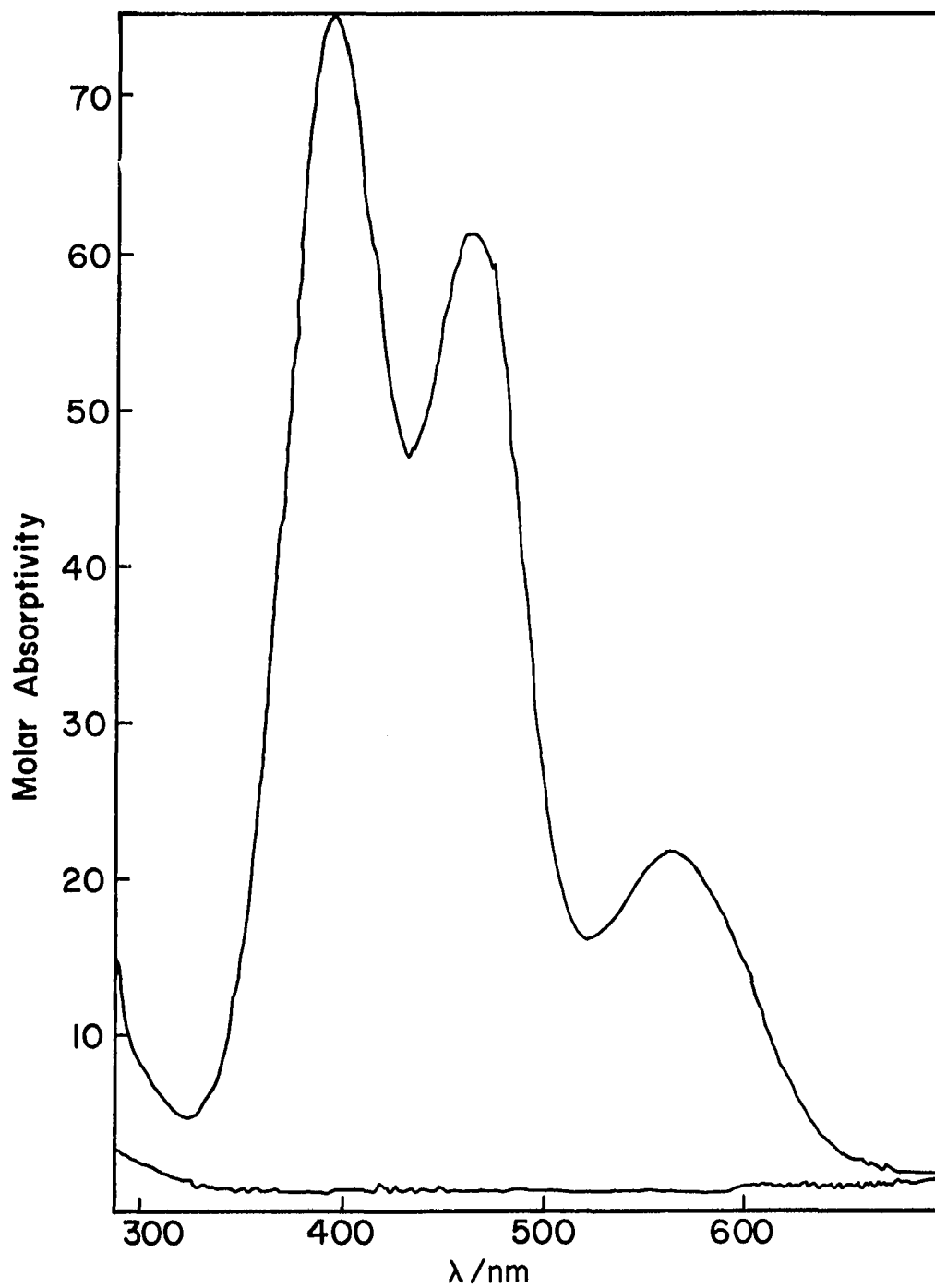


Figure I-3. The electronic spectrum of $\text{trans-CrCl(L)H}_2\text{O}^{2+}$

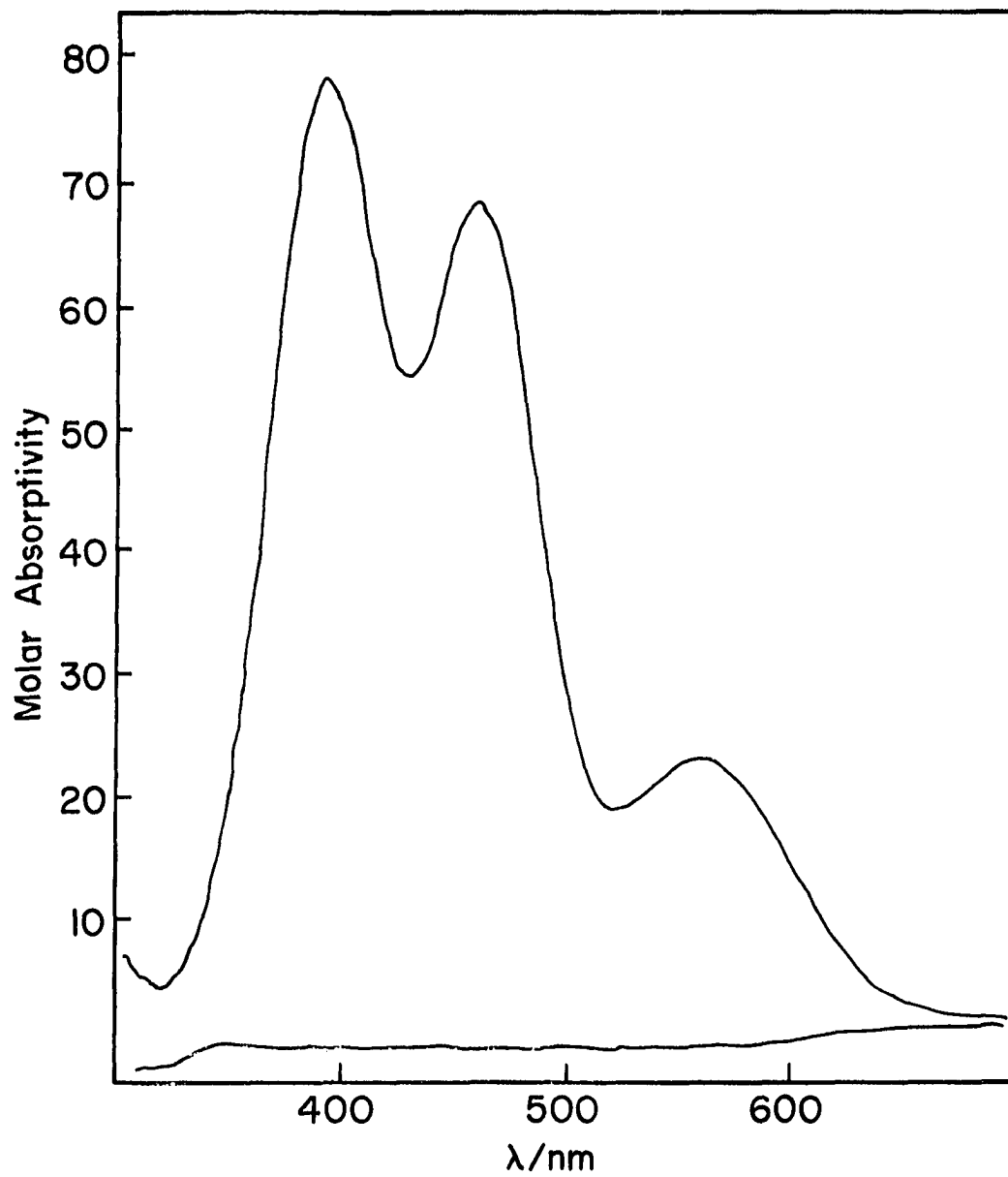


Figure I-4. The electronic spectrum of $\text{trans-BrCr(L)H}_2\text{O}^{2+}$

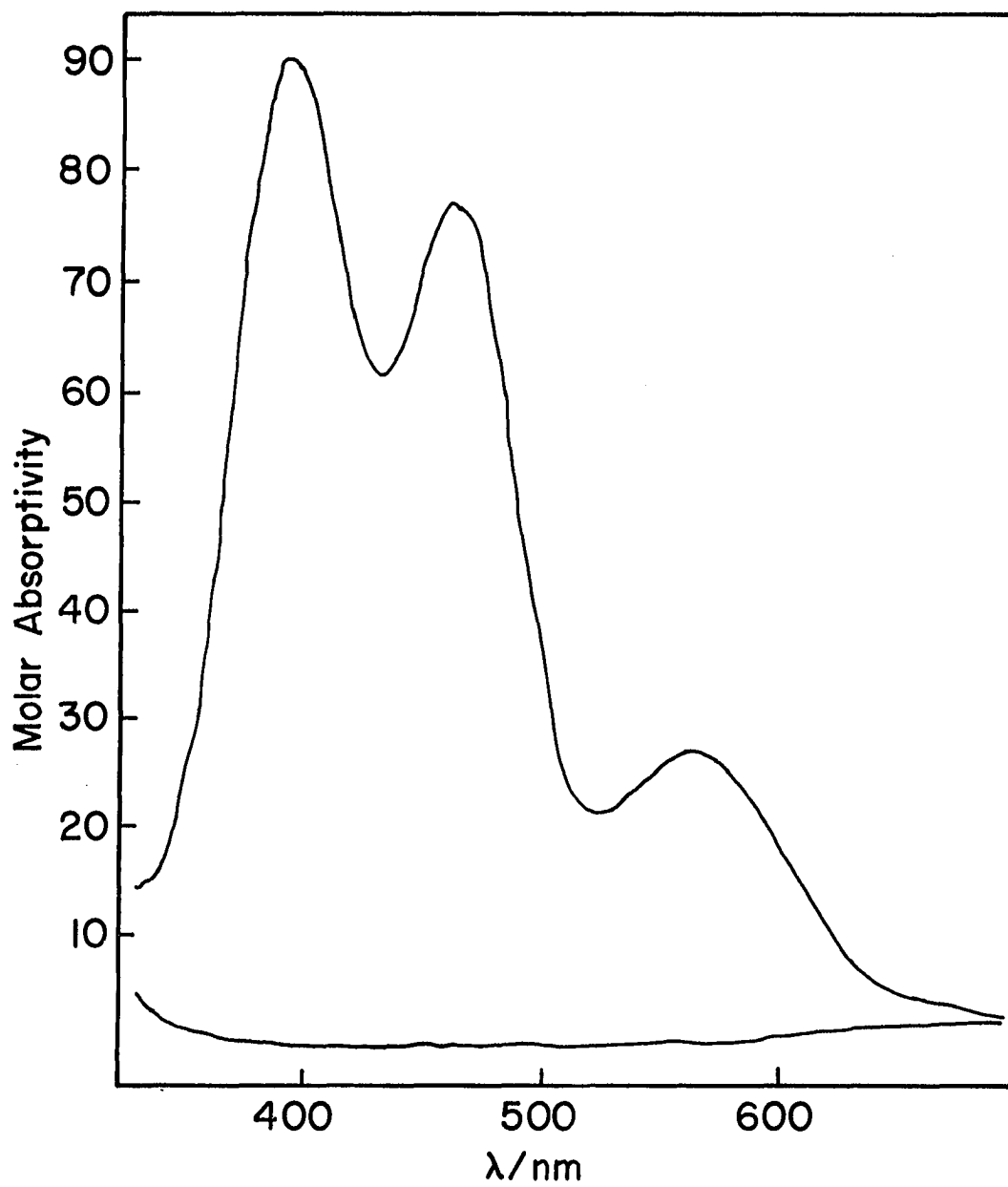


Figure I-5. The electronic spectrum of $\text{trans-ICr(L)H}_2\text{O}^{2+}$

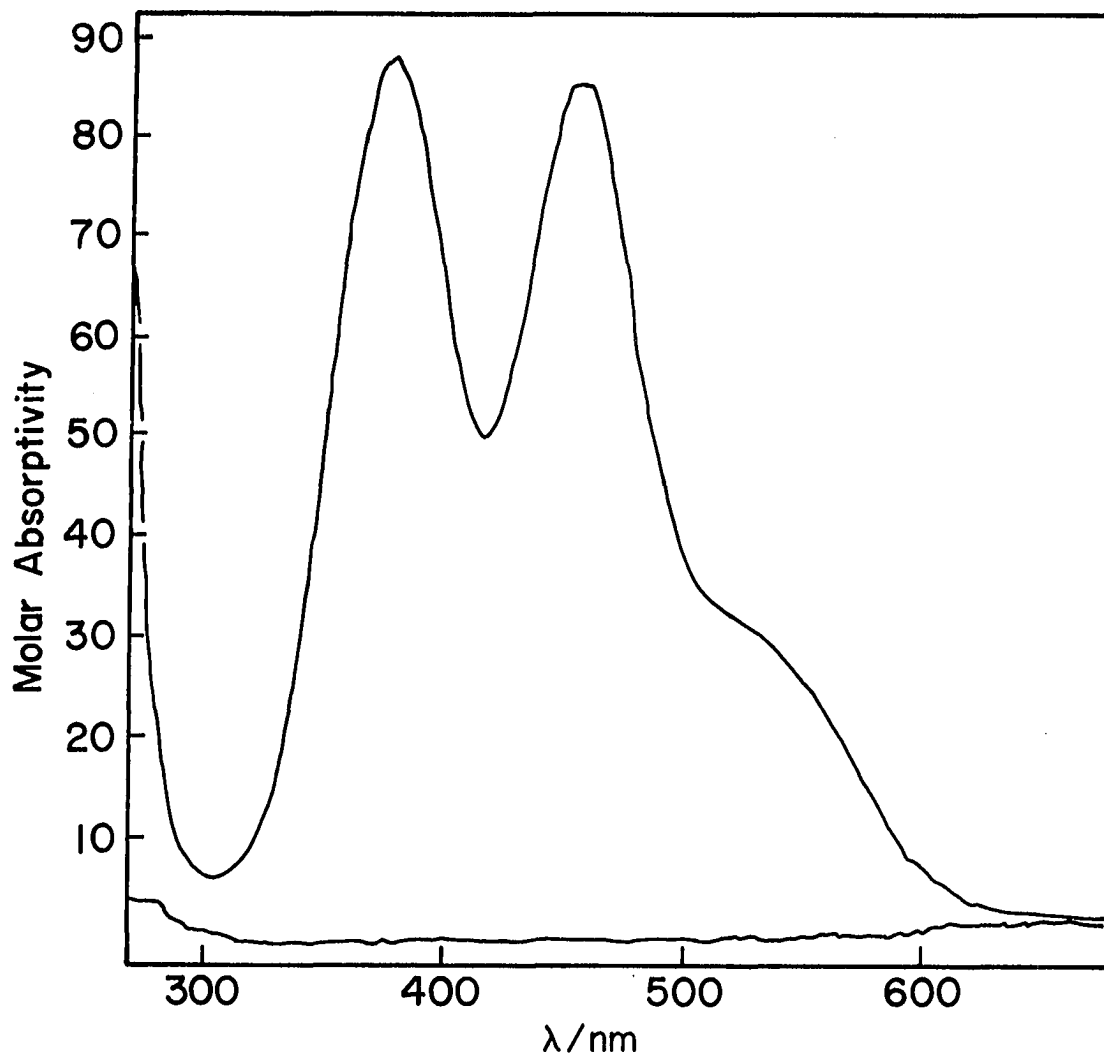


Figure I-6. The electronic spectrum of $\text{trans}-(\text{H}_2\text{O})_2\text{Cr}(\text{L})^{3+}$

Table I-4. Spectral parameters for various trans-XCr([15]aneN₄)H₂O^{n+=2,3} complexes

X	λ_{\max}, ϵ	λ_{\max}, ϵ	λ_{\max}, ϵ
Cl	393 nm (76.2±1.9)	462 nm (62.2±1.6)	564 nm (21.9±0.6)
Br	393 nm (77.5±3)	460 nm (67.5±2.7)	560 nm (22.9±0.9)
I ^a	394 nm (90±3)	462 nm (75±2.5)	562 nm (26±1)
H ₂ O	377 nm (88±3.7)	454 nm (86.5±3.6)	(sh)540 nm (28±1.2)

^aThese values are an estimate due to its thermal instability.

decomposition of the iodo complex results in the same spectrum, that of the diaquo Cr(L)^{3+} .

Characterization of the Organochromium Species

It has been shown that dibromine (27a) and mercury (27b) electrophiles cleave the carbon chromium bond. Both of these reagents may be used as a qualitative test for the presence of this bond.

Ethylchromium($[\text{15}] \text{aneN}_4$) $^{2+}$ was prepared from ethyl iodide and $\text{Cr}([\text{15}] \text{aneN}_4)^{2+}$ and purified by cation exchange chromatography. This solution was reacted with Br_2 in an apparatus attached to a mass spectrometer. The only volatile organic was ethyl bromide.

When solutions of the organochromium species react with Hg^{2+} , a pronounced change in the visible spectrum is observed. The final spectrum is that of trans- $(\text{H}_2\text{O})_2\text{Cr}([\text{15}] \text{aneN}_4)^{3+}$, Figure I-7.

Several organochromium species were prepared in bulk solution from the organic bromide (R = ethyl and n-butyl) and not purified. Upon reaction with Hg^{2+} (in solution as the perchlorate) and workup, the mixed organomercuric halides, X = Cl and Br, were isolated as solids and the mass spectra recorded. In both cases all the peaks in the respective spectra could be assigned to the organomercuric halides. The individual peaks will not be reported due to the large number resulting from the isotopes of mercury.

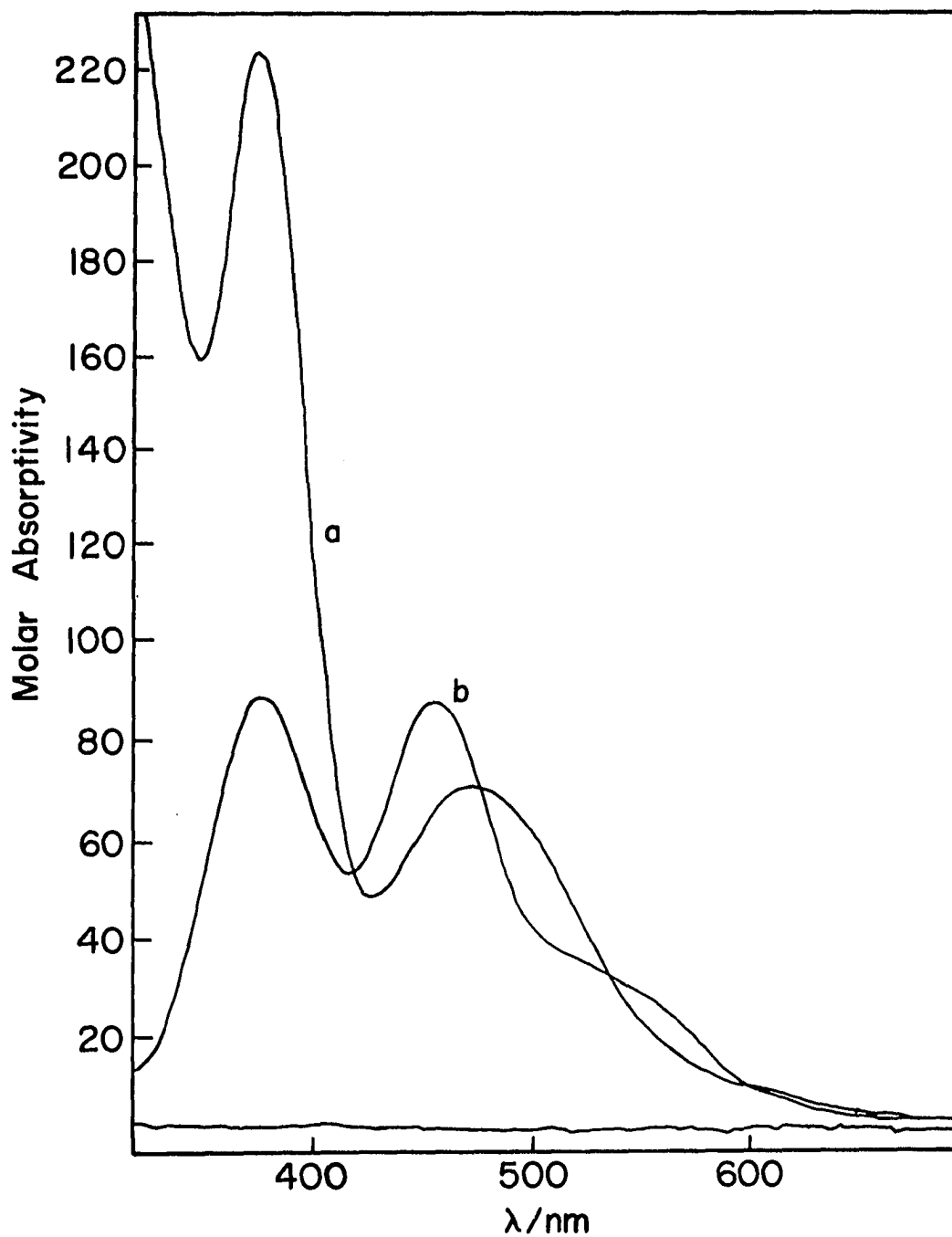


Figure I-7. Electronic Spectra

(a) The electronic spectrum of $\text{CH}_3\text{Cr}(\text{L})^{2+}$

(b) The electronic spectrum of the same solution after the addition of excess Hg^{2+}

Benzylchromium($[15]aneN_4$) $^{2+}$ was prepared in a similar manner, except in this experiment the organic chloride was used. The only halide in solution was chloride. In this case benzylmercuric chloride was isolated, m.p. = 103-4° (lit. 104°) (60). This was also confirmed by the compound's mass spectrum.

The spectra of these solutions are directly related to the nature of the organic group. The primary alkyl groups, R = methyl, ethyl, n-propyl, and n-butyl, show a pronounced low energy transition (~ 465 nm) (Figures I-8-11a), whereas the secondary alkyls, R = isopropyl and cyclohexyl, show only a shoulder at approximately the same region (Figures I-12, 12a and 13). The adamantyl moiety, the only tertiary alkyl isolated, appears much like the primary alkyls, Figure I-14. The spectrum of benzylCr($[15]aneN_4$)H $_2$ O $^{2+}$ is similar in appearance to (H $_2$ O) $_5$ CrCH $_2$ Ph $^{2+}$, Figures I-15, 15a. The neopentyl and tert-butyl chromium species were not able to be isolated from a cooled (ice-water) air-free column of Sephadex C-25. Their spectra will not be shown.

A list of the absorption max. and the corresponding extinction coefficients, as determined by the chromate method, averaged over all separate determinations, appear in Table I-5.

Solids of these organochromium species are difficult, if not impossible, to get except with tetraphenylborate

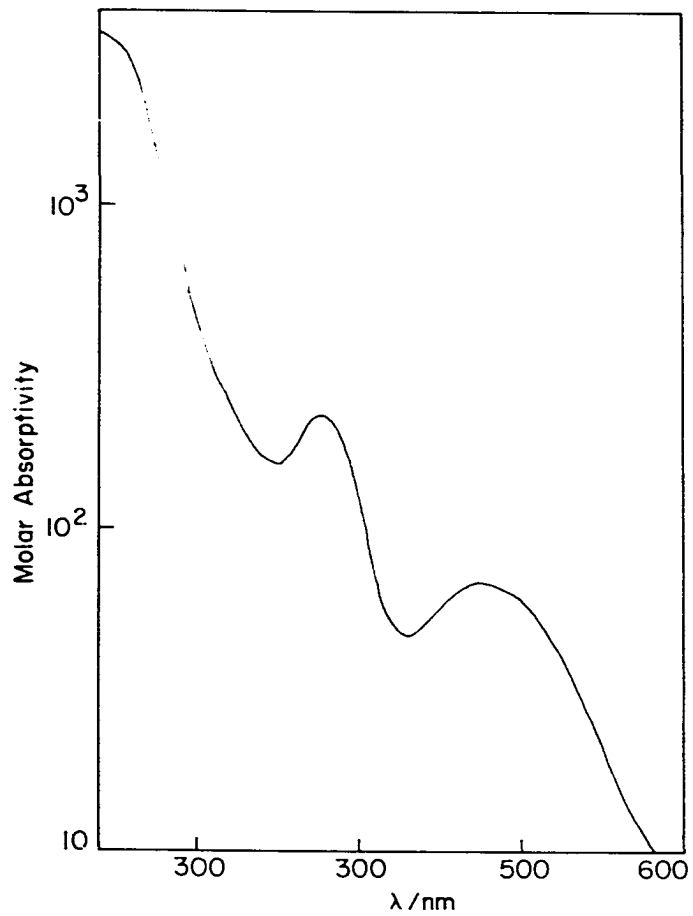


Figure I-8. The electronic spectrum of methylCr(L)²⁺

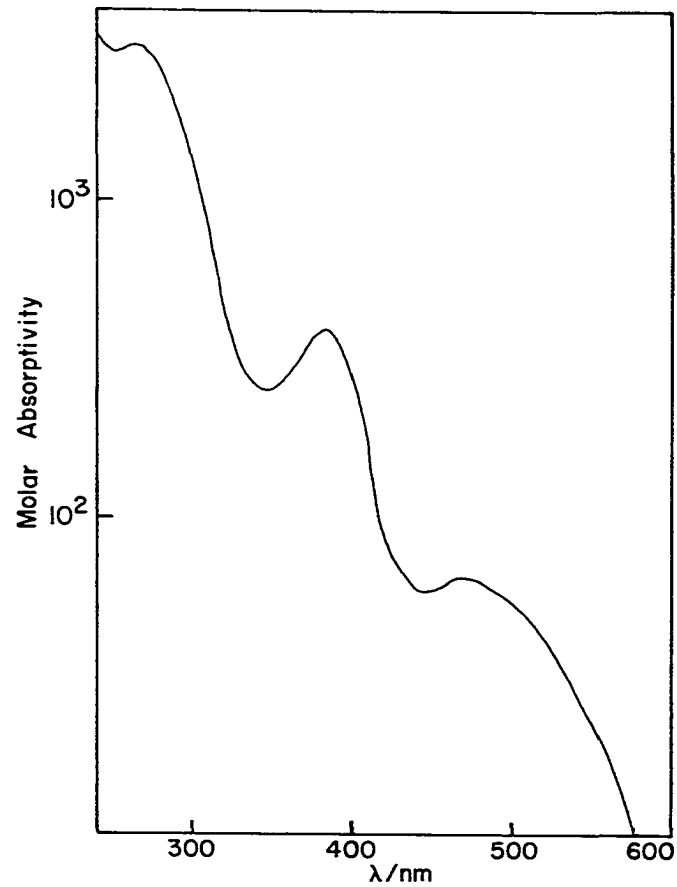


Figure I-9. The electronic spectrum of ethylCr(L)²⁺

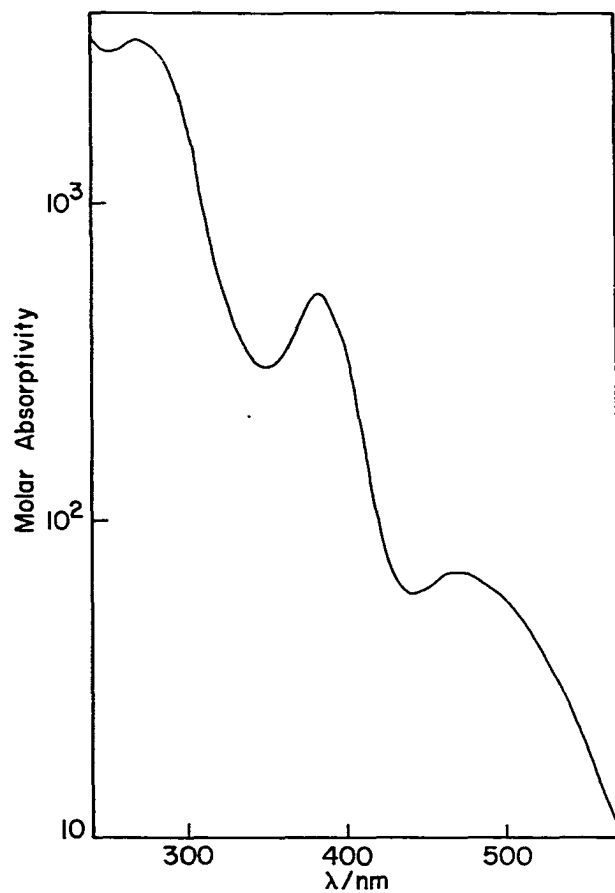


Figure I-10. The electronic spectrum of $n\text{-propylCr(L)}^{2+}$

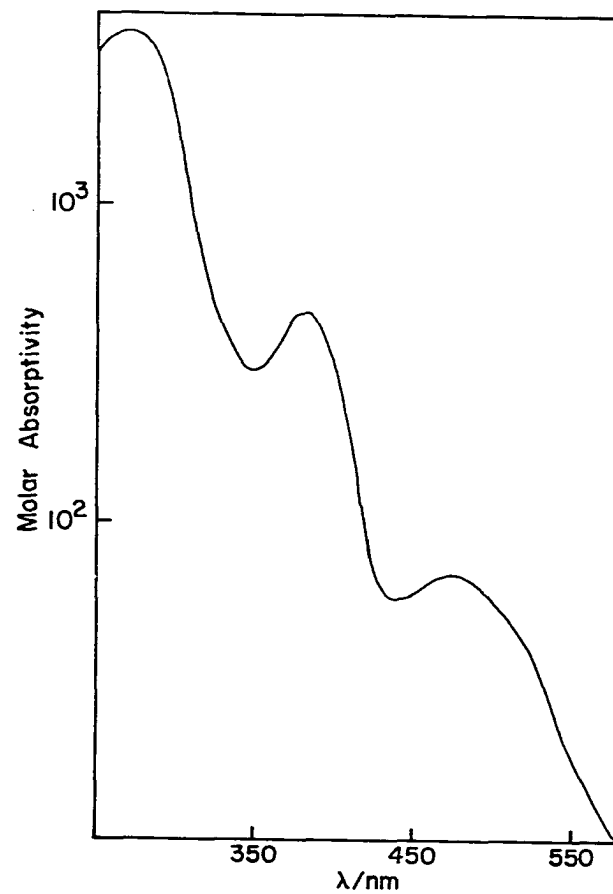


Figure I-11. The electronic spectrum of $n\text{-butylCr(L)}^{2+}$

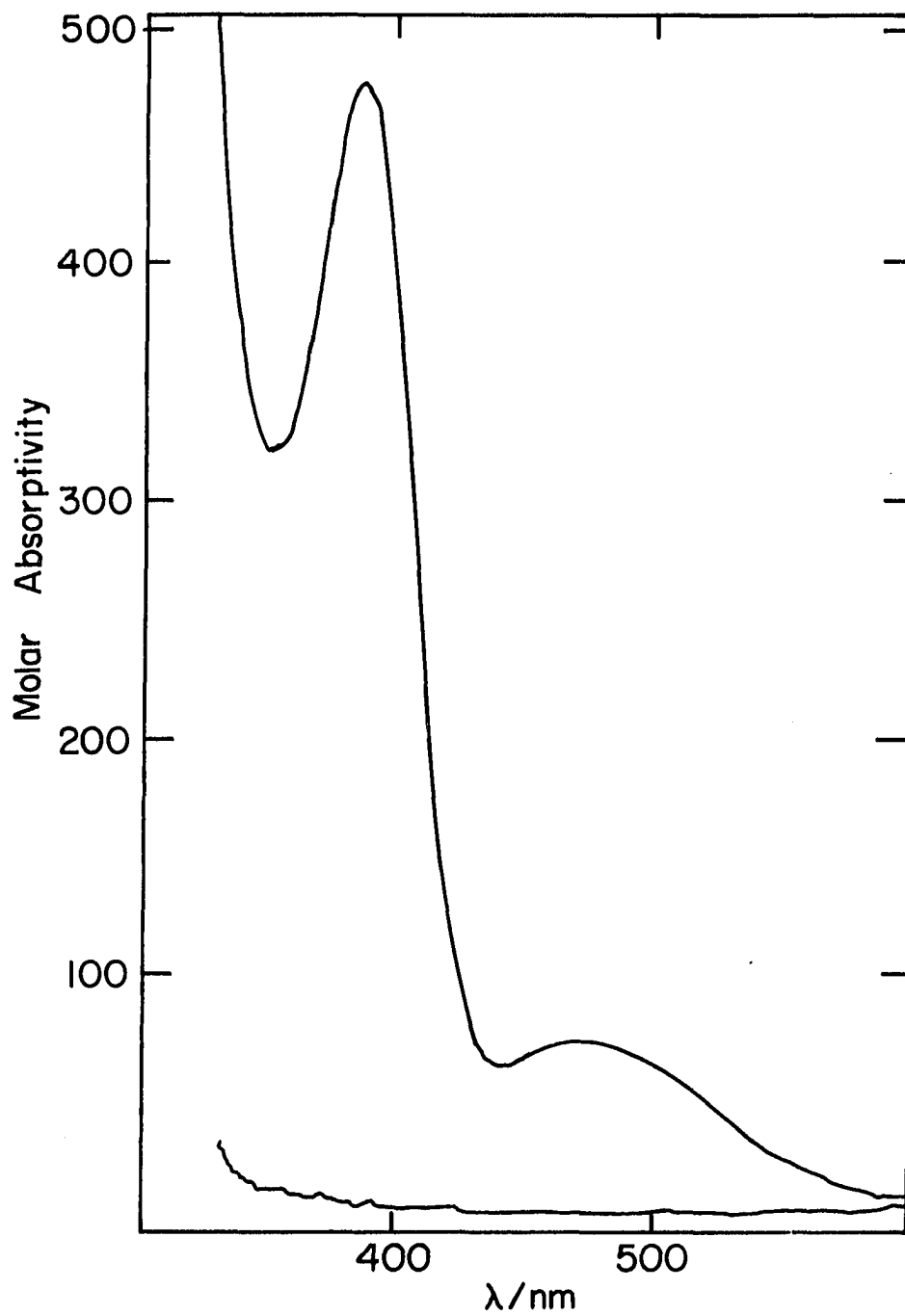


Figure I-11a. The electronic spectrum of $n\text{-butylCr(L)}^{2+}$ -non log scale

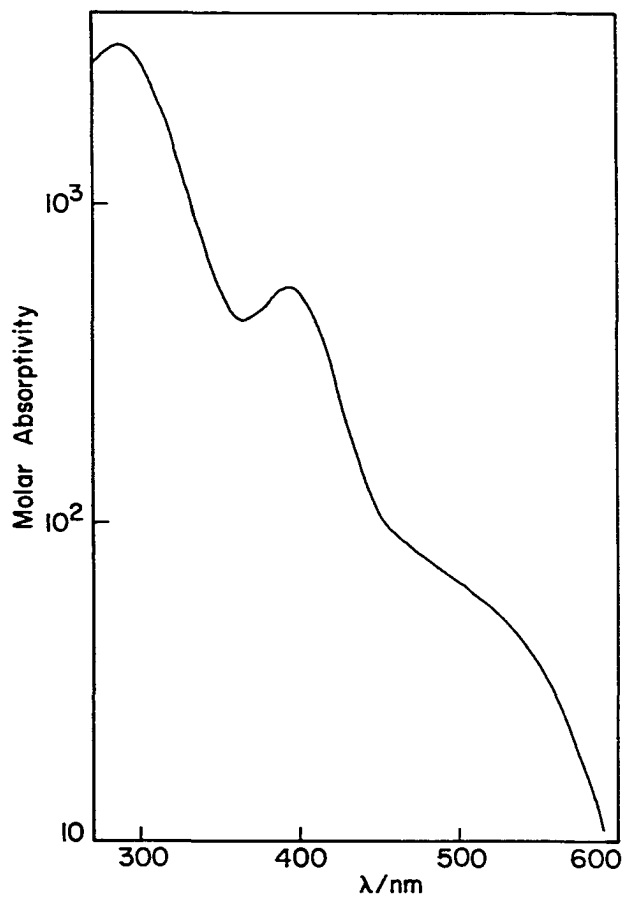


Figure I-12. The electronic spectrum of isopropylCr(L)²⁺

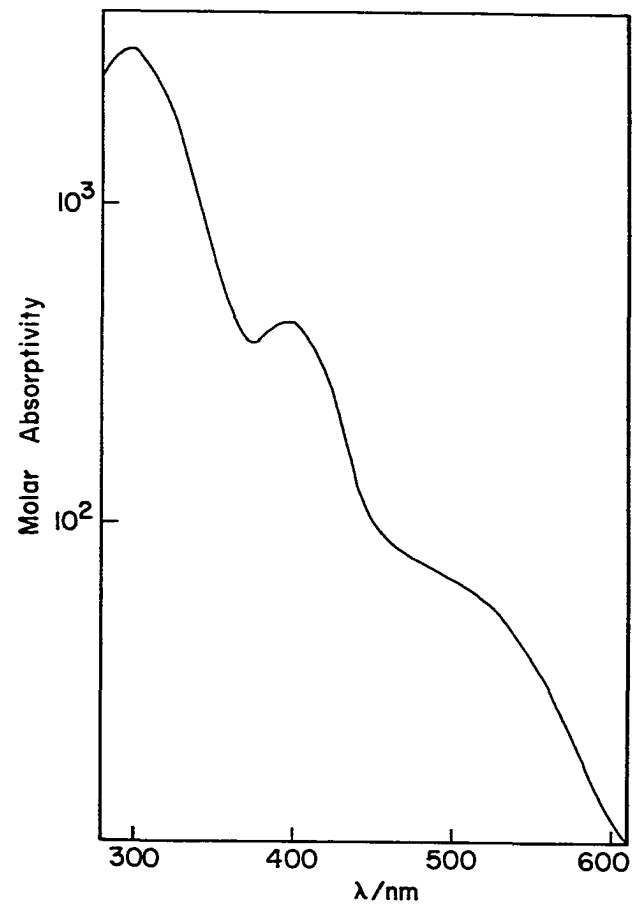


Figure I-13. The electronic spectrum of cyclohexylCr(L)²⁺

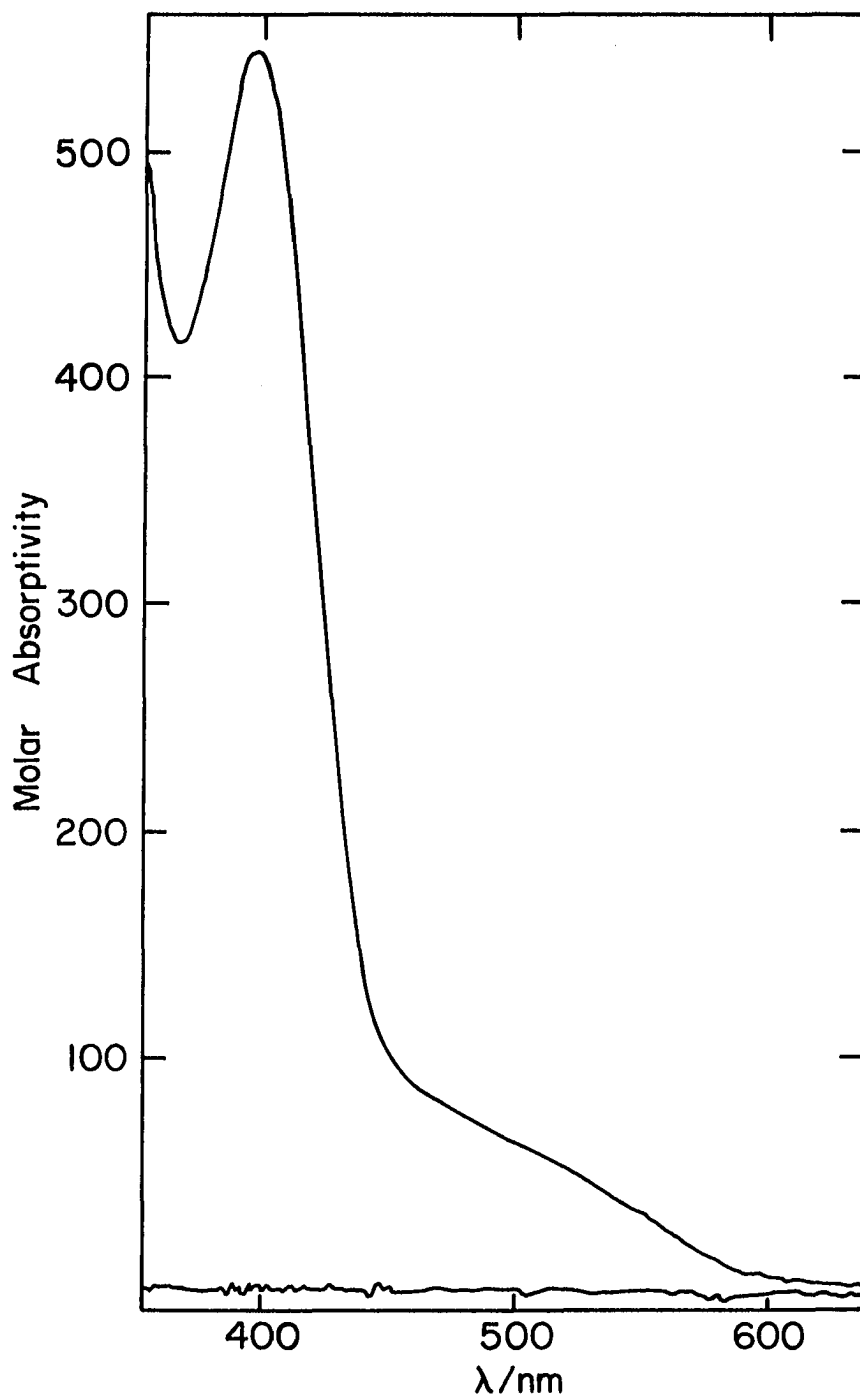


Figure I-12a. The electronic spectrum of isopropylCr(L)²⁺ - non log scale

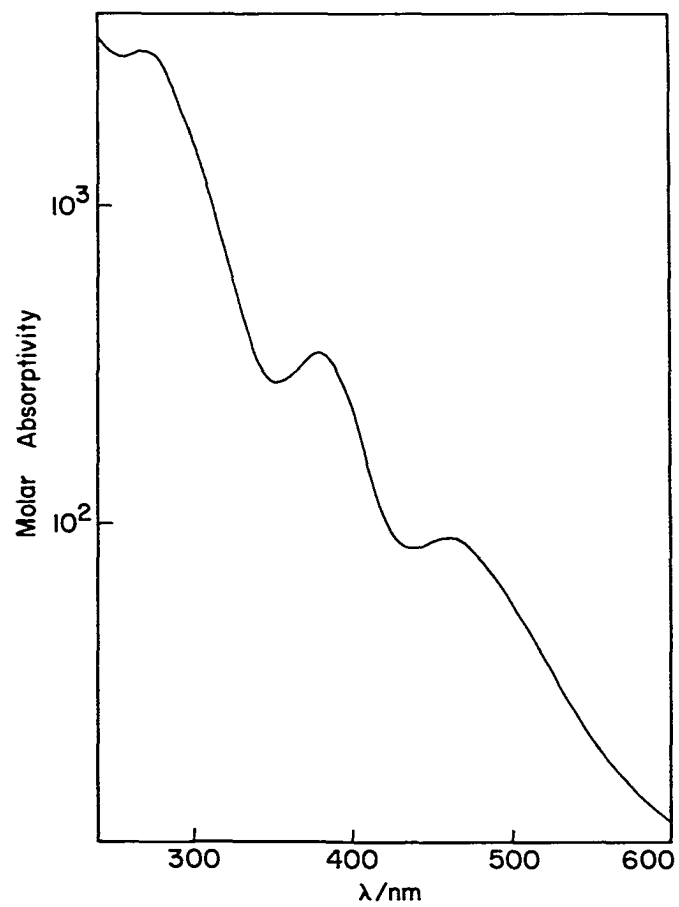


Figure I-14. The electronic spectrum of 1-adamantylCr(L)²⁺

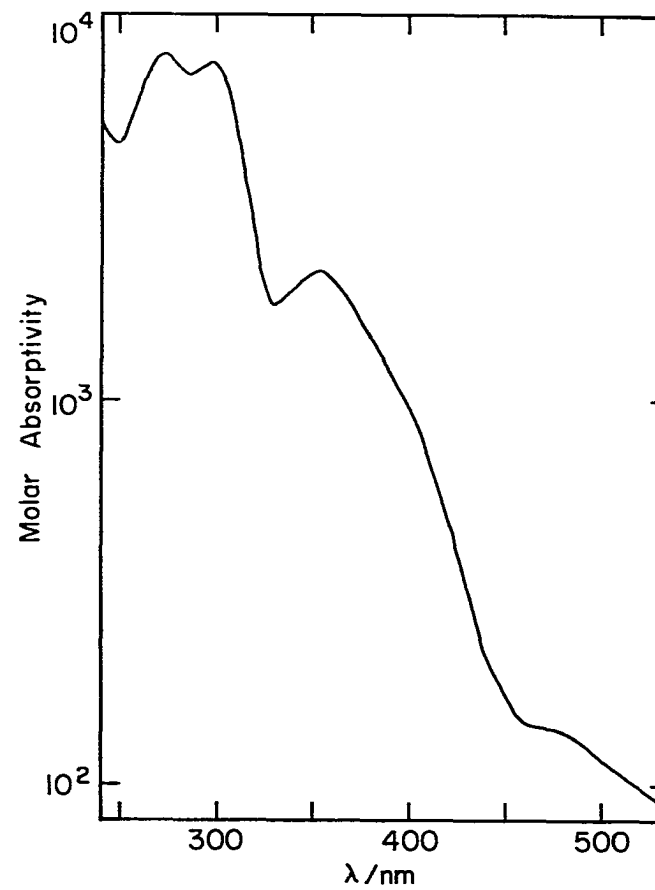


Figure I-15. The electronic spectrum of benzylCr(L)²⁺

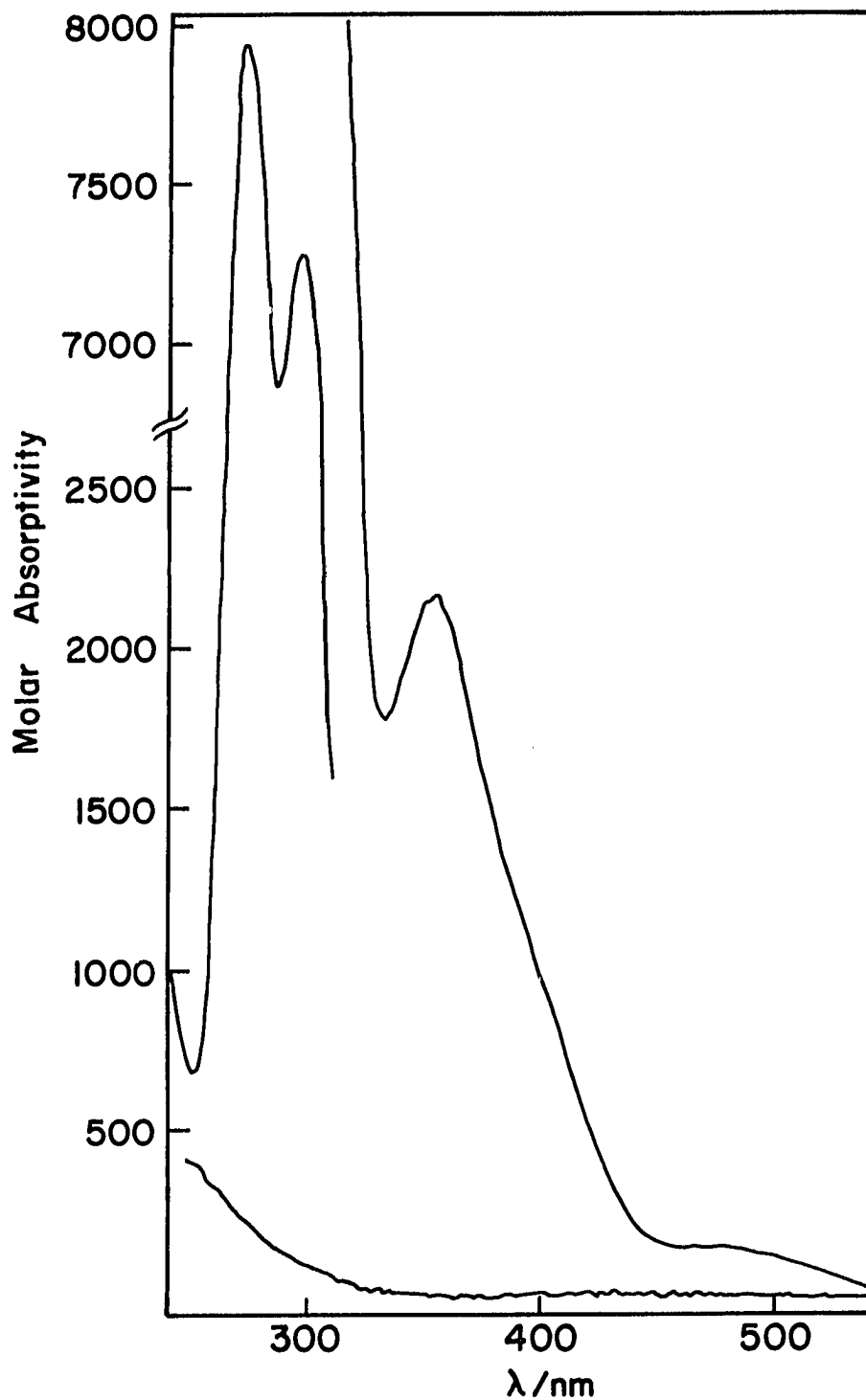


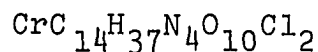
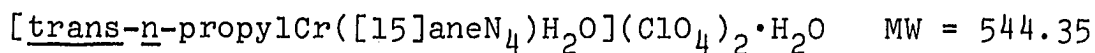
Figure I-15a. The electronic spectrum of benzylCr(L)²⁺. Note scale change, the break applies only to the maxima

Table I-5. Spectral parameters for various trans-RCr([15]aneN₄)²⁺ complexes^a

R	$\lambda_{\max}(\epsilon)$	$\lambda_{\max}(\epsilon)$	$\lambda_{\max}(\epsilon)$
Methyl	258(sh) (3300±200)	375 (227±10)	468 (68.7±3)
Ethyl	264 (3100±240)	383 (387±32)	467 (65.7±5.4)
<u>n</u> -Propyl	265 (3440±200)	383 (465±28)	468 (70.5±4.2)
<u>n</u> -Butyl	268 (3300±260)	383 (459±37)	468 (69.2±5.5)
Isopropyl	287 (3280±230)	396 (550±40)	510(sh) (68.9±4.8)
Cyclohexyl	298 (3070±45)	400 (422±6)	500(sh) (66.8±1)
Adamantyl	268 (3060±40)	383 (347±5)	463 (88±1)
Benzyl	273 (7920±166)	297 (7470±157)	353 (2170±46)

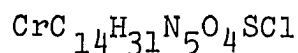
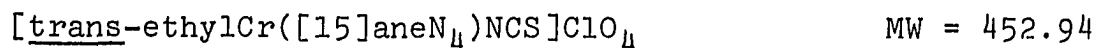
^aThese should not be regarded as absolute values but as lower limits due to possible decomposition.

which makes a meaningful elemental analysis difficult due to the presence of two of these anions. Yet, two species have been isolated as moderately stable crystalline solids. Their elemental analysis is now reported:



calc. C (30.89), H (6.85), N (10.29)

found. C (30.72), H (6.32), N (10.00)

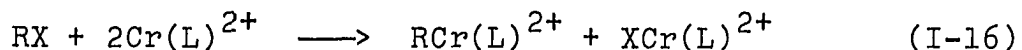
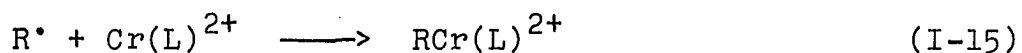
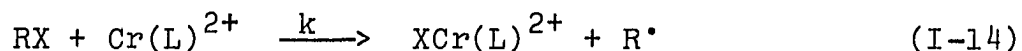


calc. C (37.12), N (6.90), N (15.46)

found. C (36.48), N (6.78), N (15.54)

Characterization of the Reaction of Organic Halides with $\text{Cr}([\text{15}]\text{aneN}_4)^{2+}$

The reaction of $\text{Cr}([\text{15}]\text{aneN}_4)^{2+}$ with organic halides is described in equations I-14 and I-15, respectively.



The characterization of the reaction products were discussed in the previous two sections.

Evidence for the stoichiometry of the reactions as written in equation I-16 comes from the spectrophotometric titration of the reaction of $\text{Cr}([\text{15}] \text{aneN}_4)^{2+}$ with benzyl bromide. Further proof for this one-to-two stoichiometry comes from a kinetic experiment.

The titration curve is shown in Figure I-16. The mole ratio of benzyl bromide to $\text{Cr}(\text{L})^{2+}$ is 0.54:1.0 indicating a 2:1 stoichiometry, 2 $\text{Cr}(\text{L})^{2+}$:1 RX.

This stoichiometry was confirmed by the value of the absolute second-order rate constants for the above reaction with respect to the excess reagent, either PhCH_2Br or $\text{Cr}([\text{15}] \text{aneN}_4)^{2+}$. The reaction rates are 1.91×10^4 and $9.74 \times 10^3 \text{ dm}^3 \text{ mol}^{-1} \text{ s}^{-1}$, respectively. This is consistent with equation I-16. Since the value of the second order rate constant is dependent upon the excess reagent which is related to each other as shown in the following expression:

$$-\frac{[\text{RX}]}{dt} = -\frac{1}{2} \frac{[\text{Cr}(\text{L})^{2+}]}{dt}$$

The factor of two appears in the rate measurements with the value of the rate constant being twice as large when halide is in excess, $2k$, than when $\text{Cr}([\text{15}] \text{aneN}_4)^{2+}$ is the excess reagent.

It is assumed that all other simple organic halides react in a similar manner. This excludes the reaction of geminal halides (i.e., BrCH_2Cl) which will be discussed next.

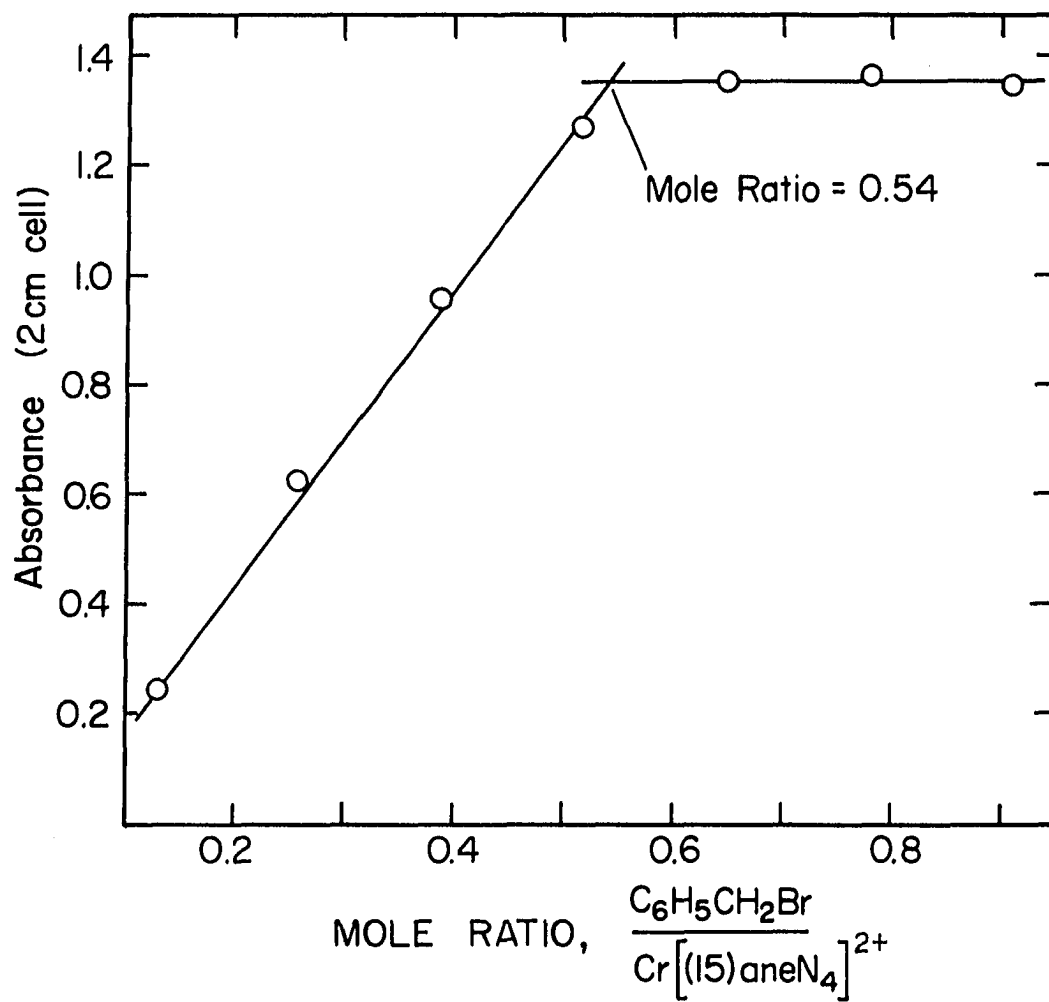


Figure I-16. Spectrophotometric titration of $\text{Cr}(\text{L})^{2+}$ by $\text{C}_6\text{H}_5\text{CH}_2\text{Br}$

Geminal Halides and their Reaction

with $\text{Cr}([\text{15}] \text{aneN}_4)^{2+}$

When $\text{Cr}([\text{15}] \text{aneN}_4)^{2+}$ reacts with geminal halides (i.e., BrCH_2Cl) and pseudo-halides (i.e., ClCH_2CN) no organochromium species result. This is in sharp contrast with $\text{Cr}_{(\text{aq})}^{2+}$, where the substituted methylpentaquo chromium(III) species are quite stable.

The inorganic products are the halo chromium (Br, Cl) and diaquo chromium species. This was determined by cation exchange chromatography of the reaction solutions and identification by their respective visible spectra.

The organic reaction products were determined for BrCCl_3 and BrCH_2Cl by mass spectrometry.

The reactions were carried out with the reaction vessel attached to the mass spectrometer so that all the volatile products could be sampled.

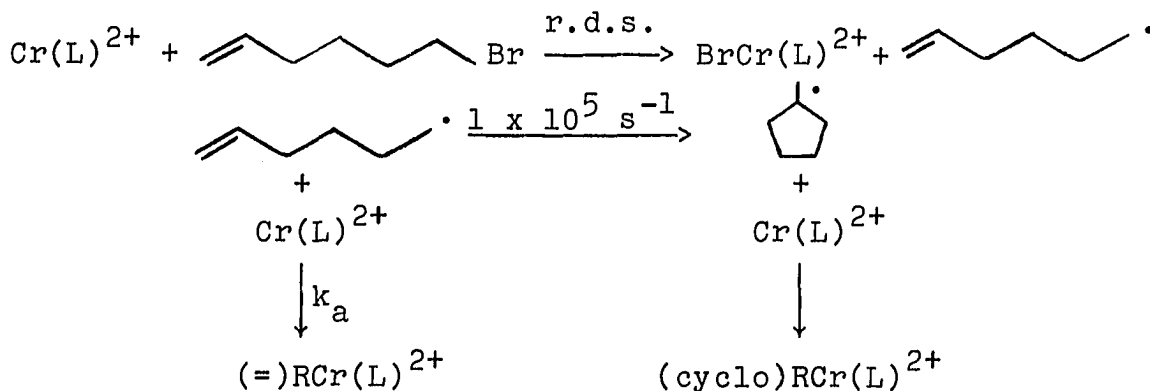
In the case of BrCCl_3 , both CO and CH_4 were present in the sample. CO_2 might be there also. The sources of their respective parent ions were confirmed by their appearance potentials (61). Due to a small air leak, a quantitative assignment of product ratios would be impossible for BrCCl_3 .

With BrCH_2Cl , different products were observed and their ratio determined. The products were CH_2CH_2 , CO_2 and

CH₄; their respective ratios are >1000:30:1. Ethylene was again confirmed by its appearance potential and the diminutive size of the oxygen peak confirmed that there was very little air in the system. Castro and Kray (62) have established that these reactions proceed by carbene or carbenoid intermediates which could form the observed products.

Radical Intermediates and the Rate of Radical Capture

In order to get definitive proof for the existence of free radical intermediates and determine their rate of capture by Cr([15]aneN₄)²⁺, several experiments were performed. 6-Bromo-1-hexene was reacted with Cr(L)²⁺ supposedly forming the 5-hexenyl radical as an intermediate. This radical is known to cyclize, rate = 1 x 10⁵ s⁻¹ (33), to the cyclopentylmethyl radical in accord with the following scheme.



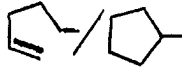
Then the identification of methylcyclopentane in the products establishes the existence and intermediacy of free radicals. Now if the reaction involves radical capture, one can measure this rate in the above system by a competition-type experiment by determining the relative amounts of olefinic to alkyl organochromium products. Since it would be quite difficult to do this, the organochromium compounds were decomposed by base to yield the respective hydrocarbons which were then measured by gas chromatography. The ratio of hydrocarbons found were used in the following expression:

$$k_a = 1 \times 10^5 \text{ s}^{-1} \left[\frac{\text{Cyclopentene}}{\text{Methylcyclopentane}} \right] / [\text{Cr(L)}^{2+}]$$

This may be derived from the rate of formation of uncyclized organochromium species substituting in the equivalent value for the concentration of olefinic radical. One then assumes that the radicals captured represent the actual hydrocarbons. With rearrangement, the above expression results yielding k_a the rate of radical capture by $\text{Cr}([\text{15}] \text{aneN}_4)^{2+}$.

The identity of the respective hydrocarbons was confirmed by the retention times when compared to authentic samples. The ratio of products was determined by the peak area. The detector (F.I.) was calibrated using a 1:1 sample of the two hydrocarbons and the detector response was essentially the same for both. The data used to compute the

values of the rate of radical capture, $k_a = 9.1 \pm 2 \times 10^6$ $\text{dm}^3 \text{mol}^{-1} \text{s}^{-1}$, are shown below:

$[\text{Cr}(\text{L})^{2+}]_{\text{ave}}$	[5-hexenyl bromide]		$10^{-6} k_a$ ($\text{dm}^3 \text{mol}^{-1} \text{s}^{-1}$)
0.0221	0.00287	1.60	7.2
0.0446	0.00448	4.88	10.9

Kinetics

Spectra of solutions of $\text{Cr}([\text{15}] \text{aneN}_4)^{2+}$ mixed with various organic halides were run to decide the best wavelength to use for kinetic experiments. Ethyl iodide was chosen for the initial gathering of kinetic data because the reaction appeared to proceed at a rate amenable to conventional spectroscopic methods of analysis and that $\text{Cr}_{(\text{aq})}^{2+}$ is known not to react with simple halides. The kinetic runs were done under pseudo-first-order conditions, $[\text{RI}] \geq 10[\text{Cr}(\text{L})^{2+}]$. The resulting first order plots were quite linear confirming the first order dependence of the reaction on the limiting reagent, $\text{Cr}([\text{15}] \text{aneN}_4)^{2+}$. In the cases where the ethyl iodide concentration was varied the value of $k_{\text{obs}}/[\text{Et-I}]$ (k_{obs} being the pseudo-first-order rate constant) was constant, confirming the first order dependence on $[\text{Et-I}]$. The run done with ethyl bromide was

again linear when plotted in a pseudo-first-order manner but the rate constant was approximately three times slower. The reaction of isopropyl iodide was too fast to catch more than the last part of it. These reactions were indicative of a dependence upon the identity of the halide, Br or I, and the nature of the organic group, primary or secondary.

To check on the sensitivity of the reaction rate upon the solvent composition, the following experiments were performed. The rate of reaction of ethyl iodide with $\text{Cr}([\text{15}] \text{aneN}_4)^{2+}$ was determined at slightly different mixed solvent ratios. In t-butanol:water 54:46 by volume, the rate was $0.363 \pm 0.02 \text{ dm}^3 \text{ mol}^{-1} \text{ s}^{-1}$ and in 56:44 by volume water:t-butanol, the rate was $0.432 \pm 0.015 \text{ dm}^3 \text{ mol}^{-1} \text{ s}^{-1}$. Both are the average of three runs at the identical ethyl iodide concentration. This indicated that the solvent would have to be made with care and handled in such a way as to prevent loss of t-butanol.

Up until this time, all the reactions were performed with the Cr^{2+} being generated by Zn/Hg reduction of solutions of $\text{Cr}_{(\text{aq})}^{3+}$. It was found that under identical conditions, except for the source of $\text{Cr}_{(\text{aq})}^{2+}$, larger absorbance changes were obtained using Cr^{2+} prepared from $\text{CrCl}_2 \cdot 4\text{H}_2\text{O}$. Acid concentrations greater than $\sim 5 \times 10^{-4} \text{ M}$ also appeared to decompose the $\text{Cr}([\text{15}] \text{aneN}_4)^{2+}$. With these observations, acid- and zinc-free solutions of

$\text{Cr}_{(\text{solvent})}^{2+}$ were used for all further work. There was no change in the observed rate constants with the source of Cr(L)^{2+} . At this point, it was also decided to set the solvents ionic strength. This was arbitrarily chosen to be $\mu = 0.20$, maintained by LiClO_4 . Again, the rate constants for the reaction of ethyl iodide showed no substantive effect upon increasing the ionic strength as required for a reaction between the charged, $\text{Cr}([\text{15}] \text{aneN}_4)^{2+}$, and an uncharged species, the organic halide.

Following the preliminary results, a systematic kinetic study of the reaction of $\text{Cr}([\text{15}] \text{aneN}_4)^{2+}$ with a wide range of organic halides was instituted.

Pseudo-first-order conditions, usually with $[\text{RX}] \geq 10[\text{Cr(L)}^{2+}]$, but always a greater than 10-fold stoichiometric excess were used in all cases except those already mentioned with benzyl bromide. The standard method was used to calculate the k_{obs} for all runs with $\tau_{1/2} \geq 5$ sec. For all the faster reactions, k_{obs} was provided by computer interface. These values were spot checked using the standard approach. The linearity of all first order plots confirmed the first-order dependence on $[\text{Cr}([\text{15}] \text{aneN}_4)^{2+}]$, Figures I-17 and I-18. The results of the experiments are shown in Tables I-6 and I-7.

The second-order rate constants, k_{RX} , were determined from the slope of plots of k_{obs} vs $[\text{RX}]$. The reactions are

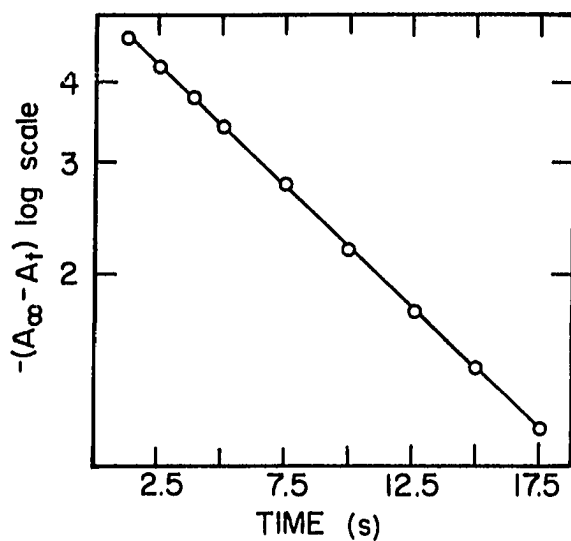


Figure I-17. A standard method plot for the reaction of isopropylbromide with Cr(L)^{2+}

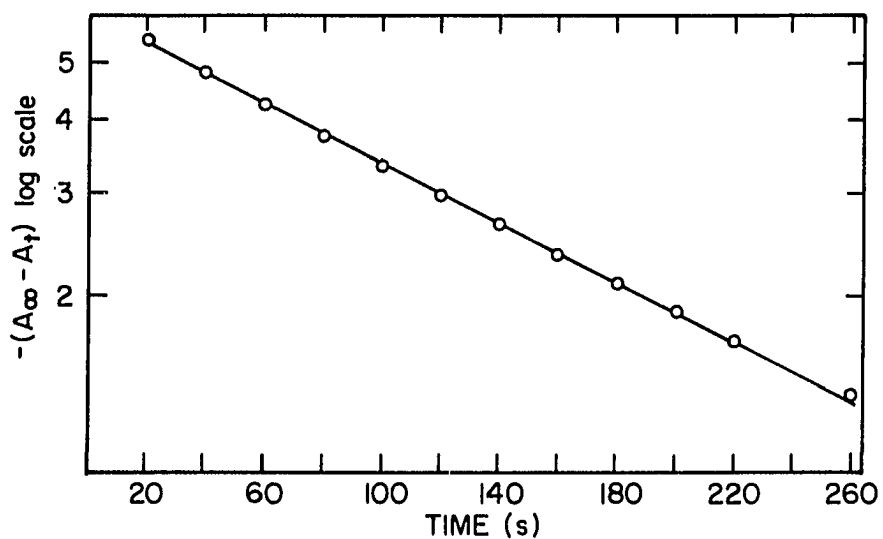


Figure I-18. A standard method plot for the reaction of n-butylbromide with Cr(L)^{2+}

Table I-6. Kinetic data for the reactions of $\text{Cr}([\text{15}] \text{aneN}_4)^{2+}$ with organic mono-halides. Conditions 1:1 v/v t-butanol/water, $\mu = 0.20 \text{ M} (\text{Li}^+)$, $T = 25^\circ$

RX	$10^3[\text{Cr}(\text{L})^{2+}]$	$10^2[\text{RX}]$	λ/nm	$k_{\text{RX}} \text{ dm}^3 \text{ mol}^{-1} \text{ s}^{-1} \pm \delta$	Comment
Methyl-I	2.60	11.68	370	0.0474	
	2.60	11.68	370	0.0447	
Ethyl-Br	2.60	7.29	390	0.169	
	2.60	7.29	390	0.179	
	2.60	7.38	390	0.150	
	2.60	7.38	390	0.156	
	2.60	7.38	390	0.169	
	3.97	7.38	390	0.161	
	3.97	7.38	390	0.195	
	1.28	7.63	390	0.140	
	1.28	7.63	390	0.147	
	2.60	12.10	390	0.168	
	2.60	12.10	390	0.174	
	Ethyl-I	2.60	2.30	390	0.409
2.60		2.30	390	0.414	
2.60		2.30	390	0.447	
2.60		6.88	390	0.446	
2.60		6.88	390	0.423	
2.60		10.89	390	0.379	
2.60		10.89	390	0.390	
2.60		10.89	390	0.399	
2.60		6.80	390	0.432	
2.60		6.80	390	0.404	
2.60		6.80	390	0.399	
2.60		6.80	390	0.411	
2.60		6.80	390	0.414	

Table I-6. (Continued)

RX	$10^3[\text{Cr(L)}^{2+}]$	$10^2[\text{RX}]$	λ/nm	k_{RX}	$\text{dm}^3 \text{ mol}^{-1} \text{ s}^{-1} \pm \delta$	Comment
<u>n</u> -Propyl-Br	2.60	2.02	390		0.174	
	2.60	2.04	390		0.172	
	2.60	6.03	390		0.166	
	2.60	6.03	390		0.184	
	2.60	6.03	390		0.150	
	2.60	10.01	390		0.161	
	2.60	10.01	390		0.174	
<u>n</u> -Butyl-Br	2.80	1.71	390		0.150	
	2.80	2.90	390		0.148	
	2.80	4.27	390		0.138	
	2.80	5.96	390		0.127	
	2.80	6.80	390		0.128	
	2.80	7.64	390		0.142	
	2.80	8.49	390		0.134	
Neopentyl-Br	2.60	2.30	390		0.122	
	2.60	3.08	390		0.153	
	2.60	3.83	390		0.124	
	2.60	5.37	390		0.102	
	2.60	6.89	390		0.086	
	2.60	7.62	390		0.089	
	2.60	9.88	390		0.088	
5-Hexenyl-Br	2.40	2.50	390		0.153	
	2.40	3.78	390		0.156	
	2.40	4.42	390		0.162	
	2.40	6.32	390		0.154	

Table I-6. (Continued)

RX	$10^3[\text{Cr(L)}^{2+}]$	$10^2[\text{RX}]$	λ/nm	k_{RX}	$\text{dm}^3 \text{ mol}^{-1} \text{ s}^{-1 \pm \delta}$	Comment
Cyclohexyl-Br	2.60	1.43	390		0.853	After two distillations
	2.60	1.83	390		0.886	
	2.60	2.92	390		0.771	
	2.60	3.73	390		0.824	
	2.60	4.40	390		0.823	
	2.60	5.18	390		0.859	
<u>t</u> -Butyl-Br	2.30	4.46	390		6.6	Done in 85% THF
	2.30	6.78	390		6.1	
1-Adamantyl-Br	2.30	3.63	380		19.4 ± 0.5	4 runs. Done in 99% MeOH
Isopropyl-Br	2.60	1.95	390		2.03	
	2.60	1.95	390		1.96	
	2.60	4.80	390		1.85	
	2.60	4.80	390		2.02	
	2.60	4.80	390		1.88	
	2.60	6.80	390		1.95	
	2.60	6.80	390		1.97	
	2.60	6.80	390		1.82	
	2.60	7.76	390		1.88	
	2.60	7.76	390		1.71	
	Isopropyl-I	2.30	5.00	390		
2.30		5.00	390		4.90	
Cyclopentyl-Br	2.30	1.95	390		5.12	2 runs
	2.30	4.75	390		4.68 ± 0.01	
	2.30	9.45	390		4.59	

Table I-6. (Continued)

RX	$10^3[\text{Cr(L)}^{2+}]$	$10^2[\text{RX}]$	λ/nm	$k_{\text{RX}} \text{ dm}^3 \text{ mol}^{-1} \text{ s}^{-1} \pm \delta$	Comment
Benzyl-Cl	0.22	0.130	280	3.59×10^2	
	0.22	0.205	280	$3.54 \pm 0.03 \times 10^2$	3 runs
	0.22	0.304	280	$3.21 \pm 0.03 \times 10^2$	2 runs
	0.22	0.569	280	$3.24 \pm 0.02 \times 10^2$	2 runs
	0.22	0.869	280	$3.32 \pm 0.02 \times 10^2$	
Benzyl-Br	3.16	0.017	300	$1.03 \pm 0.04 \times 10^4$	4 runs
					The first 2 sets of determinations are used to determine the reaction stoichiometry kinetically
	1.67	0.017	300	$0.92 \pm 0.03 \times 10^4$	4 runs
	0.11	0.042	280	$1.98 \pm 0.20 \times 10^4$	4 runs
	0.11	0.127	280	$1.60 \pm 0.14 \times 10^4$	6 runs
	0.11	0.212	280	$2.04 \pm 0.16 \times 10^4$	6 runs
	0.11	0.294	280	$1.94 \pm 0.14 \times 10^6$	7 runs
	0.11	0.356	280	$1.93 \pm 0.08 \times 10^4$	6 runs

Table I-7. Summary of the kinetic data for the reactions of $\text{Cr}([\text{15}] \text{aneN}_4)^{2+}$ with geminal dihalides and pseudo halide. Conditions: Solvent 1:1 v/v t-butanol/water, $\mu = 0.20 \text{ M}$, $T = 25^\circ$

RXY	[RXY]/M	$\text{Co(L)}^{2+}/\text{M}$	λ/nm	$k_{\text{RXY}}/\text{dm}^3\text{mol}^{-1}\text{s}^{-1} \pm \delta^a$	(#) ^b	Comment
BrCH_2Cl	$3.69\text{--}10.7 \times 10^{-3}$	2.6×10^{-3}	390	42.4 ± 3	16	linear
ClCH_2CN	$1.58\text{--}11.06 \times 10^{-3}$	2.2×10^{-3}	390	314 ± 8	21	linear
BrCHClCH_3	$2.79\text{--}5.81 \times 10^{-3}$	2.6×10^{-3}	390	~ 500	25	curved k_{obs} vs [RXY] plot

^a δ is the average deviation.

^b(#) is the number of runs performed.

shown to be first-order in RX by the linear dependence of k_{obs} on increasing [RX] with a zero intercept. Two are shown in Figures I-19 and I-20. Several halides had non zero intercepts, RX = neopentyl, cyclopentyl and t-butyl bromide, this intercept was lowered and slope increased in all cases by repeated distillation of the halides. It only took two distillations to clean up cyclohexyl bromide, Figure I-19. Purification attempts were stopped after three distillations. It is assumed that these would be well-behaved if they could be sufficiently purified. It is believed that those reactions in which only a few runs were done are also first order in [RX]. These observations confirm the following rate expression:

$$[\text{RCr(L)}^{2+}]/\text{dt} = k[\text{RX}][\text{Cr(L)}^{2+}]$$

The reaction kinetics for t-butyl bromide and 1-adamantyl bromide could not be studied in the same solvent as all the other reactions. Both solvents, 85% THF/H₂O and 99% MeOH/H₂O, respectively, were shown to be innocent by the formation and identification of CH₃Cr(L)²⁺ from CH₃I in these solvents. The solvent choices were made to prevent hydrolysis and for solubility, respectively.

1-Adamantyl and t-butyl bromide displayed a noticeable second stage of reaction. The decrease in absorbance was much greater for t-butyl bromide than 1-adamantyl bromide. This is most easily attributed to the decomposition of the

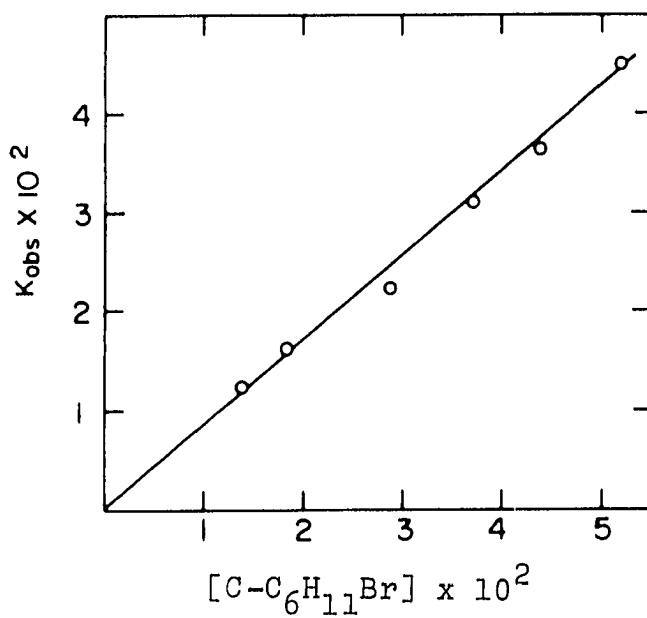


Figure I-19. Plot of k_{obs} vs $[c-C_6H_{11}Br]$

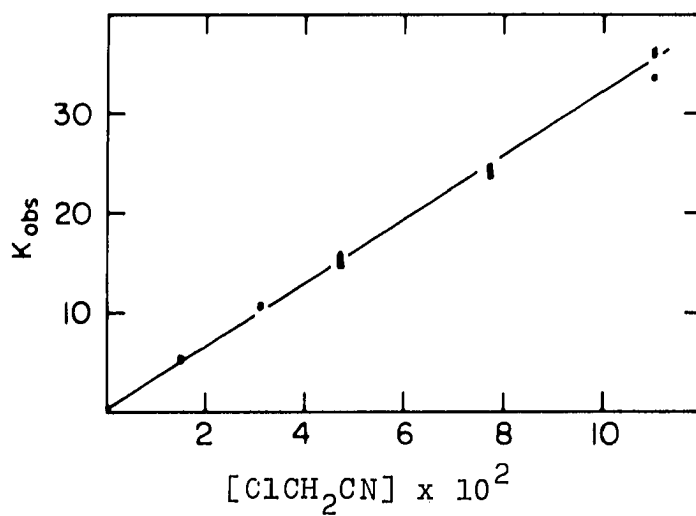


Figure I-20. Plot of k_{obs} vs $[ClCH_2CN]$

organochromium product. Other halides, RX = isopropyl, neopentyl, cyclohexyl and cyclopentyl bromide and methyl iodide showed a slow second stage of reaction, a decrease in absorbance. In the case of the methyl iodide reaction, the second stage is accounted for by the aquation of ICr(L)^{2+} with the rest of the reactions due to decomposition of the respective organochromium compounds.

Activation Parameters

The reaction rates of ethyl bromide, ethyl iodide and benzyl chloride with $\text{Cr}([\text{15}] \text{aneN}_4)^{2+}$ were determined as a function of temperature to determine activation parameters. The values of ΔH^\ddagger and ΔS^\ddagger for these reactions were calculated using the Eyring relationship,

$$\ln \frac{k}{T} = \ln \frac{R}{Nh} + \frac{\Delta S^\ddagger}{R} - \frac{\Delta H^\ddagger}{RT} \quad (\text{I-17})$$

where R is the gas constant, h is Planck's constant, and N is Avogadro's number. The values were determined by using a program which computes the slope of a plot of $\ln k/T$ vs $1/T$ by the process of least squares.

The Eyring plots for the three reactions are shown in Figures I-21, 22 and 23. The experimental points used in these calculations are found in Tables I-8, 9 and 10. For the reaction of ethyl bromide with $\text{Cr}([\text{15}] \text{aneN}_4)^{2+}$, ΔH^\ddagger and ΔS^\ddagger are $44.21 \pm 1.1 \text{ KJ mol}^{-1}$ and $-111.8 \pm 3.5 \text{ J mol}^{-1} \text{ K}^{-1}$,

Table I-8. Temperature dependence of the reaction rate of EtBr with $\text{Cr}([\text{15}] \text{aneN}_4)^{2+}$

Temp °C	[RX]	$k_2 \text{ dm}^3 \text{ mol}^{-1} \text{ s}^{-1}$
11	0.0734	0.0685
	---	0.0640
	0.1218	0.0653
18	0.0734	0.0954
	0.1218	0.0954
25	---	0.164 (ave)
35	0.0734	0.310
	---	0.295
	0.1205	0.295

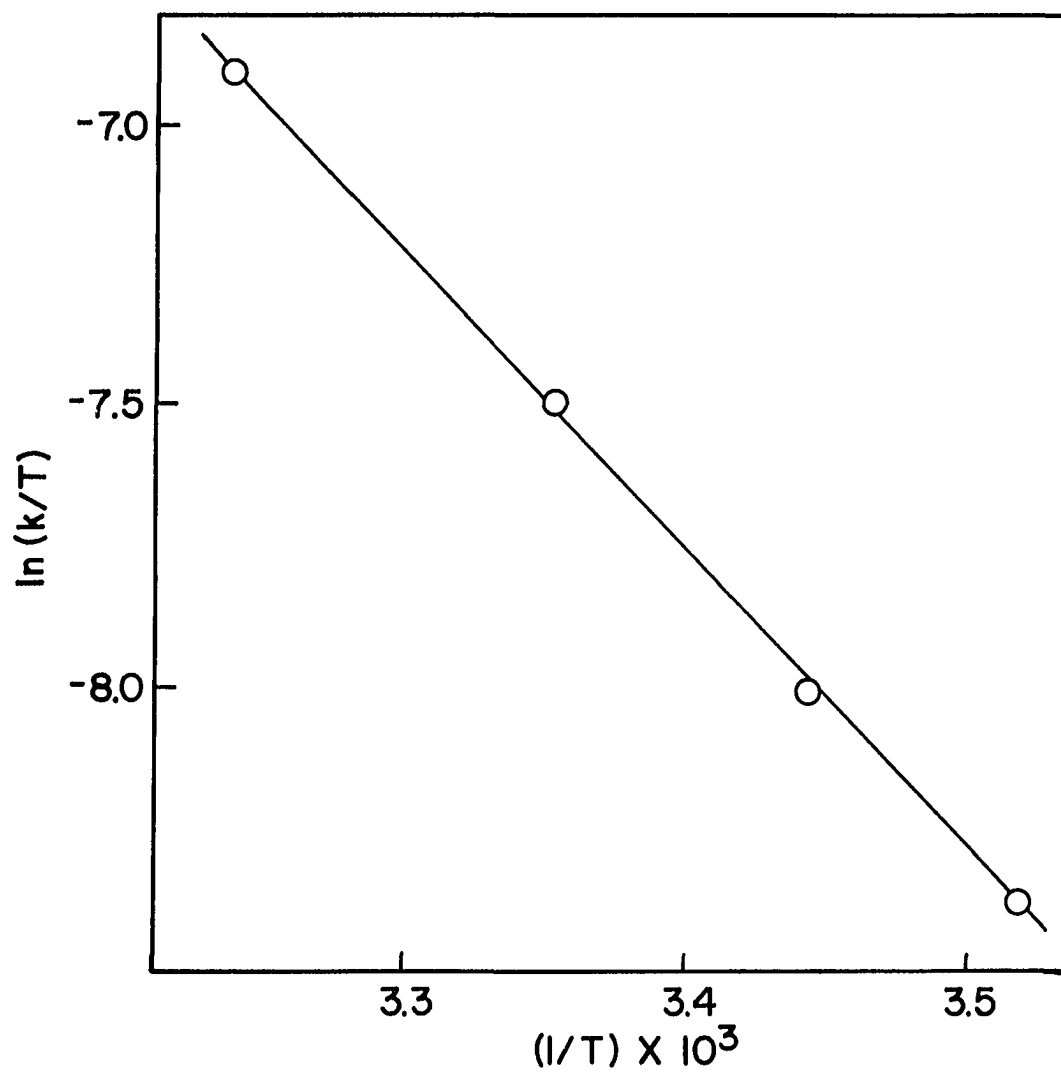


Figure I-21. Eyring plot for the reaction of EtBr with Cr(L)^{2+}

Table I-9. Temperature dependence of the reaction rate of EtI with Cr([15]aneN₄)²⁺

Temp °C	[RX]	k_2 dm ³ mol ⁻¹ s ⁻¹
11	0.0684	0.154
	---	0.159
18	0.0684	0.252
	0.1136	0.254
25	---	0.414 (ave)
35	0.0684	0.691
	0.1136	0.696
	---	0.697

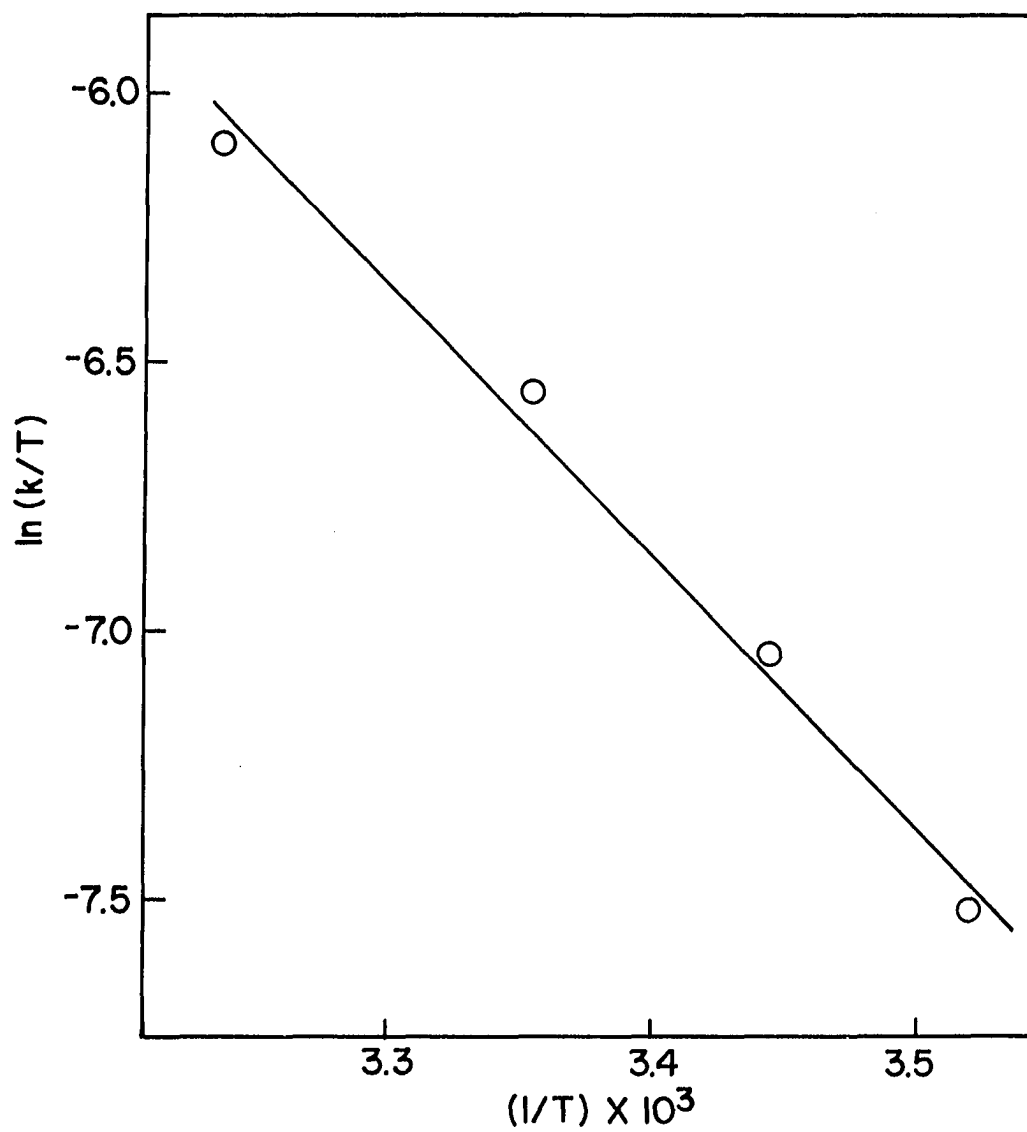


Figure I-22. Eyring plot for the reaction of EtI with Cr(L)^{2+}

Table I-10. Temperature dependence of the reaction rate of PhCH₂Cl with Cr([15]aneN₄)²⁺

Temp °C	[RX]	k ₂ dm ³ mol ⁻¹ s ⁻¹
18.5	4.24 x 10 ⁻³	245.0
	---	235.1
	---	246.9
25	---	323 (ave)
27.4	---	383.9
30.3	---	411.8
	---	410.0

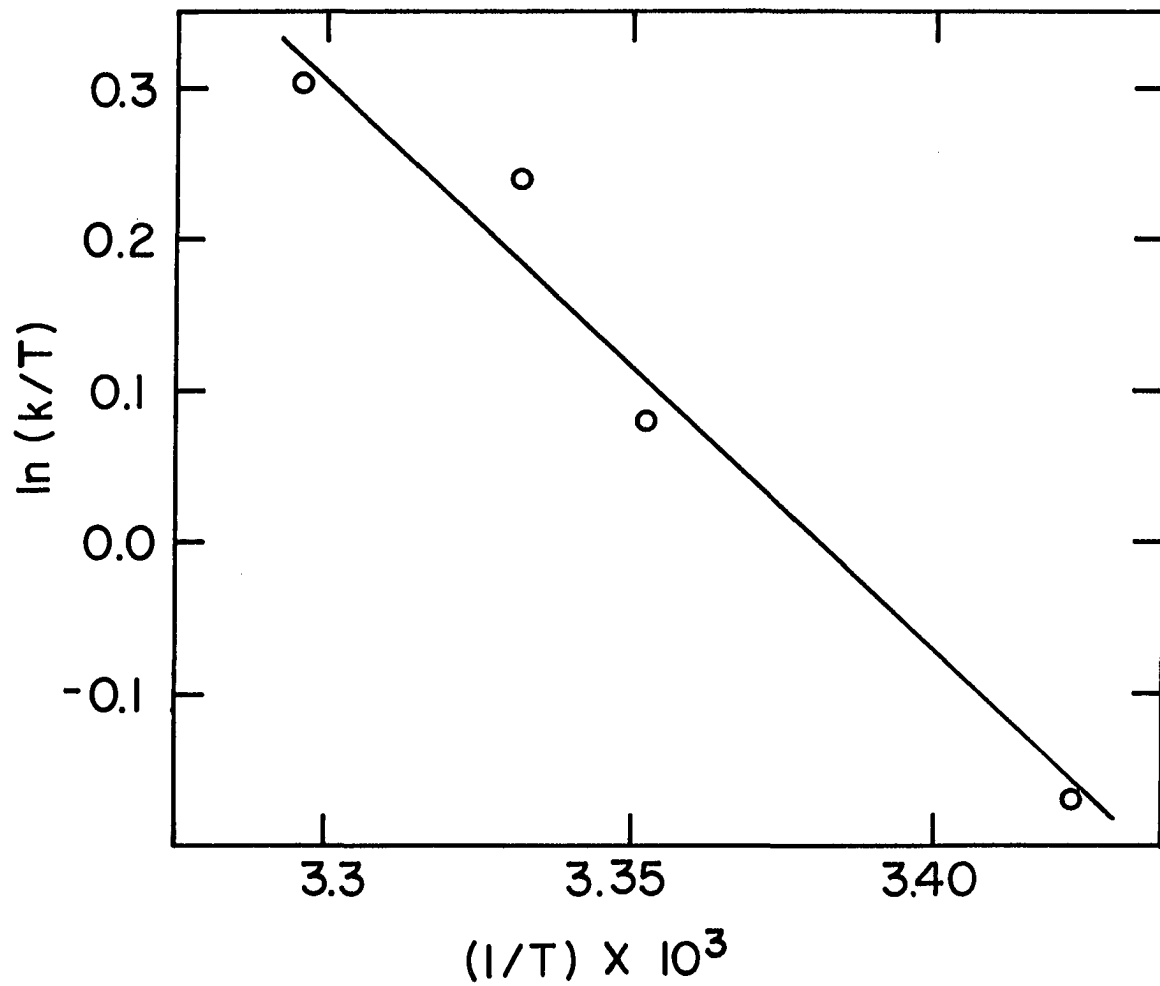


Figure I-23. Eyring plot for the reaction of $\text{C}_6\text{H}_5\text{CH}_2\text{Cl}$ with $\text{Cr}(\text{L})^{2+}$

respectively; for ethyl iodide with $\text{Cr}([\text{15}] \text{aneN}_4)^{2+}$, ΔH^\ddagger and ΔS^\ddagger are $44.1 \pm 1.3 \text{ kJ mol}^{-1}$ and $-104.4 \pm 4.3 \text{ J mol}^{-1} \text{ K}^{-1}$, respectively; for benzyl chloride with $\text{Cr}([\text{15}] \text{aneN}_4)^{2+}$, ΔH^\ddagger and ΔS^\ddagger are $30.6 \pm 1.6 \text{ kJ mol}^{-1}$ and $-94.1 \pm 5.2 \text{ J mol}^{-1} \text{ K}^{-1}$, respectively. These data will be commented upon in a later section.

DISCUSSION

As described previously, the ratio of $\text{Cr}([\text{15}] \text{aneN}_4)^{2+}$ to benzyl bromide consumed was determined by spectrophotometric titration. This value is 1.85:1.00 (Figure I-16). The result confirms the consumption of 2 moles of $\text{Cr}(\text{L})^{2+}$ to one mole of RX.

This ratio was also substantiated by the variation of the rate constant determined as a function of excess reagent, $k_{\text{obs}}/[\text{excess reagent}]$. When benzyl bromide is in pseudo-first-order excess, the average value of the rate constant is $1.91 \times 10^4 \text{ dm}^3 \text{ mol}^{-1} \text{ s}^{-1}$, whereas with $\text{Cr}(\text{L})^{2+}$ in excess the value is $0.97 \times 10^4 \text{ dm}^3 \text{ mol}^{-1} \text{ s}^{-1}$. The 2:1 ratio of rates confirms the 2:1 stoichiometry or the consumption of 2 equivalents of $\text{Cr}(\text{L})^{2+}$ per equivalent of RX.

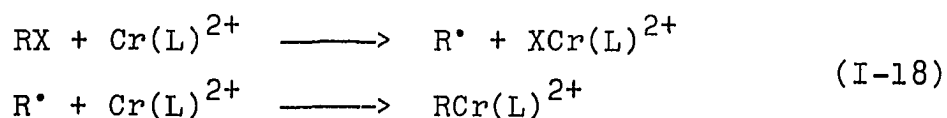
This 2:1 ratio of reduced metal to halide has been observed before in the reactions of $\text{Co}(\text{CN})_5^{3-}$ with RX (39), bis(dioximato)cobalt(II) complexes with a variety of benzylic halides (43a) and more significantly in the reduction of alkyl halides with a " $\text{Cr}(\text{en})_n$ " reagent (31). The geminal halides (i.e., BrCH_2Cl) do not follow this stoichiometry and they will be discussed separately.

The products of the reaction of monohalides with $\text{Cr}([\text{15}] \text{aneN}_4)^{2+}$ consist of a mixture of the halo- $\text{Cr}(\text{L})^{2+}$ and $\text{RCr}(\text{L})^{2+}$ species. Their respective spectral parameters

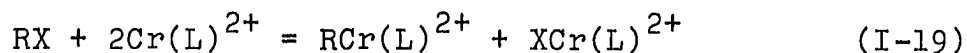
may be found in Tables I-4 and I-5. The geminal halides (pseudohalides) yield only inorganic chromium products, the respective halo and the diaquochromium($[15]aneN_4$)³⁺ complexes.

The kinetics of reaction for all the organic halides, except 1-bromo, 1-chloroethane, exhibit simple second order kinetics, first order in each reactant. The reactions of t-butyl, neopentyl, 1-adamantyl, cycloalkyl, isopropyl and methyl halides exhibit a slow second stage of reaction, slow when compared to the first phase of reaction. In the case of the first five species, this is ascribed to the decomposition of the organochromium compound. With methyl iodide, this second stage of reaction is most likely associated with the aquation of $ICr(L)^{2+}$.

Since the stoichiometry of the reaction is not reflected in the reaction order of the reagents but appears in the kinetics, implies that a slow step of reaction, the rate determining step is followed by a rapid step which consumes the second equivalent of $Cr([15]aneN_4)^{2+}$. The reactions of $Cr([15]aneN_4)^{2+}$ with organic halides are most readily explained by a simple free-radical mechanism (eq. I-18), in which the rate determining step involves halogen atom abstraction by $Cr(L)^{2+}$.



When these reaction steps are combined, the overall reaction is



The rate law which defines the mechanism results in equation I-20:

$$d\frac{[\text{RCr}(\text{L})^{2+}]}{dt} = k_{\text{RX}}[\text{Cr}(\text{L})^{2+}][\text{RX}] \quad (\text{I-20})$$

Since under the conditions of most of the rate measurements, the concentration of the organic halide was usually in a greater than 10-fold excess, the observed kinetics were pseudo-first-order, i.e.,

$$d\frac{[\text{RCr}(\text{L})^{2+}]}{dt} = k_{\text{obs}} = k_{\text{RX}}[\text{RX}]$$

The values of the reported rate constants, k_{RX} , were determined from the slope of a plot of k_{obs} vs $[\text{RX}]$ or in the instance where only a narrow concentration range was used, by the quotient of $k_{\text{obs}}/[\text{RX}]$. These values are summarized in Table I-11.

There is only one other system where accurate rate constants are available for the reaction of RX with a reduced metal system. This is the reduction of organic halides by $\text{Co}(\text{CN})_5^{3-}$. A comparison of reaction rates are listed in Table I-12. Kochi's work with " $\text{Cr}(\text{en})_n$ " provided only relative rates of reaction. With the actual rates of

Table I-11. Summary of the kinetic data for the reactions of $\text{Cr}([\text{15}] \text{aneN}_4)^{2+}$ with organic monohalides. Conditions: Solvent 1:1 v/v *t*-butanol/water, $\mu = 0.20 \text{ M}$, $T = 25.0^\circ$

RX	[RX]/M	$\text{Cr(L)}^{2+}/\text{M}$	λ/nm	$k_{\text{RX}}/\text{dm}^3 \text{ mol}^{-1} \text{ s}^{-1} \pm \delta$	(#) ^a	Comment
Methyl-I	1.17×10^{-1}	2.6×10^{-3}	375	$4.6 \pm 0.2 \times 10^{-2}$	2	Interference by aquation of $\text{ICr(L)H}_2\text{O}^{2+}$
Ethyl-Br	$7.29\text{--}12.1 \times 10^{-2}$	$1.8\text{--}3.97 \times 10^{-3}$	390	$1.64 \pm 0.2 \times 10^{-1}$	11	
Ethyl-I	$2.3\text{--}10.9 \times 10^{-2}$	2.6×10^{-3}	390	$4.14 \pm 0.2 \times 10^{-1}$	13	8 runs done with Cr^{2+} from Zn/Hg
<i>n</i> -Propyl-Br	$2.02\text{--}10.0 \times 10^{-2}$	2.6×10^{-3}	390	$1.66 \pm 0.1 \times 10^{-1}$	7	
<i>n</i> -Butyl-Br	$1.71\text{--}8.49 \times 10^{-2}$	2.8×10^{-3}	390	$1.30 \pm 0.1 \times 10^{-1}$	7	
5-Hexenyl-Br	$2.57\text{--}6.39 \times 10^{-2}$	2.6×10^{-3}	390	$1.55 \pm 0.1 \times 10^{-1}$	4	
Neopentyl-Br	$2.3\text{--}11.3 \times 10^{-3}$	2.6×10^{-3}	390	$\sim 1.1 \pm 0.2 \times 10^{-1}$	7	

^a# indicates the number of runs and δ is their average deviation.

Table I-11. (Continued)

RX	[RX]/M	Cr(L) ²⁺ /M	λ/nm	k _{RX} /dm ³ mol ⁻¹ s ⁻¹ ± δ	(#) ^a	Comment
Isopropyl-Br	1.95-7.65 x 10 ⁻²	2.6 x 10 ⁻³	390	1.84±.06	10	
Isopropyl-I	5 x 10 ⁻²	2.3 x 10 ⁻³	390	4.9±1	2	
Cyclo- pentyl-Br	1.75-9.45 x 10 ⁻²	2.6 x 10 ⁻³	390	~5.4±.5	4	
Cyclo- hexyl-Br	1.43-5.18 x 10 ⁻²	2.6 x 10 ⁻³	390	8.4±.4 x 10 ⁻¹	6	
<u>t</u> -Butyl-Br	4.46 x 10 ⁻²	2.6 x 10 ⁻³	390	~8.8±.4	2	Solvolysis of bromide solvent 85% THF corrected for solvent by factor of 1.4
1-Adamantyl-Br	3.6 x 10 ⁻²	2.3 x 10 ³	390	1±.1	4	Run in 99% MeOH corrected for solvent by factor of 0.05
Benzyl-Cl	1.3-8.69 x 10 ⁻³	2.2 x 10 ⁴	280	3.23±.05 x 10 ²	12	
Benzyl-Br	0.42-4.20 x 10 ⁻³	1.1 x 10 ⁻⁴	280	1.91±.06 x 10 ⁴	29	

Table I-11. (Continued)

RX	[RX]/M	Cr(L) ²⁺ /M	λ/nm	k _{RX} /dm ³ mol ⁻¹ s ⁻¹ ± δ	(#) ^a	Comment
BrCH ₂ Cl	3.69-10.7 x 10 ⁻³	2.6 x 10 ⁻³	390	42.4±3	16	
ClCH ₂ CN	1.58-11.06 x 10 ⁻³	2.6 x 10 ⁻³	390	314±8	21	
BrCHClCH ₃	2.79-5.81 x 10 ⁻³	2.6 x 10 ⁻³	390	~500	25	Curved k _{obs} vs [RXY] plots

Table I-12. A comparison of reaction rates of RX with reduced metal species ($\text{dm}^3 \text{mol}^{-1} \text{s}^{-1}$)

RX	rate: $(\text{Cr}(\text{L})^{2+})$	rate: $(\text{Co}(\text{CN})_5^{3-})^a$
CH_3I	$4.6 \pm 0.2 \times 10^{-2}$	$1.9 \pm 0.2 \times 10^{-2}$
$\text{CH}_3\text{CH}_2\text{I}$	$4.14 \pm 0.2 \times 10^{-1}$	$1.18 \pm 0.1 \times 10^{-1}$
$(\text{CH}_3)_2\text{CHI}$	4.9 ± 1	2.4 ± 0.06
$\phi\text{CH}_2\text{Cl}$	$3.23 \pm 0.16 \times 10^2$	$9.8 \pm 0.6 \times 10^{-4}$
$\phi\text{CH}_2\text{Br}$	$1.92 \pm 0.06 \times 10^4$	4.66 ± 0.04

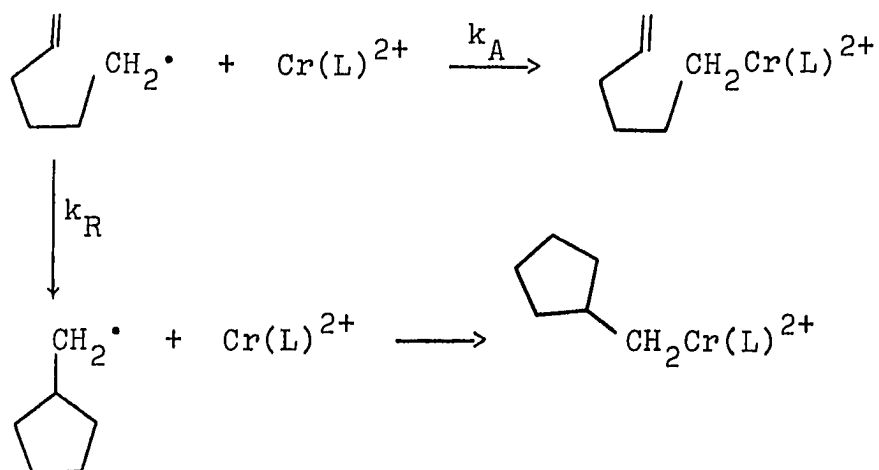
^aThese values, from reference 39, were multiplied by 2 to bring them to the same scale as the rate constants for the $\text{Cr}(\text{L})^{2+}$ reactions.

reaction dependent upon the concentration of ethylenediamine (en) (31).

The free radical nature of the reaction mechanism of $\text{Cr}(\text{L})^{2+}$ with RX is supported by the kinetic evidence. This is exemplified by the order of reactivity of the halides, $\text{I} > \text{Br} > \text{Cl}$, ethyl iodide ($0.414 \text{ dm}^3 \text{ mol}^{-1} \text{ s}^{-1}$) > ethyl bromide ($0.164 \text{ dm}^3 \text{ mol}^{-1} \text{ s}^{-1}$) and benzyl bromide ($1.91 \times 10^4 \text{ dm}^3 \text{ mol}^{-1} \text{ s}^{-1}$) > benzyl chloride ($323 \text{ dm}^3 \text{ mol}^{-1} \text{ s}^{-1}$). The structure of the halides also influences the

reaction rate in the manner expected for a free radical reaction, $3^\circ > 2^\circ > 1^\circ$, tert-butyl bromide ($\sim 8.8 \text{ dm}^3 \text{ mol}^{-1} \text{ s}^{-1}$) > isopropyl bromide ($1.84 \text{ dm}^3 \text{ mol}^{-1} \text{ s}^{-1}$) > n-propyl bromide ($0.166 \text{ dm}^3 \text{ mol}^{-1} \text{ s}^{-1}$). These patterns of reactivity have precedent in the systems of Chock and Halpern (40), and Kochi and Powers (32).

The direct evidence for the intermediacy of free radicals is provided in two experiments involving 5-hexenyl bromide. Halogen abstracting results in the formation of the 5-hexenyl radical which undergoes a rapid irreversible isomerization to the cyclopentylmethyl radical (33). Following the reduction of 5-hexenyl bromide, the resulting radical isomerization must compete with radical capture by Cr(L)^{2+} . As a consequence, two isomeric organochromium species should result as shown below.



The existence of free radicals was proved by the detection of methylcyclopentane. In the course of these experiments, it was also possible to measure the rate of radical capture by $\text{Cr}([\text{15}] \text{aneN}_4)^{2+}$. This value was determined to be $k_A = 9.1 \pm 3 \times 10^6 \text{ dm}^3 \text{ mol}^{-1} \text{ s}^{-1}$. This value is compared to $4 \times 10^7 \text{ dm}^3 \text{ mol}^{-1} \text{ s}^{-1}$ obtained by Kochi and Powers (32) in a similar manner. With the pulse radiolytic technique, Cohen and Meyerstein (29) determined rates of radical capture by $\text{Cr}_{(\text{aq})}^{2+}$. Their values cluster around $\sim 10^8 \text{ dm}^3 \text{ mol}^{-1} \text{ s}^{-1}$.

The reactions of $\text{Cr}([\text{15}] \text{aneN}_4)^{2+}$ with geminal halides present another mode of reactivity. As mentioned before, no organochromium species was detected, yet they obeyed the same second order rate expression valid for the other halides (with exception to BrCHClCH_3). For BrCCl_3 , the only organic products detected by mass spectrometry were CH_3 and CO , BrCH_2Cl produced CH_2CH_2 , CO_2 and CH_4 in a ratio of $>1000:30:1$.

These results are best explained by carbene or carbenoid-type intermediates. In the case of BrCCl_3 , the major product, CO , is rationalized as coming from dichloro-carbene and its reaction with the solvent water (63). The methane could come about through successive attacks of $\text{Cr}(\text{L})^{2+}$ upon various halomethylchromium intermediates (64). With BrCH_2Cl , ethylene was the predominate product. This

might be rationalized by methylene carbene insertion into a C-H bond of BrCH_2Cl forming BrCHClCH_3 . This then could be attacked by Cr(L)^{2+} to generate ethylene carbene which could rearrange to form ethylene.

The intermediacy of carbene or carbenoid species was previously invoked by Castro and Kray (62) in their investigations of the reductions of geminal halides by CrSO_4 in aqueous DMF.

Activation parameters have been determined for the reactions of ethyl bromide, ethyl iodide and benzyl chloride. The respective parameters are $\Delta H^\ddagger = 44.2 \pm 1 \text{ KJ mol}^{-1}$, $\Delta S^\ddagger = -111.8 \pm 3.5 \text{ J mol}^{-1} \text{ k}^{-1}$, $\Delta H^\ddagger = 44.1 \pm 1.3 \text{ KJ mol}^{-1}$, $\Delta S^\ddagger = -104.4 \pm 4.3 \text{ J mol}^{-1} \text{ k}^{-1}$ and $\Delta H^\ddagger = 30.6 \pm 1.6 \text{ KJ mol}^{-1}$, $\Delta S^\ddagger = -94.1 \pm 5.2 \text{ J mol}^{-1} \text{ k}^{-1}$. For ethyl bromide and iodide, the only significant difference is in the activation entropy, a difference of $\sim 7.4 \text{ J mol}^{-1} \text{ k}^{-1}$. The more negative value being associated with the bromide implies more order is required in its transition state than that for ethyl iodide. The reaction rate ratio for these halides is adequately explained by just the entropy difference. Taking $e^{-\Delta S/R}$ and substituting in the proper quantities results in $e^{-(111.8-104.4/8.3)} = 0.415$ which is the ratio of reaction rates. The ratio of measured rate differences is $0.164/0.414$ or 0.396 in excellent agreement with the calculated value. The activation parameter, ΔH^\ddagger , for benzyl chloride,

reflects the ease of formation of the benzyl radical compared to that of an alkyl radical, even with the differences in halide. The value of ΔS^\ddagger implies benzyl chloride has a more disordered transition state than either alkyl halide measured.

The activation data for these halides and several relevant systems are summarized in Table I-13.

Table I-13. Summary of activation parameters for the reaction of organic halides with reducing metal complexes

Reaction	ΔH^\ddagger KJ/mol	ΔS^\ddagger J/mol·K
EtBr + Cr(L) ²⁺	44.2±1	-111.8±3.5
EtI + Cr(L) ²⁺	44.1±1.3	-104.4±4.3
$\phi\text{CH}_2\text{Cl}$ + Cr(L) ²⁺	30.6±1.6	-94.1±5.2
$\phi\text{CH}_2\text{Cl}$ + Cr ²⁺ ^a	58.6	-59.8
$\text{ICH}_2\text{CH}_2\text{COO}^-$ + Co(CN) ₅ ³⁻ ^b	40.1±1.2	-112.8±4

^aFrom ref. 17, these values were multiplied by 4.18 to convert them to the same units. The reaction was run in 71.5% ethanol-water.

^bFrom ref. 40, these values were multiplied by 4.18 to convert them to the same units. The reaction was run in aqueous solution, pH \geq 12.

The kinetic data reflects an inverse dependence on the carbon halogen bond strength and also manifests resonance stabilization of the resulting free radical (benzyl-X). Similar trends are also noted for the rates of halogen abstraction from organic halides by sodium atoms and organic free radicals. This is consistent with a rather common reaction mechanism, the S_H2 -type process (65).

These sets of reactions have resulted in the formation of a new and interesting class of organometallic compounds. Their appears to be a general set of organometallic compounds emerging from this S_H2 process. These compounds are formed from a labile reducing metal species and readily available organic compounds. It seems that once the qualifications of the metal center are fulfilled, a variety of complexes would be available.

PART II. REACTIONS OF SIGMA BONDED ORGANOCHROMIUM(III)
CHELATE COMPLEXES WITH MERCURY(II) ELECTROPHILES

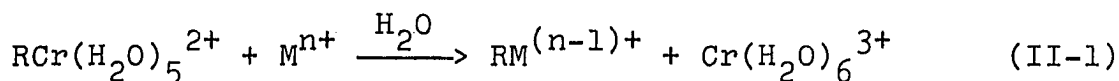
INTRODUCTION

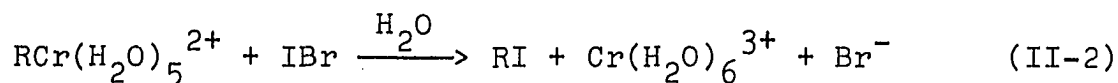
Having mechanistically characterized the preparation of a new class of sigma bonded organochromium compounds, it was of considerable interest to study the reactions that these species might undergo.

In the previous part of this work, the reaction of mercuric ion was used to verify the identity of the carbon-chromium bond. This reaction was used by Anet and Le Blanc (13) to characterize the benzylpentaquochromium(III) ion. This heterolytic cleavage, the formal transfer of a carbanion from chromium to another atom, is referred to as an electrophilic reaction. Considerable effort and interest has been expressed in the understanding of the detailed mechanism of electrophilic attack on saturated carbon in organic (66) and organometallic (67) systems.

Because of the recent review by Johnson (67) of electrophilic reactions in organotransition metal systems, only the most relevant material from this review will be highlighted.

Organopentaquochromium(III) ions react with the greatest range of electrophiles (e.g., Hg^{2+} , Hg_2^{2+} , Tl^{3+} , Br_2 , I_2 , IBr , NO^+ , NOCl , and H^+) as illustrated in the following equations, II-1,2,





in which the products of the electrophilic cleavage are consistent with the attack of the electrophile at the carbon adjacent to the metal center. As an example of this, (eqn. II-2), the reaction of several organochromium species with IBr results in the exclusive formation of the organic iodide and Cr^{3+} .

Because of their relative ease of preparation and distinctive spectra of the chromium species, they have proved to be the focus of kinetic study. The general rate law which emerges for all these reactions is shown in equation II-3. The exception to this expression is in the

$$-\frac{d[\text{RCr}^{2+}]}{dt} = k_2[\text{RCr}^{2+}][\text{electrophile}] \quad (\text{II-3})$$

case where there is a unimolecular reaction of the RCr^{2+} (R = methyl and isopropyl) species independent of the electrophile resulting in the addition of another term, $k_1[\text{RCr}^{2+}]$. This has been ascribed to the acidolysis of both of these species.

The reactivity pattern that then emerges is as follows. Of the three basic mechanisms which have been observed for electrophilic reactions, described as $\text{S}_{\text{E}}1$, $\text{S}_{\text{E}}2(\text{cyclic})$ and $\text{S}_{\text{E}}2(\text{open})$, only the $\text{S}_{\text{E}}2(\text{open})$ reaction mechanism describes

the observed reactivity and products of the reactions of electrophile with organochromium(III) ions.

One of the most extensive and best characterized electrophilic reaction series is the reactions of Hg^{2+} and CH_3Hg^+ with RCr^{2+} ions (27b,68). It was decided that in this project the reactions of Hg^{2+} and CH_3Hg^+ with a series of $\text{RCr}([\text{15}] \text{aneN}_4)^{2+}$ complexes would provide data for the comparison of two similar systems.

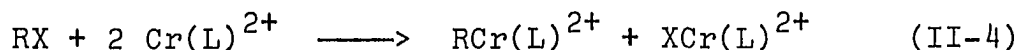
In this study the $\text{RCr}([\text{15}] \text{aneN}_4)^{2+}$ substrates investigated included species in which R = methyl, ethyl, n-propyl, n-butyl, n-pentyl, isopropyl, cyclohexyl, 1-adamantyl and benzyl. The rates of all of these reactions with Hg^{2+} have been measured along with those of R = CH_3 , CH_2CH_3 and benzyl with CH_3Hg^+ as well. In the case of the Hg^{2+} reactions, activation parameters have been determined for R = CH_2CH_3 , $\text{CH}_2\text{CH}_2\text{CH}_3$, n-butyl, n-pentyl and benzyl with the purpose of seeing if there was an isokinetic relationship for these reactions. The results obtained will be discussed in light of the previous electrophilic cleavage reactions of the organochromium bond.

EXPERIMENTAL

Preparation of Organochromium Compounds

n-Alkyl([15]aneN₄)chromium(III) complexes

All of these species were prepared in a manner analogous to that reported in the first part of this thesis except a more detailed and improved synthetic procedure will be reported. The general reaction used is outlined in equation II-4.



The detailed procedure for the preparation of ethyl-Cr(L)²⁺ is as follows: 0.10 g (0.466 mmol) of [15]aneN₄ was placed in a 50 ml round bottom flask with a serum capped side arm. ~10 ml of H₂O along with a stirring bar was added. The solution was deaerated with Cr²⁺ scrubbed N₂ for a minimum of 30 min, and a slight deficiency of Cr²⁺ (from CrCl₂·4H₂O was then added by syringe via the side arm (i.e., 0.80 ml of 0.538 M Cr²⁺, 0.430 mmol). Once the purple color had completely formed, ~3 min, ~1 ml of deaerated neat ethyl iodide or bromide (~0.01 moles) was syringed into the reaction vessel using the side arm. The solution was vigorously stirred and allowed to react under N₂ for ~20 min in the case of iodide and ~40 min for the bromide.

The unreacted halide was extracted with 2 x 15 ml portions of either CCl_4 or ether. The solution was filtered to remove the air oxidation products, green insoluble material, and placed on an ice bath jacketed column of Sephadex C-25 cation exchange resin, 7-8 x 1.6 cm, in the Na^+ form. In the case of the simple alkyl groups, the ice jacket is not necessary when using the bromides but helps prevent the aquation of the ICr(L)OH^+ species on the column. This would result in contamination of the organochromium species with Cr(L)^{3+} and lower the observed extinction coefficients.

The halohydroxochromium species is eluted first with 0.1 M NaClO_4 , $\text{pH} \approx 5.0$. If the pH is allowed to get around $\text{pH} \approx 3$, one loses the separation advantage of the lower charge, +1, on the halochromium species due to the shift in the hydrolysis equilibrium. The organochromium species is eluted next with 0.2 - 0.4 M NaClO_4 . The solutions were stored in serum capped flasks in the freezer at -10°C until ready to use. In this way the solutions kept for months.

Secondary and benzyl Cr(L)^{2+} complexes

These species were synthesized in a similar manner with an analogous work up except the exposure to atmospheric oxygen was kept to a minimum since they were mildly oxygen sensitive. When these species were purified by cation exchange chromatography, using deaerated eluent, it was

found that they were also sensitive to temperature. Because of this, all synthetic separations were done at ice bath temperatures. These solutions were collected in deaerated flasks and stored under N_2 in the freezer ($-10^\circ C$) until they were needed for kinetic work.

1-Adamantylchromium([15]aneN₄)²⁺

Since 1-adamantyl bromide could not be used in the above two phase syntheses, a different procedure was used. 0.10 g [15]aneN₄ (0.466 mmol) was dissolved in 10 ml of 4:1 v/v, THF:H₂O. The solution was deaerated for ~1 hr using a slow rate of N₂ flow making sure THF loss was kept to a minimum by using a THF bubbling tower. Then 0.80 ml of 0.538 M Cr²⁺ (0.43 mmol) was added. If sufficient H₂O is not present, a purple solid will precipitate out of solution. To this flask a deaerated solution of 1-adamantylbromide in THF (~0.5 g in 5 ml) was syringed in. The reaction was allowed to proceed under N₂ for about 40 min. Water was added, ~5 ml. The THF was removed from the reaction mixture by use of a flash evaporator at room temperature. The solution was filtered to remove the solid 1-adamantyl bromide. The separation was effected as mentioned above.

Mercury compounds

Solutions of mercuric perchlorate were prepared by heating HgO with a small excess of HClO₄. The solution was

then filtered through high retention filter paper to remove finely divided impurities. These solutions should be discarded if any precipitate is noticed -- with great care -- as the solid is very explosive.

Solid $\text{Hg}(\text{ClO}_4)_2 \cdot 2\text{H}_2\text{O}$ was also purchased from G. F. Smith, prepared from $\text{Hg}(\text{NO}_3)_2$. Solutions of methylmercuric perchlorate were prepared by dissolving CH_3HgOAc which is commercially available, in perchloric acid.

Other materials

$[\text{15}] \text{aneN}_4$ and $\text{CrCl}_2 \cdot 4\text{H}_2\text{O}$ were prepared as previously described. The halides were all commercially available and purified as before. Solid lithium perchlorate was made by neutralizing reagent grade Li_2CO_3 with HClO_4 , recrystallizing this material twice. All of the other materials used were commercially available and used as received.

Methods

Analyses

The concentrations of the $\text{RCr}([\text{15}] \text{aneN}_4)^{2+}$ were determined from their respective spectral parameters, Table I-5 of the previous section. In the case of $n\text{-pentylCr(L)}^{2+}$,

the extinction coefficients for n -butylCr(L) $^{2+}$ were used.

Stock solutions of Hg^{2+} were standardized by Volhard titration (52). Iron(III) was used as the indicator as aliquots of Hg^{2+} solution were titrated with standard NaSCN.

Solutions of CH_3Hg^+ were standardized using the dithizone method (68). The analysis uses the mixed color method where the absorbance of a CCl_4 solution of dithizone is measured before and after extraction of an aqueous solution of CH_3Hg^+ . In a typical analysis of 0.0263 M CH_3Hg^+ (1 \rightarrow 100 dilution) using a 2.51×10^{-4} M dithizone solution, the following equation is used, II-5

$$[RHg^+] = \frac{\Delta A \times V_{DZ}}{b \times \epsilon \times V_{CH_3Hg^+}} \quad (II-5)$$

For a typical analysis of 0.0263 M CH_3Hg^+ solution, the parameters in equation II-5 had the following values after a 100-fold dilution of CH_3Hg^+ :dithizone, 2.51×10^{-4} M , $V_{DZ} = 20.0$ ml, $V_{CH_3Hg^+} = 2.00$ ml, $b = 1.00$ cm and $\Delta A = 0.422$ with $\epsilon = 3.40 \times 10^4$ $M^{-1} \text{ cm}^{-1}$.

The lithium perchlorate concentration was determined by ion displacement. Aliquots of Li^+ solution were put on a column of Dowex 50W-X8 cation exchange resin in the H^+ form. After washing with H_2O , one titrates the liberated H^+ with standard NaOH to the phenolphthalein endpoint.

Spectra

The peak height ratio in the visible spectra of the organochromium cations was used to check the purity of these solutions. The mercury(II) products of some of the reactions under study were identified by their respective mass spectrum as presented in the previous section. All uv-visible spectral and absorbance data were recorded with a Cary 14 spectrophotometer using a high-intensity tungsten lamp.

Stoichiometry

The stoichiometry of the reaction of Hg^{2+} with $\text{CH}_3\text{Cr}([\text{15}] \text{aneN}_4)^{2+}$ was determined by spectrophotometric titration of $\text{CH}_3\text{Cr}(\text{L})^{2+}$ with Hg^{2+} . A 1.00 cm cell was used. The Hg^{2+} [0.0233 M] solution was added by microsyringe in increments of 0.025 ml. The change in absorbance at 320 nm for a solution 5.5×10^{-3} M in $\text{CH}_3\text{Cr}(\text{L})^{2+}$ was recorded for each addition of Hg^{2+} . A plot of absorbance vs mole ratio, $\text{Hg}^{2+}/\text{RCr}(\text{L})^{2+}$, was made. The break point of this plot represents the number of moles of Hg^{2+} that react per mole of $\text{CH}_3\text{Cr}(\text{L})^{2+}$. A similar plot was made for the reaction of CH_3Hg^+ with $\text{CH}_3\text{Cr}(\text{L})^{2+}$. In this case, the change in absorbance was measured at 310 nm after each addition of 0.05 ml of 0.0263 M CH_3Hg^+ .

Kinetics

Kinetic runs on slow reactions ($t_{1/2}$ usually ≥ 10 s) were done using a Cary 14 spectrophotometer with a thermostated cell compartment. All the reagents were placed in a spectrophotometer cell, usually of 2 cm path length, and placed in a constant temperature bath for at least 20 min. To initiate the reaction, an aliquot of thermostated $\text{RCr}([\text{15}] \text{aneN}_4)^{2+}$ solution was added and the reaction was followed by the decay of RCr(L)^{2+} absorption. For reactions in which air-free conditions were required, R = isopropyl, cyclohexyl and benzyl, the same procedure was followed except the cells were purged with N_2 for ~ 20 min before the addition of the RCr(L)^{2+} species.

The acquisition of kinetic data for the faster reactions ($t_{1/2} \leq 5$ s) was done with a Gibson-Durrum stopped flow spectrophotometer. This instrument had a thermostated Kel-F mixing block in addition to being interfaced with a PDP-15 computer for the storage and workup of raw kinetic data. A storage oscilloscope was used to display the data and could be photographed for a permanent copy of the raw data.

As above, LiClO_4 was used to maintain ionic strength. The Hg^{2+} or CH_3Hg^+ stock solution was made 0.50 M in HClO_4 and kept in a storage syringe for the flow. The

$\text{RCr}([\text{15}] \text{aneN}_4)^{2+}$ stock solution was brought to the same ionic strength with LiClO_4 and placed in the other storage syringe. As before, with the Cary 14 runs, the kinetic data were obtained by following the decrease in absorbance at a wavelength characteristic of RCr(L)^{2+}

Pseudo-first-order conditions, with the Hg(II) reagent in excess, were used for all kinetic runs. The pseudo-first-order rate constants were obtained by the standard method. As before in the standard method, $\ln(A_t - A_\infty)$ is plotted vs time in accord with

$$\ln(A_t - A_\infty) = \ln(A_0 - A_\infty) - k_{\text{obs}} t$$

and the resulting slope = $-k_{\text{obs}}$.

For the reactions done on the stopped-flow, the computer interface was used. The computer works up the raw data based upon the variable input parameters (i.e., scan rate, etc.) assigned by the user and calculates k_{obs} .

In most cases the second-order rate constant was determined from the slope of plots of k_{obs} vs $[\text{Hg(II)}]$. For the reactions with RCr(L)^{2+} , R = isopropyl, cyclohexyl and 1-adamantyl, only several runs were performed. Here the value of the second-order rate constant was obtained from the quotient of $k_{\text{obs}}/[\text{Hg}^{2+}]$.

The values of k_{obs} for the reaction of isopropyl and cyclohexyl $\text{Cr}([\text{15}] \text{aneN}_4)^{2+}$ with Hg^{2+} were determined from

the slopes of Swinbourne plots because of the inability of obtaining an accurate A_{∞} (which was measured ~ 10 hrs later) for these reactions.

In the Swinbourne method (69) A_t is plotted vs $A_{t+\tau}$ according to the following equation:

$$A_t = A_{\infty}[1 - \exp(k_{\text{obs}}\tau) + A_{t+\tau} \exp(k_{\text{obs}}\tau)]$$

In this equation τ is a uniform time interval usually between 0.5-1 half life. The respective values of τ used for R = isopropyl and cyclohexyl are 880 and 2880 seconds. The slope of the Swinbourne plot is $\exp(k_{\text{obs}}\tau)$ so that $k_{\text{obs}} = \ln(\text{slope})/\tau$.

A value for the A_{∞} of the reaction may also be obtained from a Swinbourne plot. This value is found from the intercept of the slope of the kinetic plot with a line of slope equal to one. Once A_{∞} has been determined, it is possible to use the standard method to obtain k_{obs} with the observed data.

RESULTS

Characterization

 $\text{RCr}([\text{15}] \text{aneN}_4)^{2+}$

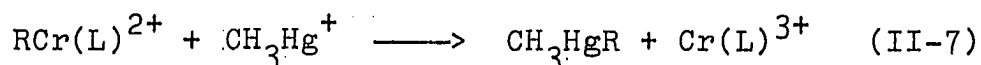
All but one of the organochromium complexes used in this investigation were characterized in Part I. In the case of n-pentylCr(L)²⁺, this was characterized by its spectral appearance which was compared to that of n-butylCr(L)²⁺. A summary of the electronic transitions and extinction coefficients may be found in Table I-5.

Organomercury(II) products

These compounds were characterized in Part I. No attempt was made to isolate the CH₃HgR species due to their extreme toxicity. As a precaution, all solutions suspected of containing any diorganomercurial compounds were disposed of by emptying the "R₂Hg" solution into acetone containing I₂.

Characterization of Reactions

The reactions of $\text{RCr}([\text{15}] \text{aneN}_4)^{2+}$ with Hg^{2+} or CH_3Hg^+ can be described by equations II-6 and II-7, respectively.



The identification of the Hg(II) product has been discussed in Part I of this thesis. The identity of Cr(L)^{3+} as the sole chromium reaction product was established by its visible spectrum, see Figures I-6, I-7 and Table I-4.

The stoichiometry of the Hg(II) reactions as described in equations II-6 and II-7 was confirmed by the spectrophotometric titration of $\text{CH}_3\text{Cr}([\text{15}] \text{aneN}_4)^{2+}$ with Hg^{2+} and $\text{CH}_3\text{Hg}^{2+}$. This was described in the Experimental section.

Titration curves for the experiments with Hg^{2+} and CH_3Hg^+ are shown in Figures II-1 and II-2, respectively. The mole ratio for the Hg^{2+} reaction is 0.48. This implies a stoichiometry of 2:1, as one would expect when $[\text{Hg}^{2+}] \leq \frac{1}{2} [\text{CrR}^{2+}]$ because the RHg^+ formed in the initial phase of the reaction reacts again with RCr(L)^{2+} to produce R_2Hg . The mole ratio for the CH_3Hg^+ reaction is 0.86, supporting a stoichiometry of 1:1, as expected. It will be assumed that all the other $\text{RCr}([\text{15}] \text{aneN}_4)^{2+}$ complexes react in the same manner with the respective Hg(II) reactants. This is supported by the previous work of Leslie and Espenson (27b).

Kinetics

Preliminary experiments

Since the reactions of Hg^{2+} and CH_3Hg^+ with RCr^{2+} had been thoroughly studied, only several preliminary reactions

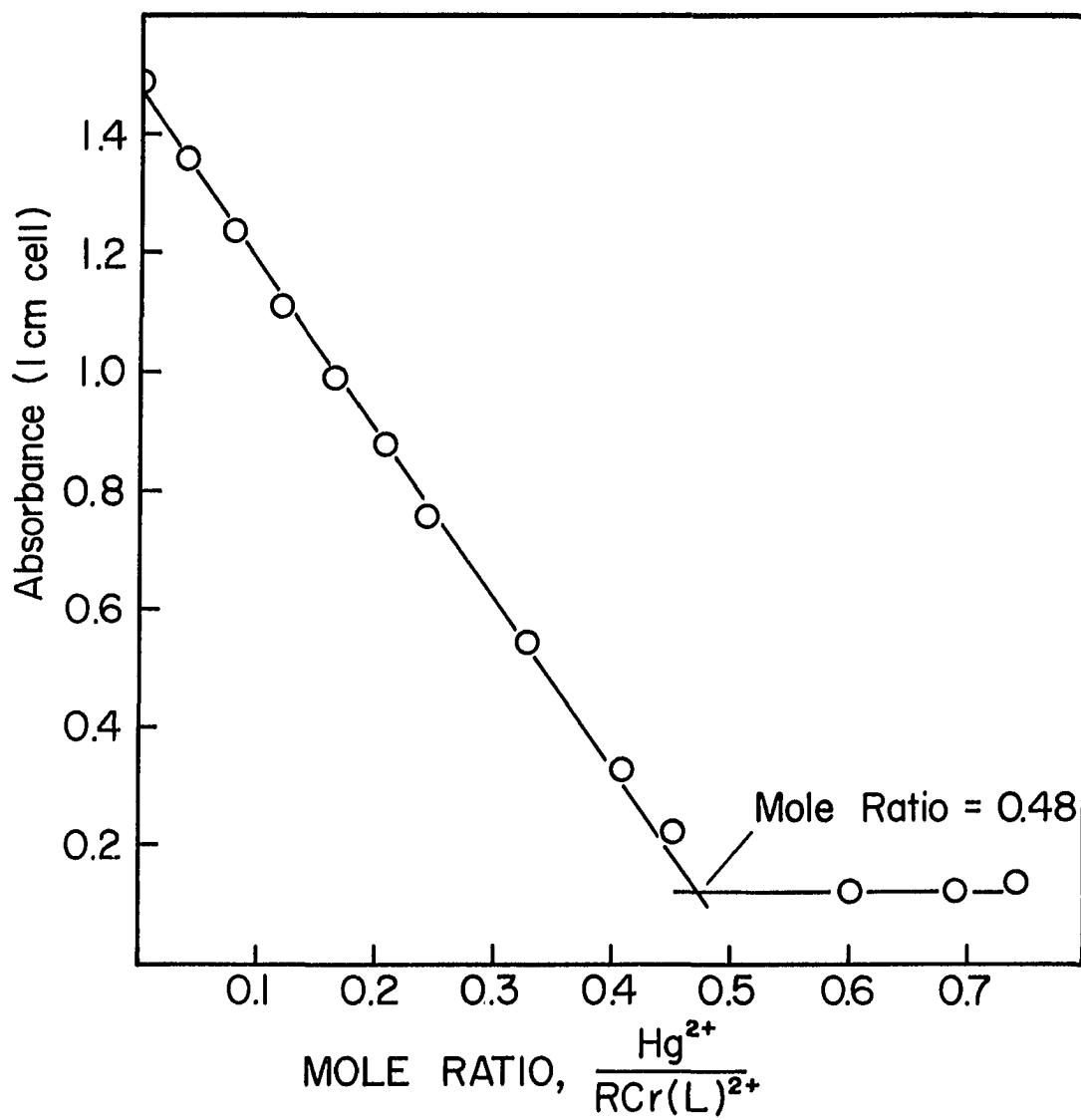


Figure II-1. Spectrophotometric titration of $\text{CH}_3\text{Cr}(\text{L})^{2+}$ by Hg^{2+}

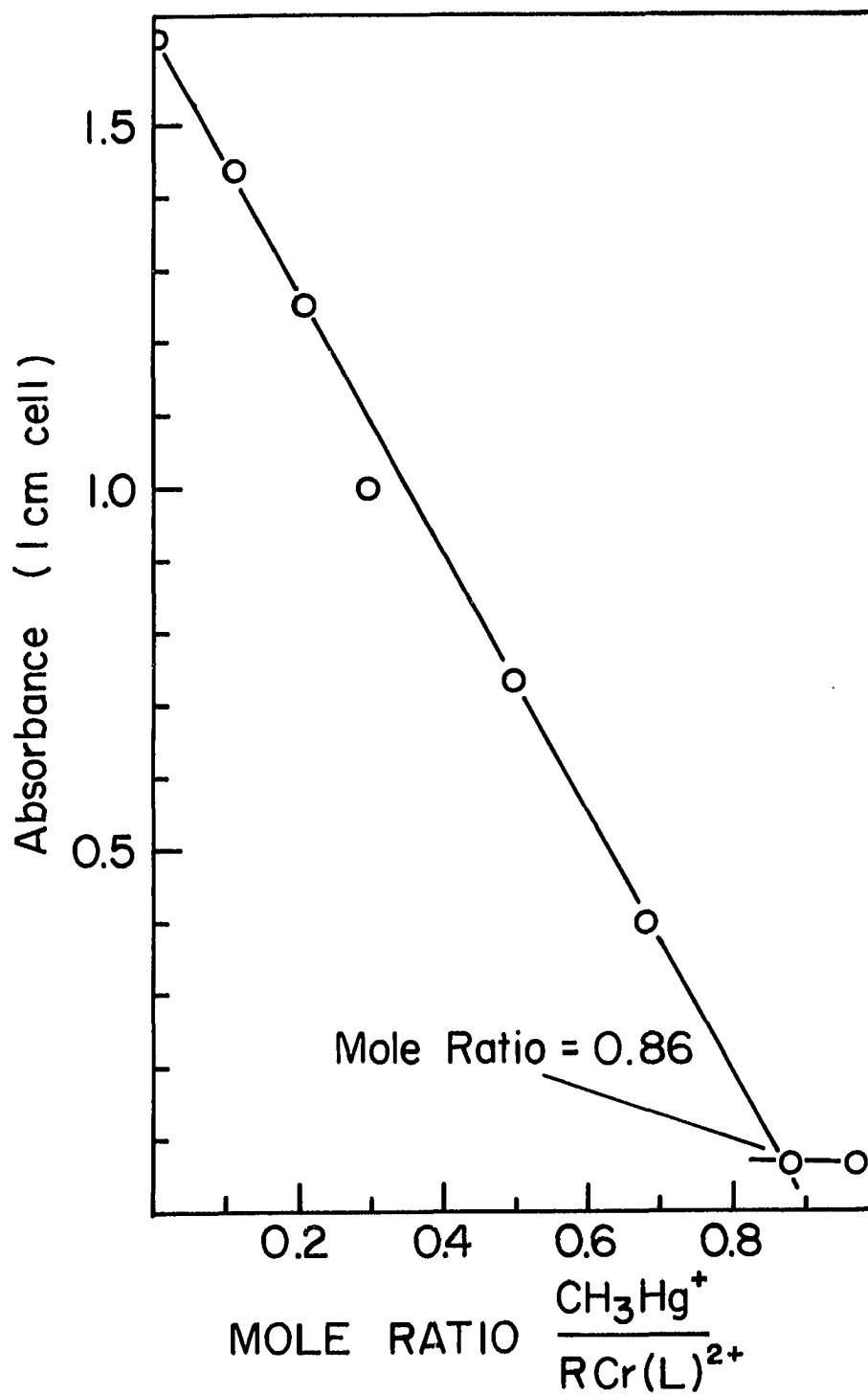
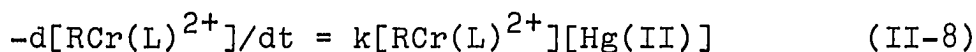


Figure II-2. Spectrophotometric titration of $\text{CH}_3\text{Cr}(\text{L})^{2+}$ by CH_3Hg^+

were investigated. This was done with the purpose of putting an approximate upper bounds on the reaction rate. Ethyl-Cr([15]aneN₄)²⁺ was chosen as the substrate because of its ease of preparation and the relatively fast reaction of Hg²⁺ with EtCr²⁺. The results of this experiment and several isolated experiments are described below.

The reaction of Hg²⁺ with EtCr(L)²⁺ proved to be quite fast, yet ~100 times slower than the analogous reaction with EtCr²⁺. These runs proved to be first order in both [Hg²⁺] and [RCr(L)²⁺] and were all done with Hg²⁺ in pseudo-first-order excess. All the first order plots were linear and when [Hg²⁺] was varied, the quotient of $k_{\text{obs}}/[\text{Hg}^{2+}]$, k_{obs} is the pseudo-first-order rate constant, was constant confirming the first-order dependence on [Hg²⁺]. These results and the previous study by Leslie and Espenson (27b) indicated that the rate law for the reaction is



This rate law is also expected to hold for the reactions involving CH₃Hg⁺. Confirmation of the rate law is given later by more systematic kinetic studies. In the previous work (68), it was found that this rate law did not strictly hold. This form of the rate law will be used and where discrepancies were found will be noted.

It was shown earlier (68) that the source of CH_3Hg^+ ($\text{CH}_3\text{HgClO}_4$ or CH_3HgOAc) did not influence the rate of reaction. This will be assumed in this study. Since CH_3HgOAc is commercially available, it was used as the source of CH_3Hg^+ in the kinetic studies.

It was again assumed that oxygen would have no effect on the reactions of Hg^{2+} or CH_3Hg^+ yet as will be shown later because of the slow rate of reaction of isopropyl and cyclohexyl $\text{Cr}([\text{15}] \text{aneN}_4)^{2+}$, oxygen had to be excluded or it competed with the desired reaction.

Since one of the major points of this study was to accurately compare the reactivity of the pentaquo vs the chelated organochromium species, the reactions were studied under identical condition of acid $[\text{H}^+] = 0.25 \text{ M}$ and ionic strength maintained at $\mu = 0.50 \text{ M}$ with LiClO_4 . In the case of $\text{R} = \text{isopropyl, cyclohexyl and 1-adamantyl}$ where the rate of reaction was so slow, the ionic strength was in practice set by the value of the $[\text{Hg}^{2+}]$ which was used in such large excess, $[\text{Hg}^{2+}] \geq 2000 [\text{RCr(L)}^{2+}]$, that its concentration was essentially unchanged. When $[\text{Hg}^{2+}]$ was varied, the ionic strength was maintained with $\text{Ba}[\text{ClO}_4]_2$. For these sets of runs, the ionic strength, $\mu = 1.46 \text{ M}$ with $[\text{H}^+] = 0.17 \text{ M}$. Only later in a narrow set of experiments designed to look at differences in electrophiles was a slight acid dependence noticed and this was at $[\text{H}^+] \leq 0.015 \text{ M}$

for the reaction of EtHg^+ with EtCr(L)^{2+} , $k_2 = 8.2 \pm 0.4 \text{ dm}^3 \text{ mol}^{-1} \text{ s}^{-1}$. This was not further investigated.

Kinetics of Hg^{2+} reactions

A systematic series of kinetic studies were performed for the reactions of Hg^{2+} with a wide range of $\text{RCr}([\text{15}] \text{aneN}_4)^{2+}$ complexes.

Pseudo-first-order conditions were used in all cases, with $[\text{Hg}^{2+}] \geq 10[\text{RCr(L)}^{2+}]$, except where $\text{R} = \text{CH}_3$. For these runs, a 9-fold excess was used. This was also treated in a pseudo-first-order manner. Figures II-3 and II-4 show typical standard methods plots resulting from data treatment. In the cases of $\text{R} = \text{isopropyl}$ and cyclohexyl , the Swinbourne method was used to calculate the observed rate constant and to also provide a value for A_∞ so that the standard method might be used. Figure II-5 illustrates a standard method plot with a Swinbourne determined A_∞ , Figure II-6, the Swinbourne treatment of data for $\text{R} = \text{cyclohexyl}$.

Except for $\text{R} = \text{CH}_3$, isopropyl , cyclohexyl and l-adamantyl , the second-order rate constants were all determined by a least squares fit of the data from a plot of k_{obs} vs $[\text{Hg}^{2+}]$. The linearity of these plots, Figures II-7, II-8, II-9 and II-10, confirms the first order dependence of the reaction upon $[\text{Hg}^{2+}]$. In all cases, the plots passed through the origin within the least squares

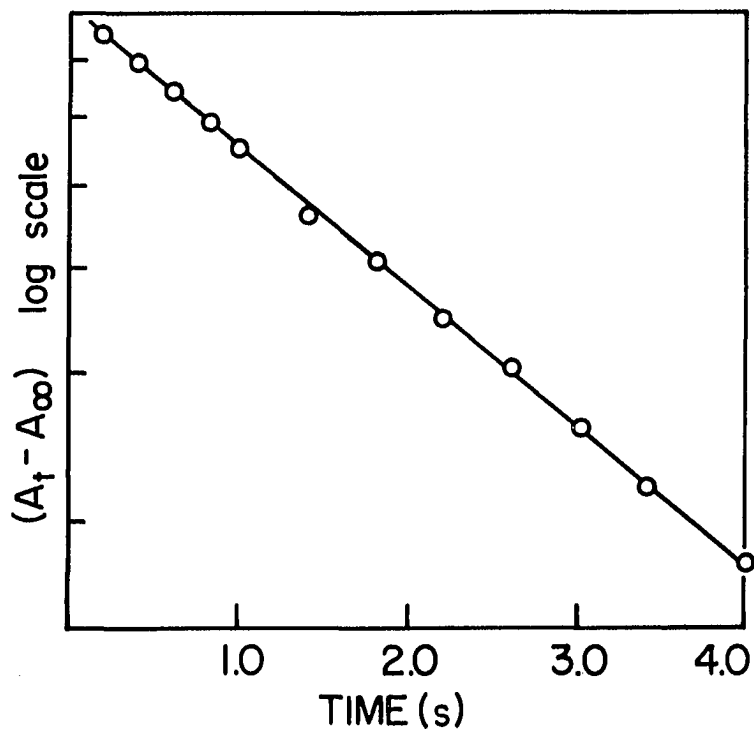


Figure II-3. Standard method plot for the reaction of $n\text{-propylCr(L)}^{2+}$ with Hg^{2+}

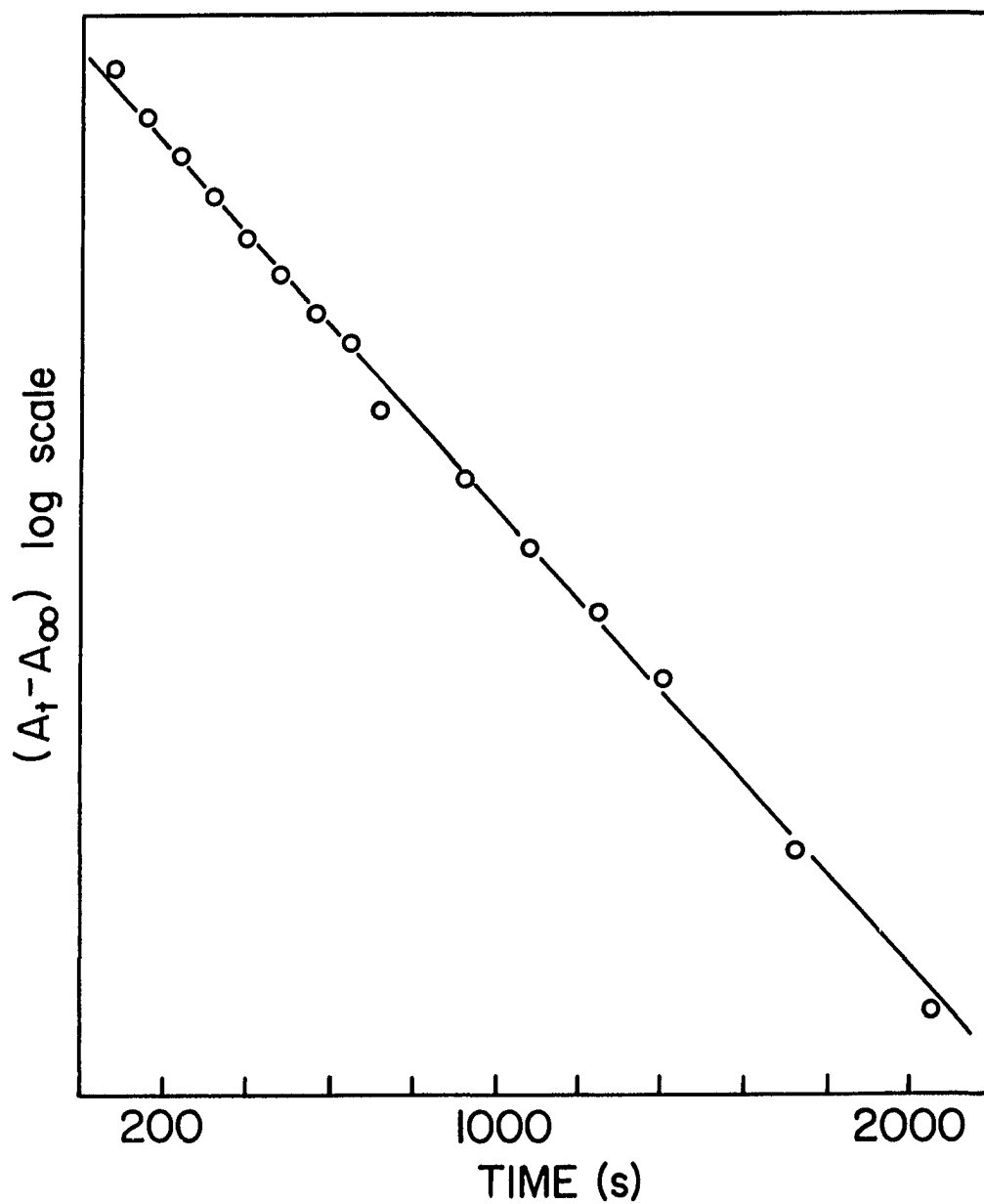


Figure II-4. Standard methods plot for the reaction of 1-adamantylCr(L)²⁺ with Hg²⁺

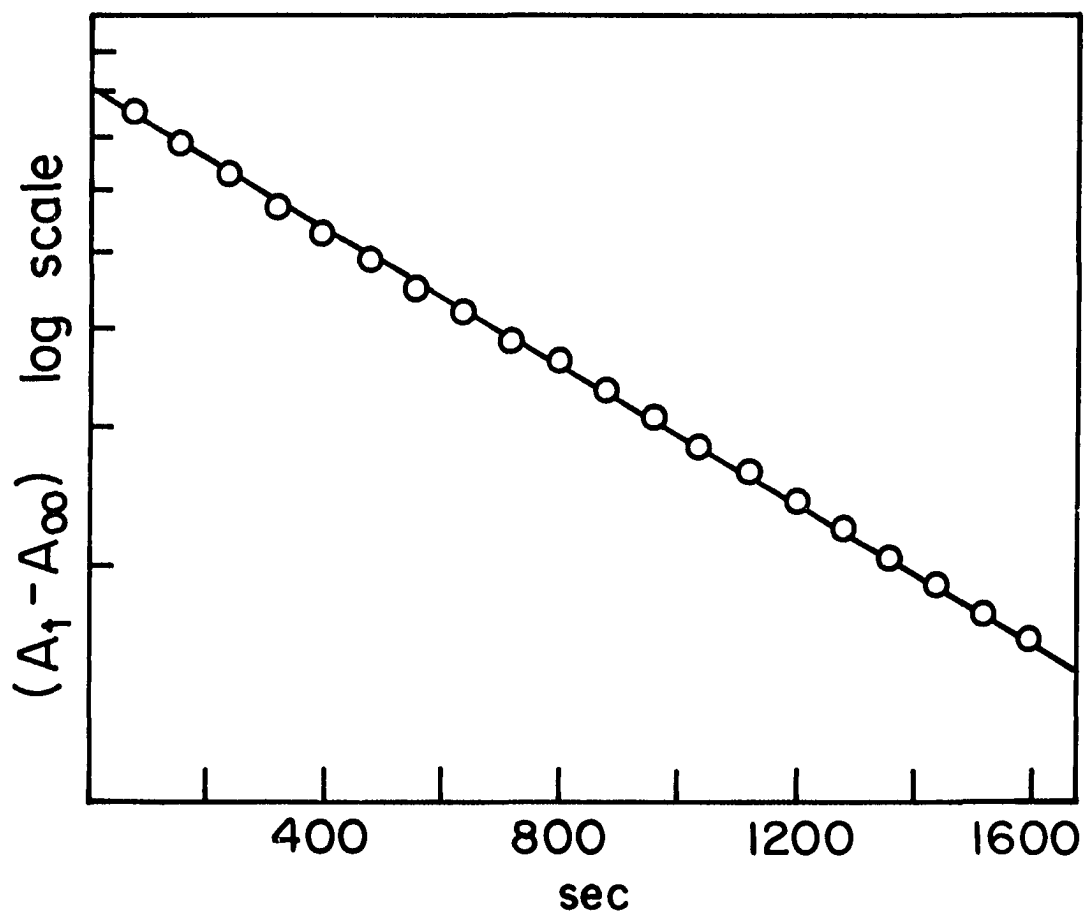


Figure II-5. Standard methods plot of the reaction of isopropylCr(L)²⁺ with Hg²⁺ using a Swinbourne determined A_{∞} .

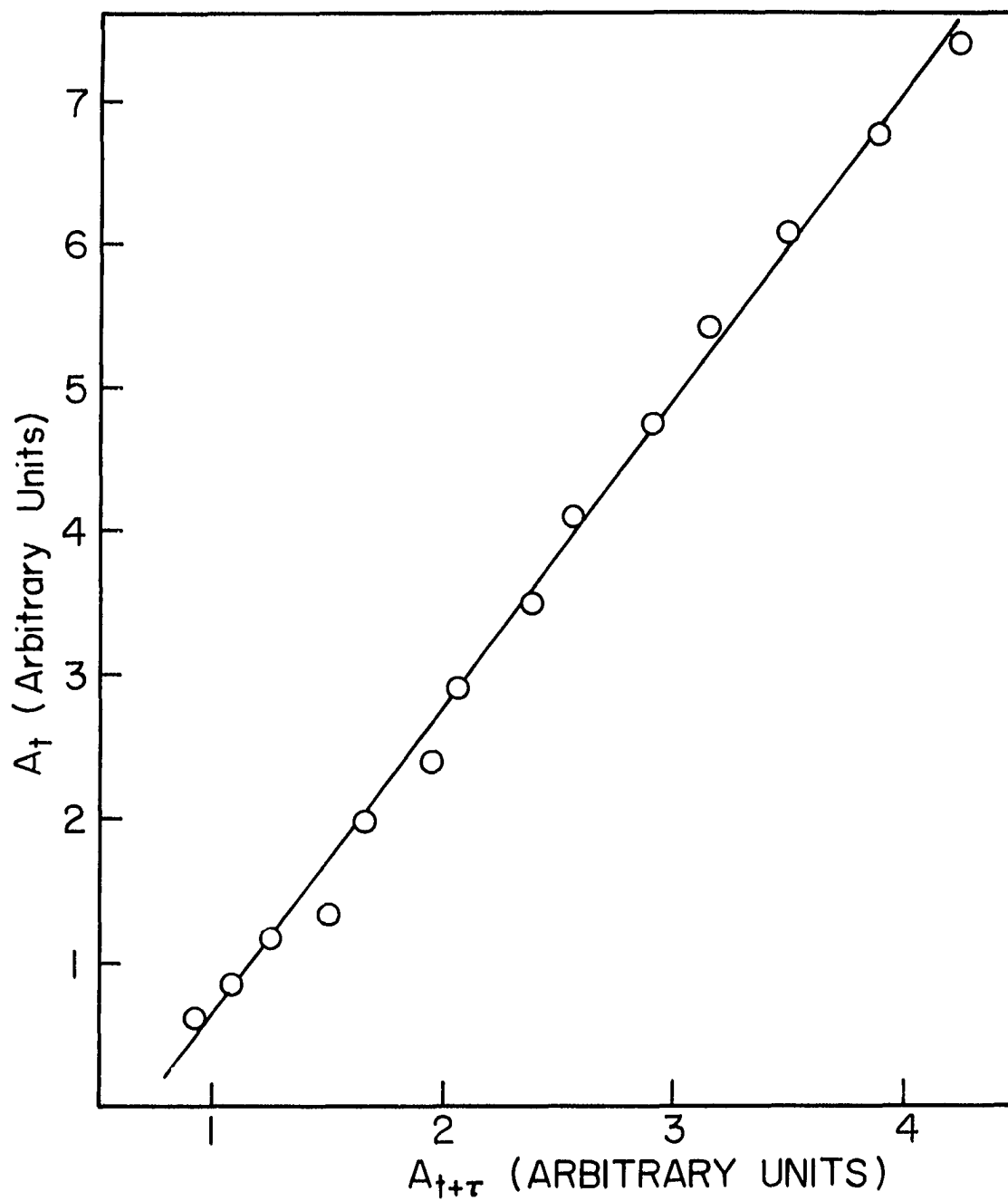


Figure II-6. Swinbourne plot for the reaction of cyclohexylCr(L)²⁺ with Hg²⁺

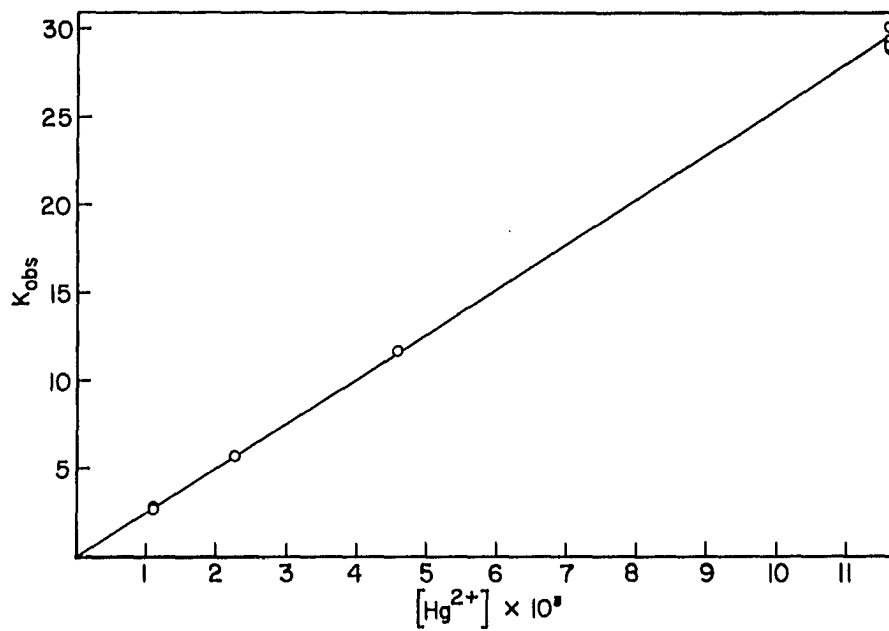


Figure II-7. Plot of k_{obs} vs $[Hg^{2+}]$ for the reaction of $ethylCr(L)^{2+}$ with Hg^{2+}

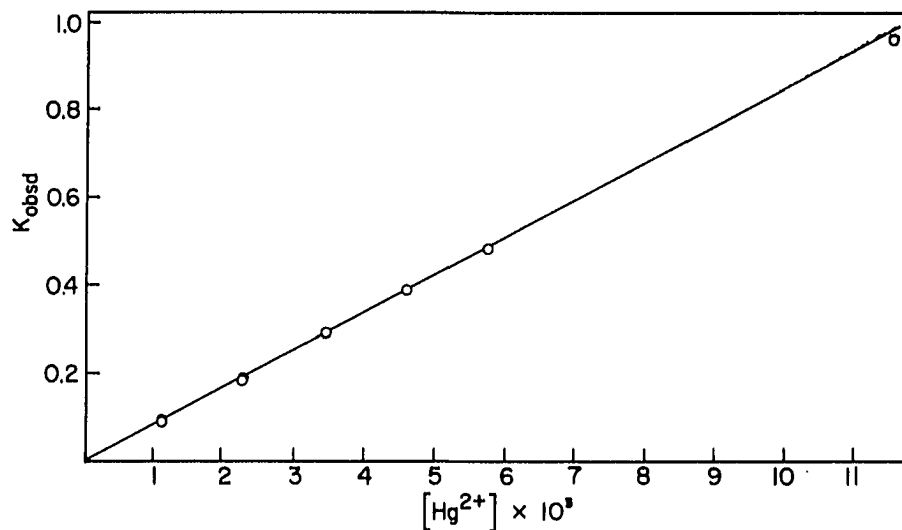


Figure II-8. Plot of k_{obs} vs $[Hg^{2+}]$ for the reaction of n -propylCr(L) $^{2+}$ with Hg^{2+}

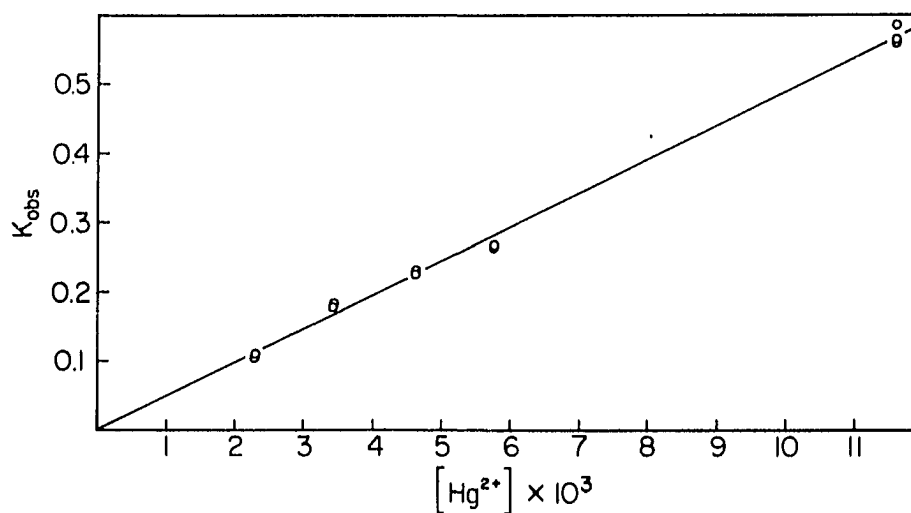


Figure II-9. Plot of k_{obs} vs $[Hg^{2+}]$ for the reaction of n -butylCr(L) $^{2+}$ with Hg^{2+}

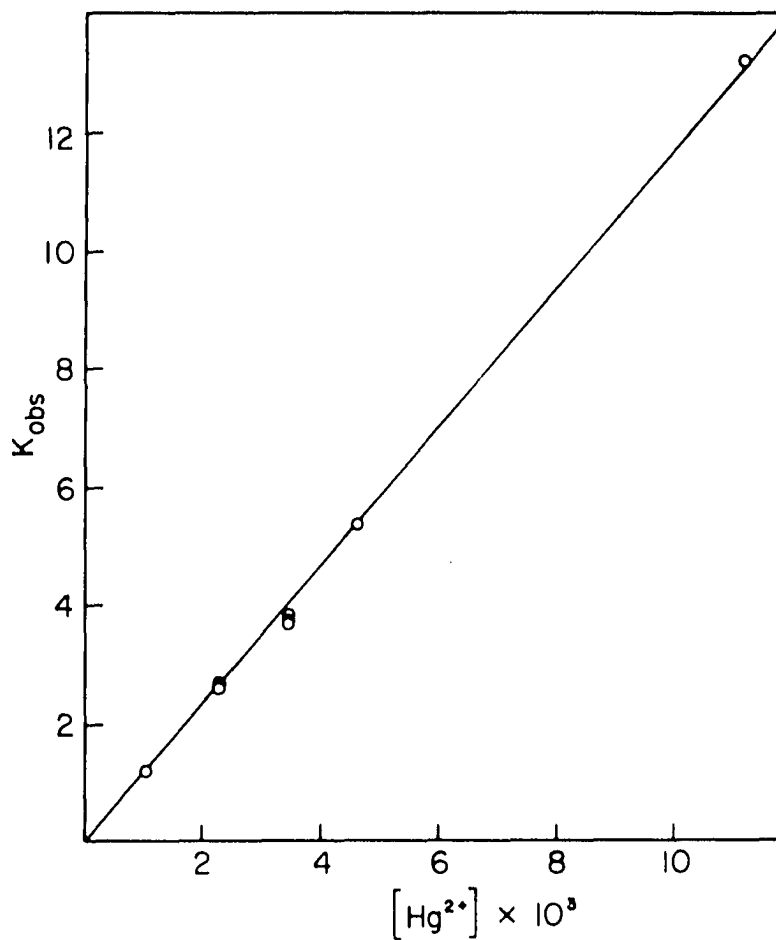


Figure II-10. Plot of k_{obs} vs $[Hg^{2+}]$ for the reaction of $benzylCr(L)^{2+}$ with Hg^{2+}

error establishing that there is no other reaction of significance except that of electrophilic attack by mercuric ion and that the reaction is properly described by equation II-8.

The results of the kinetic experiments are shown in Tables II-1 and II-2.

Though the reaction of Hg^{2+} with $\text{CH}_3\text{Cr}(\text{L})^{2+}$ was done under pseudo-first-order conditions, the concentrations used were so low, $[\text{Hg}^{2+}] = 4.66 \times 10^{-5} \text{ M}$, $[\text{RCr}(\text{L})^{2+}] = 5 \times 10^{-6} \text{ M}$, and the absorbance change even at $\lambda = 255 \text{ nm}$ so small, ~ 0.05 absorbance units, that the value of the rate constant for this reaction should be considered approximate.

It is assumed that all of the reactions of Hg^{2+} with $\text{RCr}([\text{15}] \text{aneN}_4)^{2+}$, just as in the case of its reactions with RCr^{2+} , are independent of $[\text{H}^+]$ at the concentrations used in this study.

Kinetics of CH_3Hg^+ reactions

Systematic kinetic studies were also carried out for the reactions of CH_3Hg^+ (from CH_3HgOAc in dilute HClO_4 , 0.50 M) with several of the above complexes, $\text{R} = \text{CH}_3$, CH_2CH_3 and benzyl. It proved near impossible to get accurate kinetic data on the rest of the complexes for two reasons. First, the CH_3HgR product insolubility clouded up the spectrophotometer cells and second, the slow rate at which the complexes would apparently react, i.e., $\text{R} = \text{isopropyl}$.

Table II-1. Kinetic data for the reactions of Hg^{2+} with $\text{RCr}([\text{15}] \text{aneN}_4)^{2+}$ complexes, R = primary alkyls. Conditions: $[\text{H}^+] = 0.25 \text{ M}$, $\mu = 0.50 \text{ M}$, $T = 25.0^\circ$

R	$10^4[\text{RCr(L)}^{2+}]$	$10^3[\text{Hg}^{2+}]$	λ/nm	$k_{\text{Hg}}(\text{dm}^3\text{mol}^{-1}\text{s}^{-1}) \pm \delta$ (#) ^a	Comment
Methyl	0.05	0.0466	255	$3.1 \pm 0.2 \times 10^6$ (2)	
Ethyl	1.3	1.165	268	$2.48 \pm 0.02 \times 10^3$ (2)	
	1.3	2.33	268	$2.60 \pm 0.03 \times 10^3$ (4)	
	1.3	4.66	268	$2.58 \pm 0.01 \times 10^3$ (2)	
	1.3	11.65	268	$2.54 \pm 0.04 \times 10^3$ (4)	
<u>n</u> -Propyl	0.9	1.165	268	81.2 ± 0.6 (2)	
	0.9	2.33	268	82.8 ± 0.6 (2)	
	0.9	3.495	268	83.7 ± 0.4 (2)	
	0.9	4.66	268	84.0 ± 0.7 (2)	
	0.9	5.825	268	82.8	
	0.9	11.65	268	81.1 ± 0.2 (2)	

^a δ is the average deviation with (#) the number of runs.

Table II-1. (Continued)

R	$10^4[\text{RCr(L)}^{2+}]$	$10^3[\text{Hg}^{2+}]$	λ/nm	$k_{\text{Hg}}(\text{dm}^3\text{mol}^{-1}\text{s}^{-1})\pm\delta$ (#) ^a	Comment
<u>n</u> -Butyl	2.0	2.33	268	46.6±0.8 (3)	
	2.0	3.495	268	52.4±0.3 (5)	
	2.0	4.66	268	48.2±0.1 (2)	
	2.0	5.825	268	45.8±0.5 (6)	
	2.0	11.65	268	48.9±1.0 (3)	
<u>n</u> -Pentyl	2.0	4.54	268	42.9±0.1 (2)	
	2.0	5.85	268	37.8±0.2 (2)	
	2.0	8.39	268	43.0±0.4 (3)	
	2.0	11.68	268	47.5±0.1 (2)	
Benzyl	1.0	1.165	297	1.08±0.01 x 10 ³ (3)	Done under O ₂ free conditions
	1.0	2.33	297	1.17±0.02 x 10 ³ (3)	
	1.0	3.495	297	1.11±0.02 x 10 ³ (4)	
	1.0	4.66	297	1.18±0.01 x 10 ⁴ (4)	
	1.0	11.65	297	1.15±0.01 x 10 ³ (3)	

Table II-2. Kinetic data for the reactions of Hg^{2+} with $\text{RCr}([\text{15}] \text{aneN}_4)^{2+}$ complexes, R = secondary and tertiary alkyls. Conditions: $[\text{H}^+] \cong 0.17 \text{ M}$, $\mu \cong 1.46 \text{ M}$, $T = 25.0^\circ$

R	$10^4 [\text{RCr}(\text{L})^{2+}]$	$[\text{Hg}^{2+}]$	λ/nm	$k_{\text{Hg}} (\text{dm}^3 \text{mol}^{-1} \text{s}^{-1})_{\pm\delta} (\#)^a$	Comment	
Isopropyl	2.0	0.216	310	4.7×10^{-3}	Apparent acidolysis needed Swinbourne value for A_∞ to give linear standard method plots	
	2.0	0.432	310	3.9×10^{-3}		
Cyclohexyl	2.0	0.216	323	2.0×10^{-3}		
	2.0	0.432	323	1.2×10^{-3}		
1-Adamantyl	2.0	0.216	310	3.2×10^{-3}		These runs were nicely linear with observed value for A_∞
	2.0	0.432	310	3.0×10^{-3}		

^a δ is the average deviation with (#) the number of runs.

Pseudo-first-order conditions were used in all cases with $[\text{CH}_3\text{Hg}^+]$ usually $\geq 10[\text{RCr(L)}^{2+}]$. Typical first-order plots using the standard method are shown in Figures II-11 and II-12. The linearity of these plots and all the others confirm the first-order dependence on $[\text{RCr(L)}^{2+}]$.

The results of these experiments are given in Table II-3. The second-order rate constants, $k_{\text{CH}_3\text{Hg}}$, were determined from the slope of k_{obs} vs $[\text{CH}_3\text{Hg}^+]$ plots, Figures II-13 - II-15. First-order dependence of the reaction rate on $[\text{CH}_3\text{Hg}^+]$ was confirmed by their linearity.

As in the case of the Hg^{2+} reactions, it again will be assumed that there is no dependence on $[\text{H}^+]$. Though a slight acid dependence was found for the reaction of CH_3Hg^+ with $\text{CH}_3\text{Cr}^{2+}$, no attempt was made to investigate this effect in the system under study. So a comparison between the very analogous reactions could be made, the same conditions were used, $[\text{H}^+] = 0.25 \text{ M}$ and $\mu = 0.50 \text{ M}$.

Activation Parameters - Isokinetic Relationships

The reaction of Hg^{2+} with RCr(L)^{2+} , R = ethyl, n-propyl, n-butyl, n-pentyl and benzyl were studied at different temperatures to provide the data necessary to

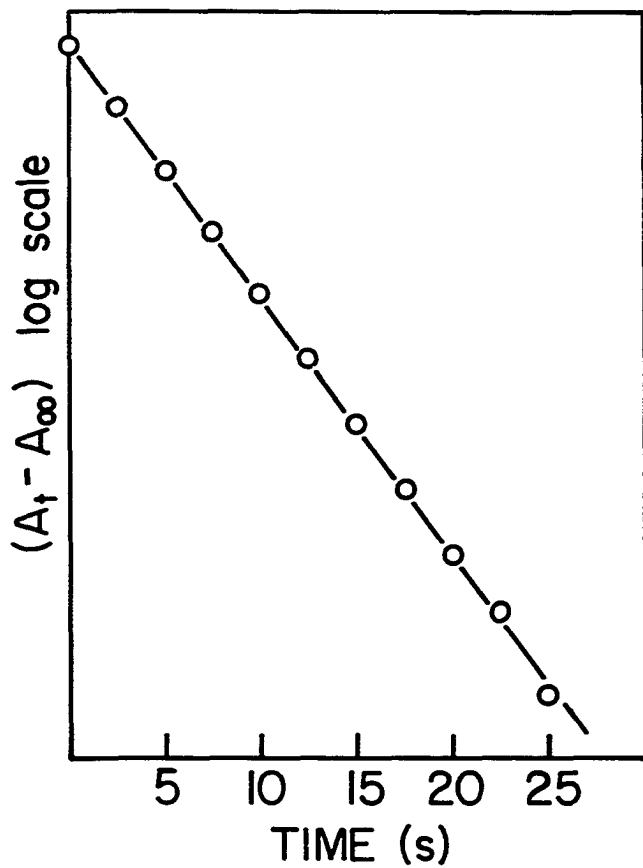


Figure II-11. Standard method plot for the reaction of ethylCr(L)²⁺ with CH₃Hg⁺

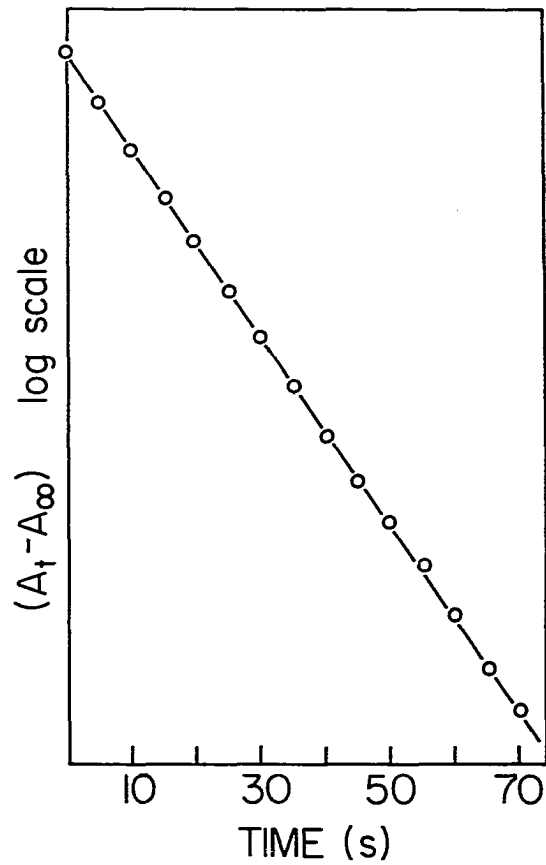


Figure II-12. Standard method plot for the reaction of benzylCr(L)²⁺ with CH₃Hg⁺

Table II-3. Kinetic data for the reaction of CH_3Hg^+ with $\text{RCr}([\text{15}] \text{aneN}_4)^{2+}$.
 Conditions: $[\text{H}^+] = 0.25 \text{ M}$, $\mu = 0.50 \text{ M}$, $T = 25.0^\circ$

R	$[\text{RCr(L)}]^{2+}$	$10^3[\text{CH}_3\text{Hg}^+]$	λ/nm	$k_{\text{CH}_3\text{Hg}}$ ($\text{dm}^3\text{mol}^{-1}\text{s}^{-1}$) $\pm\delta$ (#) ^a
Methyl	2.4×10^{-5}	1.04	285	$1.57 \pm 0.03 \times 10^3$ (3)
		2.09	285	$1.55 \pm 0.04 \times 10^3$ (3)
		3.67	285	$1.50 \pm 0.02 \times 10^3$ (3)
		6.31	285	$1.65 \pm 0.02 \times 10^3$ (3)
		8.93	285	$1.67 \pm 0.03 \times 10^3$ (3)
Ethyl	1.8×10^{-4}	0.94	300	11.2
		0.94	300	9.0
		3.76	300	11.2
		4.78	300	9.63
		6.02	300	9.97
		7.43	300	10.1
Benzyl	6×10^{-5}	0.94	300	5.43
		1.88	300	5.29
		2.81	300	5.34
		3.76	300	5.24
		4.70	300	5.44
		6.57	300	5.19

^a δ is the average deviation with (#) the number of runs.

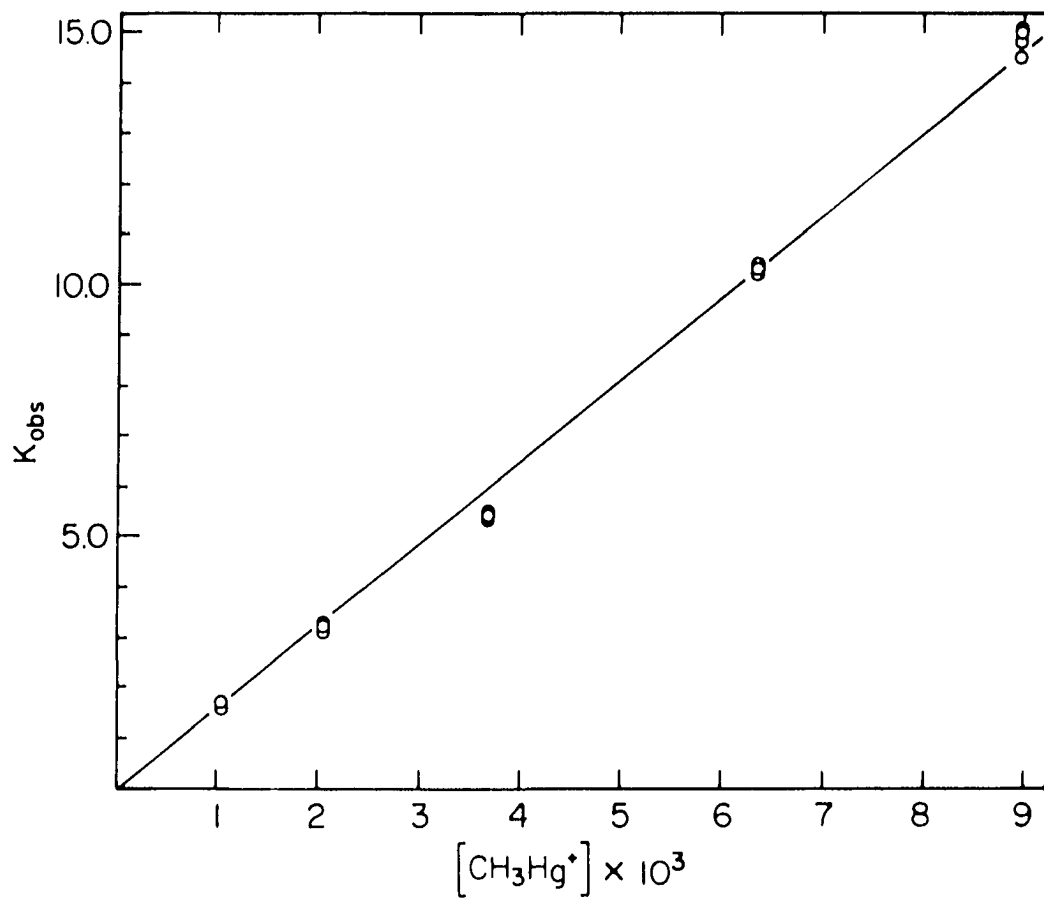


Figure II-13. Plot of k_{obs} vs $[\text{CH}_3\text{Hg}^+]$ for the reaction of methylCr(L)^{2+} with CH_3Hg^+

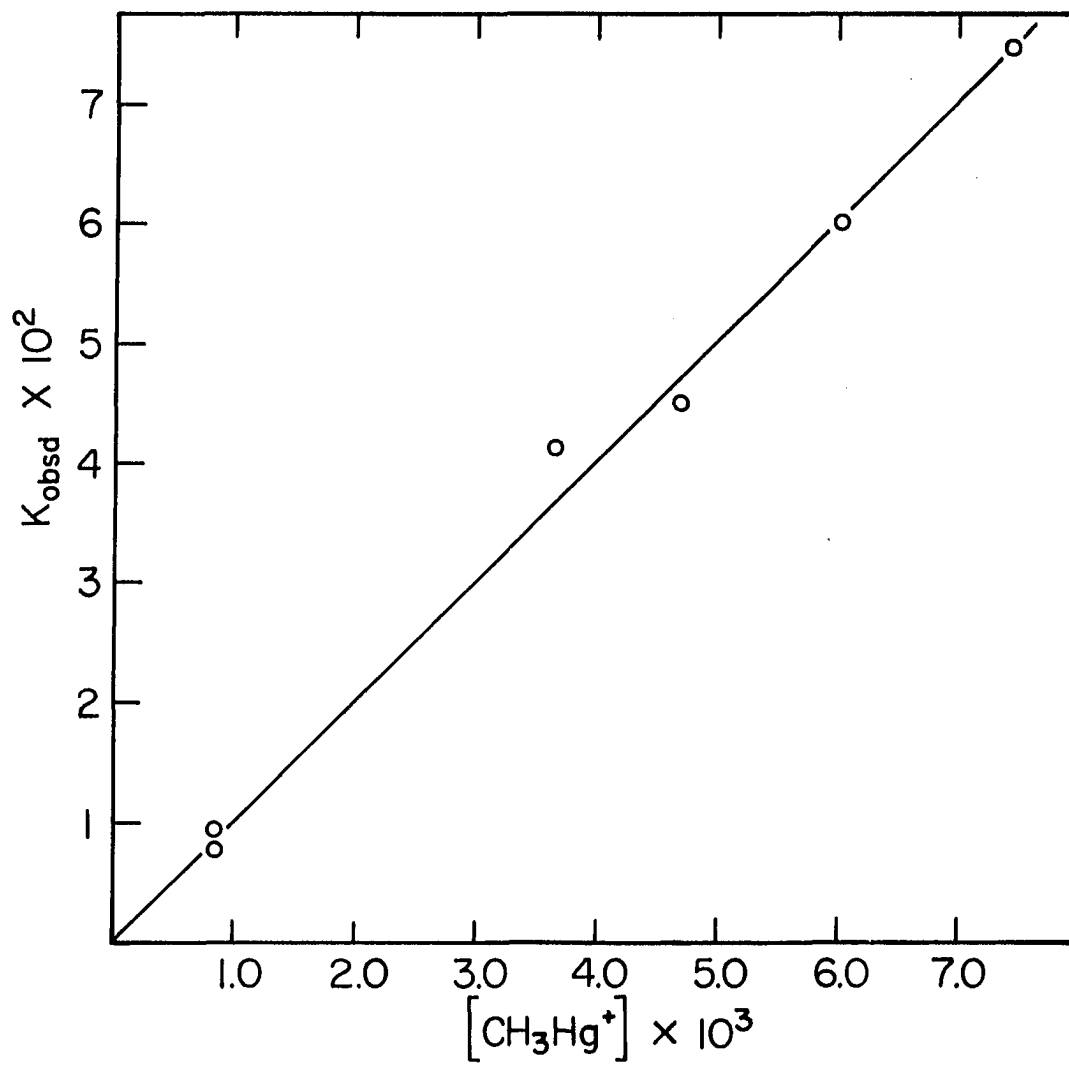


Figure II-14. Plot of k_{obs} vs $[\text{CH}_3\text{Hg}^+]$ for the reaction of ethylCr(L)^{2+} with CH_3Hg^+

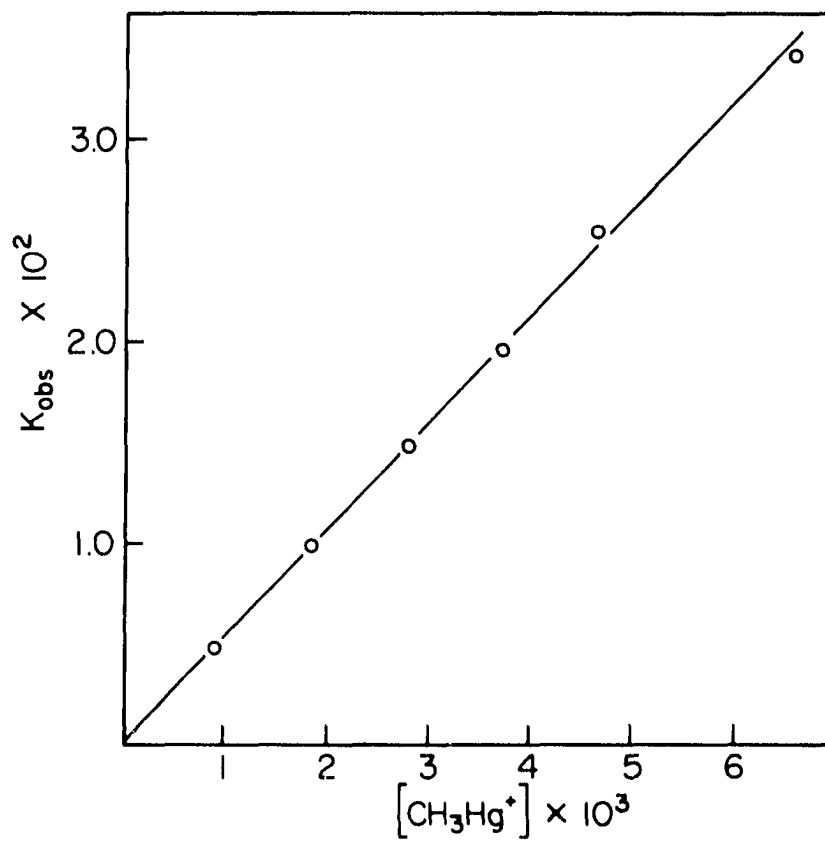


Figure II-15. Plot of k_{obs} vs $[\text{CH}_3\text{Hg}^+]$ for the reaction of benzylCr(L)^{2+} with CH_3Hg^+

evaluate activation parameters. These data are shown in Tables II-4 - II-8. The values of ΔH^\ddagger and ΔS^\ddagger for the above reactions were computed using the Eyring equation,

$$\ln \frac{k}{T} = \ln \frac{R}{Nh} + \frac{\Delta S^\ddagger}{R} - \frac{\Delta H^\ddagger}{RT} \quad (\text{II-9})$$

with R being the gas constant, N is Avogadro's number and h is Plank's constant. From a plot of $\ln(k/T)$ vs $1/T$, the values of ΔH^\ddagger and ΔS^\ddagger were determined from the slope and intercept by a least squares fit of the data.

Representative Eyring plots are shown in Figures II-16 - II-19, with the experimental points used for the calculation. The values at 25° have the appropriate error bars. These results are summarized in Table II-9 and will be discussed later.

In the field of organic chemistry, it is not uncommon that changes in reaction rate for a series of reactions involving common type reactants to be correlated by parallel changes in ΔH^\ddagger and ΔS^\ddagger . This concept has made little impact in the area of transition metal reactions.

Because of requirements of the thermodynamic equation II-10 proportionality of any of the variations, i.e., ΔH ,

$$F = H - TS \quad (\text{II-10})$$

to any of the others, i.e., ΔF , demands proportionality to the third.

Table II-4. Temperature dependence of the rate of reaction of Hg^{2+} with ethylCr(L)^{2+} . Conditions: $[\text{H}^+] = 0.25 \text{ M}$, $\mu = 0.50 \text{ M}$

$T(^{\circ}\text{C})$	k_{Hg} ($\text{dm}^3\text{mol}^{-1}\text{s}^{-1}$)
18.2	1.82×10^3
18.2	1.82×10^3
20.7	2.04×10^3
20.7	2.05×10^3
25.0	$2.53 \pm 0.02 \times 10^3$ (ave)
26.8	2.74×10^3
26.8	2.76×10^3
26.8	2.73×10^3
30.3	3.11×10^3
30.3	3.07×10^3
30.3	3.13×10^3

Table II-5. Temperature dependence of the rate of reaction of Hg^{2+} with $n\text{-propylCr(L)}^{2+}$. Conditions: $[\text{H}^+] = 0.25 \text{ M}$, $\mu = 0.50 \text{ M}$

$T(^{\circ}\text{C})$	k_2 ($\text{dm}^3\text{mol}^{-1}\text{s}^{-1}$)
15.5	39.4
15.5	38.9
17.7	47.8
17.7	49.1
20.5	58.7
20.5	59.4
25.0	82.1 \pm 0.4 (ave)
29.0	102.0
29.0	103.0

Table II-6. Temperature dependence of the rate of reaction of Hg^{2+} with n -butylCr(L) $^{2+}$. Conditions: $[\text{H}^+] = 0.25 \text{ M}$, $\mu = 0.50 \text{ M}$

$T(^{\circ}\text{C})$	k_{Hg} ($\text{dm}^3\text{mol}^{-1}\text{s}^{-1}$)
19.8	38.2
19.8	37.8
22.5	44.9
22.5	44.8
25.0	48.9 \pm 1.7 (ave)
28.1	57.7
28.1	57.8
28.1	58.4
31.9	69.6
31.9	69.4

Table II-7. Temperature dependence of the rate of reaction of Hg^{2+} with $n\text{-pentylCr(L)}^{2+}$. Conditions: $[\text{H}^+] = 0.25 \text{ M}$, $\mu = 0.50 \text{ M}$

$T(^{\circ}\text{C})$	k_{Hg} ($\text{dm}^3\text{mol}^{-1}\text{s}^{-1}$)
19.7	33.4
20.0	33.9
20.0	34.6
22.6	37.6
22.6	37.8
25.0	43.3 \pm 2
29.0	48.5
29.0	49.6
30.8	54.7
30.8	55.0
30.8	55.5

Table II-8. Temperature dependence of the rate of reaction of Hg^{2+} with benzylCr(L)^{2+} . Conditions: $[\text{H}^+] = 0.25 \text{ M}$, $\mu = 0.50 \text{ M}$

$T(^{\circ}\text{C})$	k_{Hg} ($\text{dm}^3\text{mol}^{-1}\text{s}^{-1}$)
19.6	846
19.6	848
19.6	864
22.8	959
22.8	975
22.8	990
25.0	1140±33
28.9	1320
28.9	1374
28.9	1296
28.9	1332
31.9	1539
31.9	1543
31.9	1536

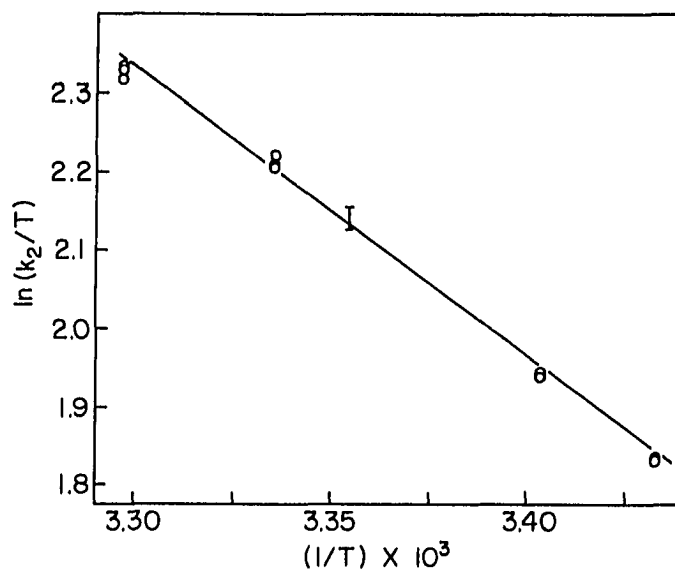


Figure II-16. Eyring plot for the reaction of ethylCr(L)²⁺ with Hg²⁺

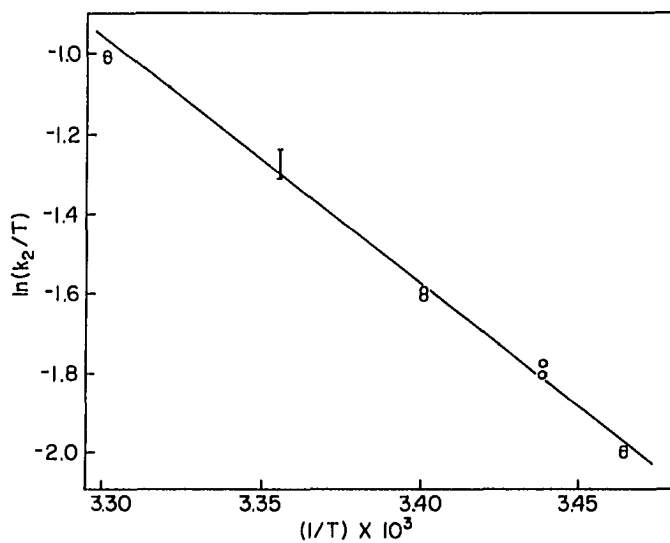


Figure II-17. Eyring plot for the reaction of n-propylCr(L)²⁺ with Hg²⁺

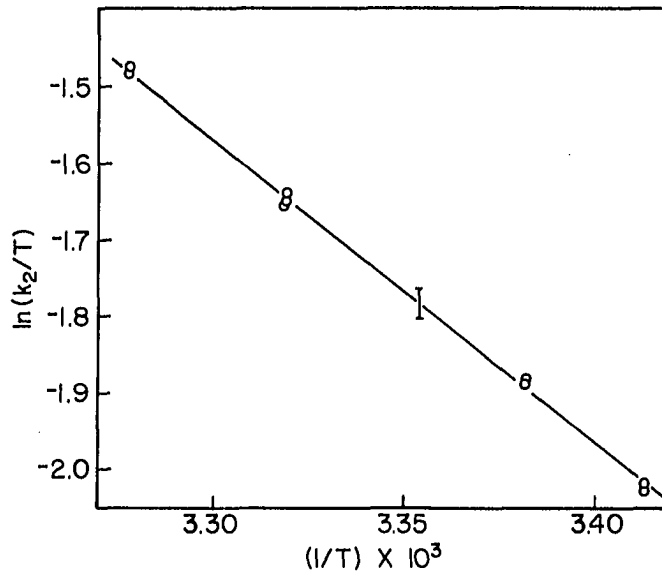


Figure II-18. Eyring plot for the reaction of n -butylCr(L) $^{2+}$ with Hg^{2+}

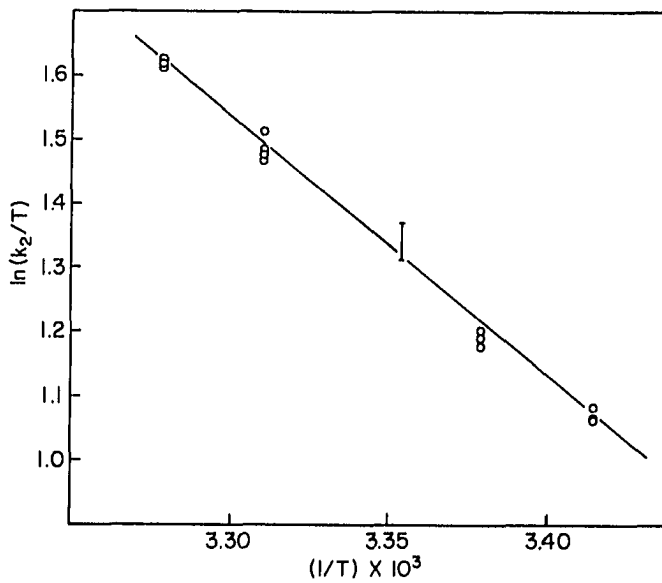


Figure II-19. Eyring plot for the reaction of benzylCr(L) $^{2+}$ with Hg^{2+}

Table II-9. Activation parameters for the reaction of Hg^{2+} with $\text{R-Cr}([\text{15}] \text{aneN}_4)^{2+}$

#	R	ΔH^\ddagger KJ(mol) ⁻¹	ΔS^\ddagger J(mol) ⁻¹ K ⁻¹
1	Ethyl	30.2±1.2	-77.2±3.9
2	<u>n</u> -Propyl	48.8±1.5	-44.7±5.1
3	<u>n</u> -Butyl	33.5±2.1	-99.9±7.0
4	<u>n</u> -Pentyl	29.7±1.2	-114.1±4.0
5	Benzyl	33.4±1.6	-74.5±5.2

Since fairly accurate values of ΔH^\ddagger and ΔS^\ddagger have been obtained for five $\text{R-Cr}([\text{15}] \text{aneN}_4)^{2+}$ complexes in their reactions with Hg^{2+} (Table II-9), a thermodynamic relationship to correlate the reaction rates was sought.

A plot of $\Delta \bar{H}^\ddagger$ vs $-\Delta \bar{S}^\ddagger$ was constructed as shown in Figure II-20. There is no apparent correlation in this plot. What might have been expected was a linear relationship with the slope of the plot equal to the absolute temperature, T, the isokinetic temperature at which all the represented reactions would occur at the same rate (70,71).

Since it is clear that there is no correlation, there must be a reason for this. Leffler and Grunwald (72) consider a failure to obtain a correlation for an isokinetic

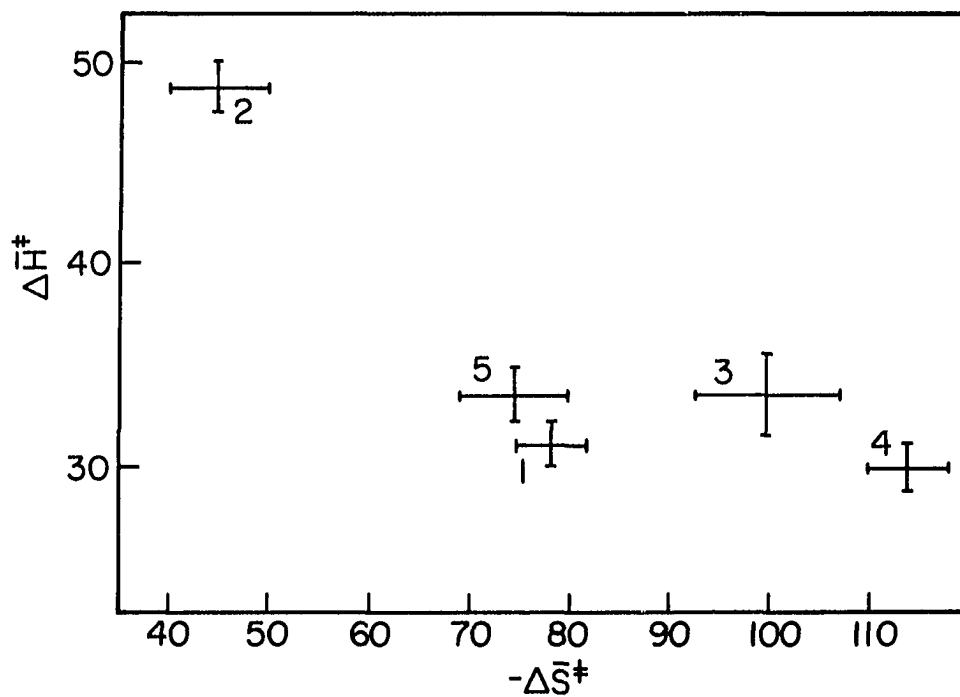


Figure II-20. Plot of ΔH^\ddagger vs $-\Delta S^\ddagger$. The numbers correspond to the data in Table II-9

relationship indicative of more than one manner in which a substituent may influence the reaction site. Besides the added electronic effect of more alkyl substituents on the carbon attached to chromium, there is also steric crowding at the site of reaction due to this addition. It is just this sort of influence which can cause the failure in an attempted isokinetic relationship (71).

DISCUSSION

The rate law for the reactions of Hg(II) electrophiles with all $\text{RCr}([\text{15}] \text{aneN}_4)^{2+}$ complexes is as written in equation II-8. Thus, all of the reactions studied are second order as required by the $\text{S}_{\text{E}}2$ mechanism.

In the case of the reaction with Hg^{2+} , their rates are much faster than the corresponding reaction rates of CH_3Hg^+ with the same substrate. This is readily explained and is the expected rate trend for Hg^{2+} which is a much more potent electrophile than CH_3Hg^+ . In the reaction with Hg^{2+} in excess, it is assumed that only Hg^{2+} reacts even though some CH_3Hg^+ is present after the reaction is initiated because $[\text{Hg}^{2+}] > [\text{CH}_3\text{Hg}^+]$ and that Hg^{2+} is the better electrophile.

The rate of reaction with only one other organomercurial, EtHg^+ , was determined. Its rate of reaction with $\text{EtCr}(\text{L})^{2+}$, $k = 8.2 \text{ dm}^3 \text{ mol}^{-1} \text{ s}^{-1}$, is only slightly different from that of CH_3Hg^+ , $k = 9.9 \text{ dm}^3 \text{ mol}^{-1} \text{ s}^{-1}$. There does not appear to be much of a steric effect in agreement with the results obtained by Leslie and Espenson (27b). The electrophilicity does not differ significantly in these two species as expected since the charge resides primarily upon the metal. As before, the change of R on RHg^+ does not alter the reaction.

A summary of the second-order rate constants for the reaction of Hg^{2+} with $\text{RCr}([\text{15}] \text{aneN}_4)^{2+}$ may be found in

Table II-10. The values for the reaction of CH_3Hg^+ with $\text{RCr}([\text{15}] \text{aneN}_4)^{2+}$ may be found in Table II-11. A comparison of these rate constants with the reactions of the same two electrophiles with RCr^{2+} is located in Table II-12. The trends in these data will be discussed below.

The most apparent trend in Table II-10 is the rapid decrease in reaction rate as one progresses from methyl on down the linear alkyls. Yet, a plateau appears in the data approximately after n -butyl $\text{Cr}(\text{L})^{2+}$. The most apparent explanation would seem to be a steric leveling in the rate. Based upon stick models, the α carbon becomes more and more sterically blocked, by various conformations, as the size of the alkyl chain increases. But when models of n -butyl and n -pentyl $\text{Cr}(\text{L})^{2+}$ are compared, there appears to be little difference in the shielding of the carbon-chromium bond.

Another dramatic drop in the reaction rate is manifest when one compares the rate of reaction of a primary alkyl with that of either secondary alkyl. Again, steric hindrance at the site of reaction appears to be the simplest explanation for the sharp decrease in rate. Here also, the rate for the less hindered isopropyl complex is a factor of 2 faster than that of the more hindered cyclohexyl complex. The decrease in rate with increase in chain length and branching is seen for the reactions of Hg^{2+} with RCr^{2+} (Table II-12), yet the rate of decrease is not as sharp. In

Table II-10. Summary of reaction rates for Hg^{2+} with RCr(L)^{2+} .

Conditions: $[\text{H}^+] = 0.25 \text{ M}$, $\mu = 0.50 \text{ M}$, $T = 25.0^\circ$

R	$[\text{RCr(L)}^{2+}]$	$[\text{Hg}^{2+}]$	λ/nm	$k_{\text{Hg}} \pm \delta \text{ (dm}^3\text{mol}^{-1}\text{s}^{-1}\text{)}$
Methyl	5×10^{-6}	4.66×10^{-5}	255	$3.1 \pm 0.2 \times 10^6$
Ethyl	1.3×10^{-4}	$1.16\text{--}11.65 \times 10^{-3}$	268	$2.53 \pm 0.03 \times 10^3$
<u>n</u> -Propyl	9×10^{-5}	$1.16\text{--}11.65 \times 10^{-3}$	268	$82.1 \pm 0.4 \times 10^1$
<u>n</u> -Butyl	2×10^{-4}	$2.33\text{--}11.65 \times 10^{-3}$	268	$4.88 \pm 0.17 \times 10^1$
<u>n</u> -Pentyl	2×10^{-4}	$4.54\text{--}11.65 \times 10^{-3}$	268	$4.33 \pm 0.2 \times 10^1$
Isopropyl ^{a,b}	2×10^{-4}	$2.16\text{--}4.32 \times 10^{-1}$	310	$4.3 \pm 0.4 \times 10^{-3}$
Cyclohexyl ^{a,b}	2×10^{-4}	$2.16\text{--}4.32 \times 10^{-1}$	323	$1.6 \pm 0.4 \times 10^{-3}$
Adamantyl ^a	2×10^{-4}	$2.16\text{--}4.32 \times 10^{-1}$	310	$3.1 \pm 0.1 \times 10^{-3}$
Benzyl ^b	1×10^{-4}	$1.16\text{--}11.65 \times 10^{-3}$	297	$1.14 \pm 0.03 \times 10^3$

^aConditions $[\text{H}^+] \cong 0.17 \text{ M}$, $\lambda \cong 1.46 \text{ m}$, $T = 25.0^\circ$.

^bOxygen free. $\delta =$ Average deviation.

Table II-11. Summary of reaction rates for CH_3Hg^+ with RCr(L)^{2+} .
 Conditions: $[\text{H}^+] = 0.25 \text{ M}$, $\mu = 0.50 \text{ M}$, $T = 25.0^\circ$

R	$[\text{RCr(L)}^{2+}]$	$[\text{CH}_3\text{Hg}^+]$	λ/nm	$k_{\text{CH}_3\text{Hg}^+} \pm \delta \text{ (dm}^3\text{mol}^{-1}\text{s}^{-1}\text{)}$
Methyl	2.4×10^{-5}	$1.04\text{--}8.93 \times 10^{-3}$	285	$1.63 \pm 0.02 \times 10^3$
Ethyl	1.8×10^{-4}	$0.94\text{--}7.43 \times 10^{-3}$	300	9.9 ± 0.4
Benzyl ^a	6×10^{-5}	$0.94\text{--}6.57 \times 10^{-3}$	300	5.2 ± 0.1

^aOxygen free conditions. δ is the average deviation.

Table II-12. Summary of reaction rates of Hg(II) with organochromium cations, $k/\text{dm}^3\text{mol}^{-1}\text{s}^{-1}$. Conditions: $[\text{H}^+] = 0.25 \text{ M}$, $\mu = 0.50 \text{ M}$, $T = 25.0^\circ$

R	$\text{Hg}^{2+}/\text{RCr(L)}^{2+}$	$\text{Hg}^{2+}/(\text{H}_2\text{O})_5\text{CrR}^a$	$\text{CH}_3\text{Hg}^+/\text{RCr(L)}^{2+}$	$\text{CH}_3\text{Hg}^+/\text{(H}_2\text{O)}_5\text{Cr}_5\text{R}^a$
Methyl	3.1×10^6	1×10^7	1.63×10^3	1.0×10^4
Ethyl	2.53×10^3	1.4×10^5	9.9	1.99×10^2
<u>n</u> -Propyl	8.2×10^1	3.5×10^4	---	---
Isopropyl	$4.3 \times 10^{-3}{}^{b,c}$	1.56^c	---	---
Benzyl	$1.14 \times 10^3{}^c$	$4.87 \times 10^4{}^c$	5.2^c	$9.8 \times 10^1{}^c$

^aData from reference 27(b).

^b $[\text{H}^+] \cong 0.17 \text{ M}$, $\mu \cong 1.46 \text{ M}$.

^cOxygen free conditions.

the case of the reaction of Hg^{2+} with isopropylCr^{2+} , two additional side reactions of the chromium complex were noticed. The first being its sensitivity to oxygen and second, hydrolysis of the carbon-chromium bond. Neither of these reactions interfere with the electrophilic cleavage of this bond. The sensitivity toward oxygen of RCr(L)^{2+} , $\text{R} = \text{isopropyl}$ and cyclohexyl , was qualitatively observed on the bench top. Since only a narrow $[\text{H}^+]$ was used, no attempt was made to investigate the hydrolysis of these species.

The rate of reaction of $\text{l-adamantylCr(L)}^{2+}$ is just as rapid if not more so than that of $\text{cyclohexylCr(L)}^{2+}$. Yet, this chromium-carbon bond has no readily approachable avenue for electrophilic attack and its rate of reaction was expected to be much slower. The reaction is bimolecular and first order in $[\text{Hg}^{2+}]$ as testified by Figure II-4, which rules out a unimolecular reaction independent of $[\text{Hg}^{2+}]$. It was also shown in a single experiment with $[\text{H}^+] = 0.17 \text{ M}$, $\mu = 1.46 \text{ M}$ that the rate of disappearance of RCr(L)^{2+} was $k_2 < 8 \times 10^{-6} \text{ s}^{-1}$.

The only major difference between RCr(L)^{2+} and RCr^{2+} is the macrocycle, $[\text{15}] \text{aneN}_4$. There appear to be at least two factors at work. First, the macrocycle adds considerable bulk around the chromium-carbon bond, the site of reactivity. This added hydrophobic "skirt" could increase steric

hindrance of the reaction site and mediate the rate at which Hg^{2+} (hydrophilic) approaches the α -carbon. Second would be the increased electron density on the chromium center due to the fact that amine nitrogens are much better sigma electron donors than the oxygen of water. This would reduce the effective positive charge on chromium resulting in a decreased polarization of the carbon chromium bonds making the α -carbon less susceptible to electrophilic attack.

As in the case of the reactions with RCr^{2+} , the rates of the CH_3Hg^+ reactions do not exactly parallel the reactions of Hg^{2+} (68), Tables II-11 and II-12. The rate differences seem to be more pronounced for the CH_3Hg^+ reactions. The only significant difference between these two species is their electrophilicity. As shown before (68), and illustrated with an example from this work, EtHg^+ , the rate differences between electrophiles do not appear to be steric in origin.

The slightly steeper change in rate for the CH_3Hg^+ reactions as compared to Hg^{2+} might be due to the differences in solvation of these ions. Because of the lower charge and hydrophobic nature of the methyl group on CH_3Hg^+ , this species would not be as highly solvated as Hg^{2+} . Since the waters of solvation would be more strongly bound by Hg^{2+} , one might expect it to exhibit more steric crowding at the site of reaction. The methyl group attached to the mercury,

in the case of CH_3Hg^+ , might also help this electrophile to more easily overcome the hydrophobic barrier induced by the macrocycle.

Due to the presence of radical intermediates in the formation of these complexes, $\text{RCr}([\text{15}] \text{aneN}_4)^{2+}$, it is experimentally impossible to synthesize an optically active organochromium species using this method. Because of this inherent difficulty, it is impossible to definitively assign a stereochemical course to the electrophilic cleavage reactions induced by CH_3Hg^+ and Hg^{2+} . Yet, as before (68), it might be possible to suggest a stereochemistry for this reaction by comparison of rate trends for $\text{S}_{\text{E}}2$ reactions of known stereochemistry. The results of these reactions are shown in Table II-13.

There is no good comparison with any of the reactions in Table II-13 that are of known stereochemistry. Yet, if one had to choose a reaction stereochemistry, the data best fits an inversion process. Again, it can be seen for all these reactions the one with the most definitive steric effect on the rate is the reaction of Hg^{2+} with $\text{RCr}([\text{15}] \text{aneN}_4)^{2+}$. The only complex which shows even a comparable range in reaction rates is, curiously enough, the chelated organocobalt complex, $\text{RCo}(\text{dmgH})_2\text{OH}_2$. One should be wary of this conclusion for there are only a

Table II-13. Relative rate trends, k_R/k_{Et} , for various S_E2 (open) reactions of metal alkyls, R = aliphatic^a

Reaction	Stereochemistry	R=CH ₃	C ₂ H ₅	C ₃ H ₇	CH(CH ₃) ₂
RCr(L) ²⁺ + Hg ²⁺ ^{b,c}		1180	1.0	0.032	1.6 x 10 ⁻⁶
(H ₂ O) ₅ Cr-R ²⁺ + Hg ²⁺ ^c		71	1.0	0.25	1.1 x 10 ⁻⁵
RCr(L) ²⁺ + CH ₃ Hg ⁺ ^{b,c}		1650	1.0	---	---
(H ₂ O) ₅ Cr-R + CH ₃ Hg ⁺ ^c		50	1.0	0.61	---
RCo(dmgh) ₂ OH ₂ + Hg ²⁺ ^c	Inversion	530	1.0	0.74	<5 x 10 ⁻⁶
RSn(neoC ₅ H ₁₁) ₃ + Br ₂ ^d	Inversion	6.9	1.0	0.28	5.2 x 10 ⁻²
RHgBr + HgBr ₂ ^e	Retention	2.4	1.0	---	---

^aThese data were taken from references 27(b) and 68 though this was not the original source.

^bThis work.

^cIn H₂O at 25°.

^dIn methanol, T = 45°.

^eIn ethanol, T = 100°.

Table II-13. (Continued)

Reaction	Stereochemistry	R=CH ₃	C ₂ H ₅	C ₃ H ₇	CH(CH ₃) ₂
HCl + R ₂ Hg ^f	Retention	0.16	1.0	0.62	0.68
"S _N 2"	Inversion	33	1.0	0.04	3 x 10 ⁻³

^fIn DMSO, T = 50°.

limited number of examples of inversion for the electrophilic reactions of Hg(II) species (66(a), p. 111, (73), (74) and (75)).

The activation parameters for the reaction of Hg^{2+} with $\text{RCr}([\text{15}] \text{aneN}_4)^{2+}$ were previously tabulated in Table II-9. These values along with the parameters determined for several RCr^{2+} complexes are listed in Table II-14. The large rate variations for all the $\text{RCr}(\text{L})^{2+}$ complexes are best explained by changes in ΔS^\ddagger , except $\text{R} = \text{n-propyl}$. The values of ΔS^\ddagger for these four reactions roughly parallel the increase in bulk around the reaction site; this seems to imply that the alkyl chain must become more ordered in the transition state. The anomaly in this series is $\text{n-propylCr}(\text{L})^{2+}$. The reason for its high ΔH^\ddagger and low ΔS^\ddagger is not readily apparent. This behavior is also manifest in the isokinetic plot, Figure II-20. Though this plot has no apparent correlation, for all but $\text{R} = \text{n-propyl}$ there seems to be an isoenthalpic relationship, such that the change of the R-group does not influence the value of ΔH^\ddagger . One would like to say that the value of ΔH^\ddagger is related to the carbon-chromium bond strength with all the other factors (*i.e.*, solvent rearrangement) being essentially constant.

There is a striking difference when one compares these reactions to those of RCr^{2+} . Here the value of ΔS^\ddagger is essentially constant for very different compounds,

Table II-14. Summary of the activation parameters for the reaction of Hg(II) with organochromium cations.
 Conditions: $[H^+] = 0.25 \text{ M}$, $\mu = 0.50 \text{ M}$

Reaction	$\Delta H^\ddagger / \text{kJ mol}^{-1}$	$\Delta S^\ddagger / \text{J mol}^{-1} \text{K}^{-1}$
$\text{Hg}^{2+} + \text{C}_2\text{H}_5\text{Cr(L)}^{2+}$	30.2 ± 1.2	-77.2 ± 3.9
$\text{Hg}^{2+} + \text{n-C}_3\text{H}_7\text{Cr(L)}^{2+}$	48.8 ± 1.5	-44.7 ± 5.1
$\text{Hg}^{2+} + \text{n-C}_4\text{H}_9\text{Cr(L)}^{2+}$	33.5 ± 2.1	-99.9 ± 7.0
$\text{Hg}^{2+} + \text{n-C}_5\text{H}_{11}\text{Cr(L)}^{2+}$	29.7 ± 1.2	-114.1 ± 4.0
$\text{Hg}^{2+} + \text{C}_6\text{H}_5\text{CH}_2\text{Cr(L)}^{2+}$	33.4 ± 1.6	-74.5 ± 5.2
$\text{Hg}^{2+} + \text{n-C}_3\text{H}_7\text{-Cr(H}_2\text{O)}_5^{2+ \text{a}}$	13.8 ± 3.3	-111 ± 11
$\text{Hg}^{2+} + \text{ClCH}_2\text{Cr(H}_2\text{O)}_5^{2+ \text{a}}$	39.8 ± 0.8	-116 ± 3
$\text{CH}_3\text{Hg}^+ + \text{n-C}_3\text{H}_7\text{Cr(H}_2\text{O)}_5^{2+}$	28.6 ± 2.4	-109 ± 8

^aData from reference 26(b).

R = $\underline{n}\text{-C}_3\text{H}_7$ vs $\underline{\text{CH}_2\text{Cl}}$ and different reactions, Hg^{2+} and CH_3Hg^+ .

In the case of the reaction of Hg^{2+} with RCr^{2+} and RCr(L)^{2+} , R = $\underline{n}\text{-C}_3\text{H}_7$, the values in Table II-14 are quite different. Even after taking into account the apparent anomalous behavior of $\underline{n}\text{-C}_3\text{H}_7\text{Cr(L)}^{2+}$ and using average values for ΔH^\ddagger and ΔS^\ddagger , the value of ΔH^\ddagger for the RCr(L)^{2+} species is still twice as large as the corresponding value for the reaction of Hg^{2+} with $\underline{n}\text{-C}_3\text{H}_7\text{Cr}^{2+}$ with the corresponding values of ΔS^\ddagger are being approximately the same.

PART III. THE CRYSTAL STRUCTURE OF [trans-CHLOROQUO-
(1,4,8,12-TETRAAZACYCLOPENTADECANE)-
CHROMIUM(III)]DIODIDE-DIHYDRATE

INTRODUCTION

With the large amount of data available for chromium complexes with nitrogen donors (53), it is surprising that comparatively few structures have been determined (76). Chromium complexes with macrocyclic ligands containing nitrogen donors have been devoted little attention considering the different properties that they impart upon the metal center, i.e., stabilization of unusual oxidation states (77) and the aid they have provided in the elucidation of reaction mechanisms (78).

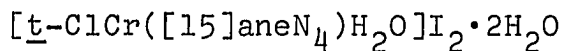
The prototypes for all the macrocyclic amine ligands are saturated cyclic tetraamines.

The structures of metal complexes of 1,4,8,11-tetraazacyclotetradecane([14]aneN₄) (79) and related tetraazacycloalkanes (80) have been reported. 1,5,9,13-Tetraazacyclohexadecane([16]aneN₄) has had its structure determined as a free amine (81). Yet, as of this time, no one has reported the structure of a saturated 15-member tetraazamacrocyclic.

The structural determination of [trans-chloroaquo-(1,4,8,12-tetraazacyclopentadecane)chromium(III)]diiodidedihydrate is now reported.

EXPERIMENTAL

Preparations



This complex was prepared from a solution of $t\text{-BrCr(L)}^{2+}$ ($\sim 3 \text{ M}$, 20 ml) resulting from the reaction of $n\text{-propyl}$ bromide with Cr(L)^{2+} which was acidified, $\text{pH} \approx 2$ with HCl and had NaI (0.3 M) added in an attempt to prepare the analogous bromide complex. The solution was allowed to sit in a freezer for several months before black crystals were noticed. The chlorine/chromium/iodine ratio, 1:1:2, was determined by electron microprobe (82), using the peak area, Figure III-1, before data analysis was started.

Crystal data

A multifaceted cone-shaped fragment suitable for analysis was cut from a larger grouping of black crystals. Its maximum dimensions were approximately $0.3 \times 0.15 \times 0.13$ mm. The crystal was mounted on the end of a glass fiber with Duco cement. Using preliminary ω oscillation photographs on an automated four-circle diffractometer at several χ and ϕ settings, ten moderately strong reflections were recorded and input into an automatic indexing program (83). The reduced cell and reduced cell scalars which were determined indicated a monoclinic crystal system. The monoclinic system, m symmetry, was confirmed by inspection

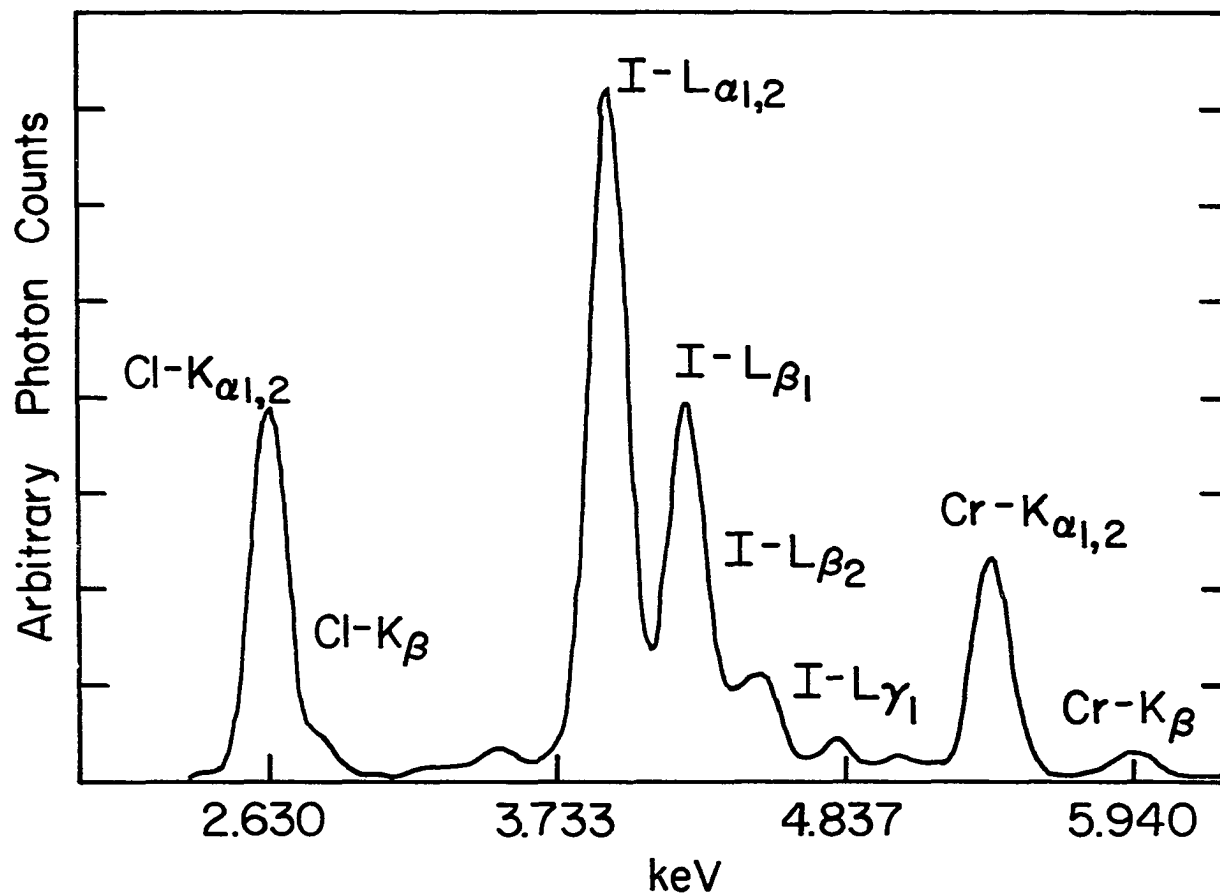


Figure III-1. X-ray emission from electron microprobe analysis of [trans-ClCr(L)H₂O](I)₂·2H₂O

of the three axial ω -oscillation photographs which were then taken.

A least-squares refinement of the lattice constants (84) determined by the $\pm 2\theta$ measurements of ten reflections, $27.9^\circ < 2\theta < 40.7^\circ$, on a previously aligned four-circle diffractometer (graphite-monochromated Mo K_α radiation, $\lambda = 0.70954\text{\AA}$) at 25°C , yielded $a = 12.978(7)$, $b = 11.898(5)$, and $c = 15.236(9)$ with $\beta = 114.10(5)^\circ$. The measured density of 1.76 gcm^{-3} obtained by flotation in $\text{CH}_3\text{I-HCCl}_3$ agrees well with the calculated density of 1.72 gcm^{-3} for $Z=4$.

Collection and Reduction of X-ray

Intensity Data

Data were collected at 25°C using an automated four-circle diffractometer designed and built in the Ames Laboratory. The upper full circle was purchased from STOE and is equipped with Baldwin Optical encoders and drive motors. The design of the base allows the encoders to be directly connected to the main θ and 2θ shafts, using solid- and hollow-shaft encoders, respectively. The diffractometer is interfaced to a PDP-15 computer in a time-sharing mode and is equipped with a scintillation counter. Graphite-monochromated Mo K_α radiation ($\lambda = 0.70954\text{\AA}$) was used for data collections. Stationary-crystal, stationary counter background measurements for

6 seconds were made $\pm 0.5^\circ$ from the calculated peak center ω value (B_1 and B_2). Scans from peak center in both positive and negative directions of ω were made in steps of 0.01° , counting for 0.5 seconds at each step until the increment count was less than or equal to the minimum of the backgrounds, after adjustment for counting time. All data (4364 reflections) within a 2θ sphere of 50° ($(\sin\theta)/\lambda = 0.596$) in the hkl and $hk\bar{l}$ octants were measured in this manner, using a take-off angle of 4.5° .

As a general check on electronic and crystal stability, the intensities of three standard reflections were re-measured every 75 reflections. These standards showed a steady decrease throughout the collection period with a total change in intensity of 25.3%. A decay correction was applied to the data with the standards fitted to the line

$$y = AX + BX^2 + CX^3 + D$$

where y = sum of the three standards, X = reflection #/100, $A = -973.7563$, $B = 39.5153$, $C = -0.8389$ and $D = 16982.5$. Examination of the data revealed systematic absences of the 00ℓ reflections for $\ell = 2n+1$ and $h0\ell$, $h = 2n+1$, thus defining the space group as P_{2_1} / a an alternate setting of P_{2_1} / c (No. 14). The measured intensities were corrected for Lorentz and polarization effects. No attempt was made

to correct for absorption due to the highly irregular shape of the crystal. The variance in each intensity was calculated by

$$\sigma_2 = C_T + k_t C_B + (0.03C_T)^2 + (0.03C_B)^2$$

where C_T and C_B represent the total and background counts, k_t is a counting time constant and the factor of 0.03 represents an estimate of nonstatistical errors.

Reflections for which $F_o > 3\sigma_{F_o}$ (2734 reflections) were used in the refinement of the structure.

Solution and Refinement

The positions of the Cl, Cr and I atoms were found by the use of three successive three dimensional superposition maps (85). The remaining atoms were found by successive structure factor (86) and electron density map calculations (87). The scattering factors used for nonhydrogen atoms were those of Hanson et al. (88) modified for the real part of anomalous dispersion. In addition to positional parameters for all atoms, the anisotropic thermal parameters for all nonhydrogen atoms were refined by a full matrix least-squares procedure (89). The equivalent reflections in the hk and hk^- octants were averaged with the related $(F)_{ave}$ calculated as $\left\{ \sum_{i=1}^N \sigma_i^2(F) \right\}^{1/2} N$, where N is the number of

observed reflections for a "unique" reflection to be averaged. There were consequently 2734 independent reflections used in the calculations. The hydrogen scattering factors used were those of Stewart et al. (90).

The final positional and thermal parameters are listed in Tables III-2 and III-2, respectively. The standard deviations were calculated from the inverse matrix of the final least-squares cycle. Hydrogen atoms were put in calculated positions (1.0\AA) with their isotropic thermal parameters fixed at 5.0\AA^2 . The observed and calculated structure factor amplitudes are available upon request.

Table III-1. Final atomic positions^a

Atom	x	y	z
I-1	0.8453(1)	0.9475(1)	0.5656(1)
I-2	0.2648(1)	0.9427(1)	0.1542(1)
Cr	0.2817(2)	0.4860(2)	0.2080(1)
Cl	0.1373(3)	0.3774(3)	0.1061(3)
O-1	0.4086(8)	0.5843(8)	0.3005(7)
O-2	0.1093(25)	0.4566(21)	0.5895(23)
O-3	0.1241(15)	0.2446(17)	0.6061(15)
N-1	0.1911(8)	0.6338(9)	0.1574(8)
N-2	0.3369(10)	0.5185(11)	0.1002(9)
N-3	0.3941(9)	0.3514(10)	0.2501(8)
N-4	0.2202(8)	0.4661(9)	0.3143(8)
C-1	0.1803(13)	0.6524(13)	0.0571(12)
C-2	0.3001(15)	0.6384(13)	0.05994(12)
C-3	0.4555(12)	0.5077(16)	0.1231(13)
C-4	0.4869(14)	0.3815(14)	0.1363(11)
C-5	0.4171(11)	0.3054(12)	0.1678(11)
C-6	0.3631(13)	0.2926(16)	0.3824(13)
C-7	0.3379(14)	0.2536(13)	0.2991(12)
C-8	0.2224(12)	0.3456(14)	0.3521(11)
C-9	0.1062(11)	0.5123(15)	0.2953(12)
C-10	0.0912(12)	0.6355(15)	0.2617(14)
C-11	0.0814(11)	0.6528(12)	0.1611(12)
H-1A	0.1482	0.7288	0.0338
H-1B	0.1267	0.5943	0.0130
H-2A	0.3539	0.6971	0.1005
H-2B	0.2988	0.6451	-0.0081

^aEstimated standard deviations are in parentheses for all but the hydrogen atoms.

Table III-1. (Continued)

Atom	x	y	z
H-3A	0.5012	0.5505	0.1849
H-3B	0.4744	0.5412	0.0707
H-4A	0.5678	0.3758	0.1860
H-4B	0.4838	0.3532	0.0736
H-5A	0.4837	0.2529	0.1889
H-5B	0.3504	0.2671	0.1174
H-6A	0.4252	0.1976	0.3208
H-6B	0.2926	0.2159	0.2490
H-7A	0.3394	0.2244	0.4218
H-7B	0.3974	0.3458	0.4203
H-8A	0.2024	0.3523	0.4086
H-8B	0.1638	0.3037	0.2995
H-9A	0.959	0.5096	0.3592
H-9B	0.475	0.4638	0.2484
H-10A	0.1578	0.6799	0.3048
H-10B	0.0208	0.6663	0.2639
H-11A	0.0564	0.7327	0.1385
H-11B	0.0249	0.6000	0.1148
H-N1	0.2475	0.6885	0.2016
H-N2	0.2937	0.4603	0.0511
H-N3	0.4637	0.3898	0.2969
H-N4	0.2817	0.5128	0.3642

Table III-2. Anisotropic thermal parameters ($\times 10^4$)^a

Atom	β_{11}	β_{22}	β_{33}	β_{12}	β_{13}	β_{23}
I-1	90	160	78	-18	-7	34
I-2	88	93	77	7	14	-2
Cr	47	59	49	-2	2	-4
Cl	67	84	63	-2	2	-11
O-1	72	82	66	4	17	-9
O-2	338	233	287	6	125	53
O-3	176	215	220	22	31	145
N-1	42	86	49	-1	-4	3
N-2	79	106	72	-17	28	-10
N-3	77	70	63	-4	14	-11
N-4	60	73	57	-4	7	0
C-1	93	91	77	12	20	16
C-2	124	67	81	15	36	8
C-3	80	105	96	-2	36	-3
C-4	102	92	64	4	23	6
C-5	64	73	87	12	22	-19
C-6	92	75	86	-5	23	9
C-7	95	111	84	-8	16	32
C-8	89	93	74	-17	31	5
C-9	52	119	77	9	22	-3
C-10	64	104	113	13	28	-12
C-11	66	70	82	12	0	6

^aThe temperature factors are in the form $\exp[-(h^2\beta_{11} + k^2\beta_{22} + l^2\beta_{33} + 2hk\beta_{12} + 2hl\beta_{13} + 2kl\beta_{23})]$.

DESCRIPTION AND DISCUSSION

A perspective (91) drawing of $t\text{-ClCr}([\text{15}]aneN_4)H_2O^{2+}$ depicting 50% probability ellipsoids is shown in Figure III-2. Interatomic bond distances and angles (92) are listed in Tables III-3 and III-4, respectively.

The Cr-N distances of the complex range from $2.079(13)\text{\AA}$ to $2.092(12)\text{\AA}$, averaging 2.084\AA , and the N-Cr-N angles range from $82.8(5)^\circ$ to $96.6(5)^\circ$. The C-N distances range from $1.438(18)\text{\AA}$ to $1.549(20)\text{\AA}$, averaging 1.495\AA . Only the Cr-N-C angles for the five-member ring approach the tetrahedral value, Cr-N₁-C₁ ($107.9(9)^\circ$) and Cr-N₂-C₂ ($109.5(9)^\circ$), whereas the other Cr-N-C angles range from $112.1(12)^\circ$ to $121.7(9)^\circ$ indicative of some strain in the six-member rings. This is also reflected in the conformation of these rings with one being skewed, the other two being in the more stable chair form. The C-C distances range from $1.500(24)\text{\AA}$ to $1.547(25)\text{\AA}$, averaging 1.524\AA . The C-C-C angles (see Table III-4) are greater than the tetrahedral value. The Cr-Cl and Cr-O distances are $2.284(4)$ and $2.042(9)\text{\AA}$, respectively, with a Cl-Cr-O angle of $178.7(3)^\circ$. These distances compare quite well with those already in the literature and are shown in Table III-5 along with the other parameters.

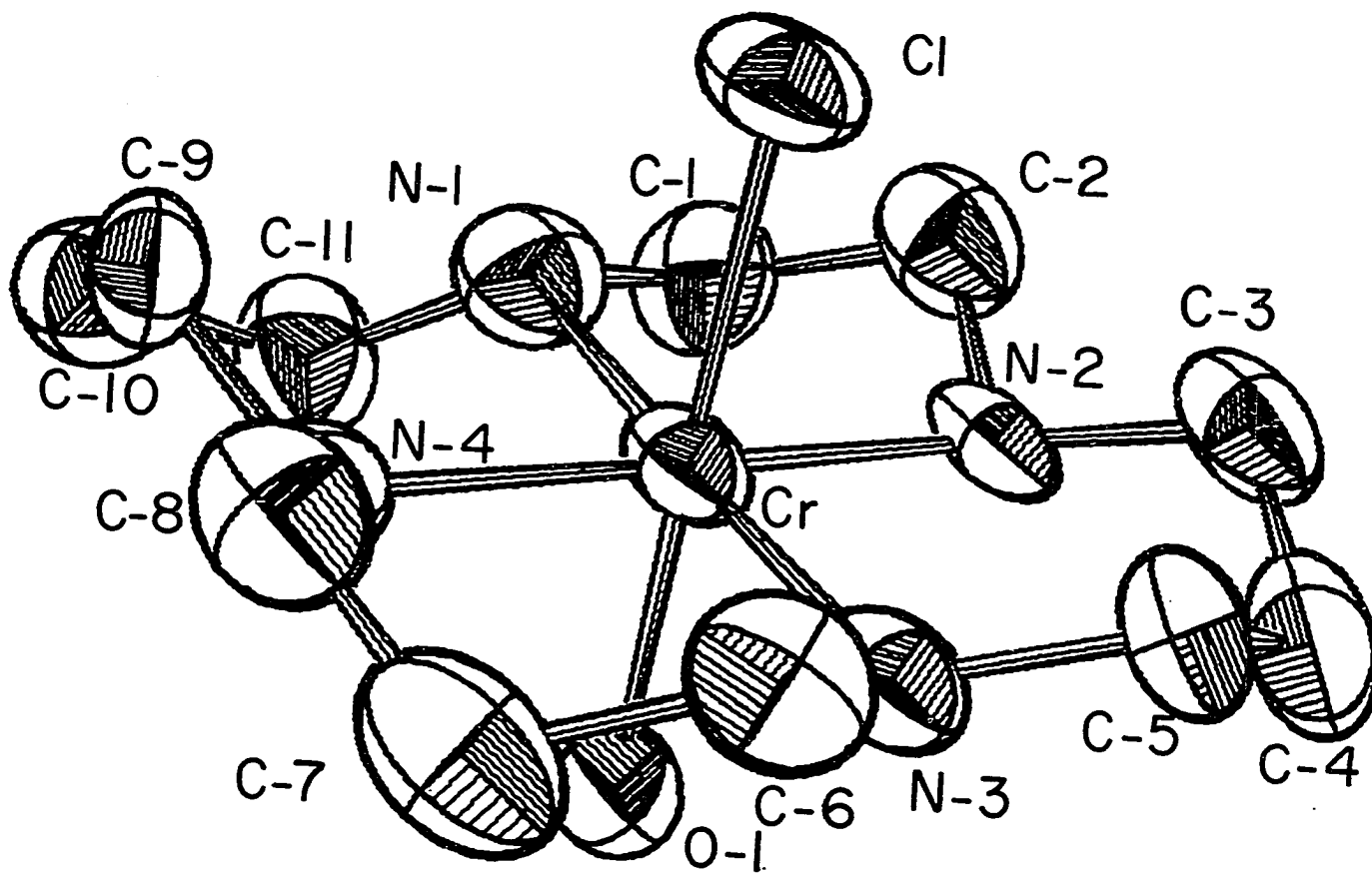


Figure III-2. Perspective drawing of the $[\text{trans-ClCr}([\text{15]aneN}_4)\text{H}_2\text{O}]^{2+}$ cation showing 50% probability thermal ellipsoids

Table III-3. Bond lengths (Å) for $\text{ClCr(L)H}_2\text{O}^{2+}$ ^a

Cr-Cl	2.284(4)	N ₃ -C ₆	1.523(19)
Cr-O ₁	2.042(9)	N ₄ -C ₈	1.496(19)
Cr-N ₁	2.080(10)	N ₄ -C ₉	1.491(17)
Cr-N ₂	2.079(13)	C ₁ -C ₂	1.546(22)
Cr-N ₃	2.083(11)	C ₃ -C ₄	1.547(25)
Cr-N ₄	2.092(12)	C ₄ -C ₅	1.493(22)
N ₁ -C ₁	1.494(19)	C ₆ -C ₇	1.507(24)
N ₁ -C ₁₁	1.465(17)	C ₇ -C ₈	1.535(22)
N ₂ -C ₂	1.549(20)	C ₉ -C ₁₀	1.539(25)
N ₂ -C ₃	1.438(18)	C ₁₀ -C ₁₁	1.500(24)
N ₃ -C ₅	1.506(18)		

^aEstimated standard deviations are in parentheses.

Table III-4. Bond angles (degrees)^a

Cl-Cr-O ₁	178.7(3)	Cr-N ₃ -C ₆	116.6(12)
N ₁ -Cr-N ₂	82.8(5)	Cr-N ₄ -C ₈	116.8(9)
N ₁ -Cr-N ₃	169.3(4)	Cr-N ₄ -C ₉	118.0(12)
N ₁ -Cr-N ₄	92.6(5)	Cr-N ₁ -C ₁₁	121.7(9)
N ₂ -Cr-N ₃	87.8(5)	N ₁ -C ₁ -C ₂	106.4(12)
N ₂ -Cr-N ₄	175.4(5)	C ₁ -C ₂ -N ₂	104.8(12)
N ₃ -Cr-N ₄	96.6(5)	C ₂ -N ₂ -C ₃	107.8(13)
N ₁ -Cr-Cl	92.5(3)	N ₂ -C ₃ -C ₄	108.5(13)
N ₂ -Cr-Cl	91.2(4)	C ₃ -C ₄ -C ₅	117.9(13)
N ₃ -Cr-Cl	93.0(3)	C ₄ -C ₅ -N ₃	113.5(12)
N ₄ -Cr-Cl	89.7(3)	C ₅ -N ₃ -C ₆	108.2(12)
N ₁ -Cr-O ₁	86.9(4)	N ₃ -C ₆ -C ₇	111.6(13)
N ₂ -Cr-O ₁	89.9(4)	C ₆ -C ₇ -C ₈	113.9(14)
N ₃ -Cr-O ₁	87.8(4)	C ₇ -C ₈ -N ₄	112.8(12)
N ₄ -Cr-O ₁	89.2(4)	C ₈ -N ₄ -C ₉	106.1(11)
Cr-N ₁ -C ₁	107.9(9)	N ₄ -C ₉ -C ₁₀	113.4(12)
Cr-N ₂ -C ₂	109.5(9)	C ₉ -C ₁₀ -C ₁₁	114.7(14)
Cr-N ₂ -C ₃	118.1(15)	C ₁₀ -C ₁₁ -N ₁	109.8(11)
Cr-N ₃ -C ₅	112.1(12)	C ₁₁ -N ₁ -C ₁	109.2(11)

^aEstimated standard deviations are in parentheses.

Table III-5. Comparison of bond distances

Compound	Cr-Cl	Cr-O	Cr-N	N-C	C-C	Reference
$\text{ClCr(L)H}_2\text{O}^{2+}$	2.284	2.042	2.084	1.495	1.524	This work
$\underline{t}\text{-Cl}_2(\text{H}_2\text{O})_2\text{Cr(en)}^+$	2.32	2.05	2.08	1.49(7)	1.58,1.71	93
$\text{ClCr}(\text{NH}_2\text{CH}_3)_5^{2+}$	2.299	---	2.098	1.466	---	94
Cr(en)_3^{3+}	---	---	2.081	1.481	1.489	95
$\text{Cr(en)}_2(\text{SCH}_2\text{CO}_2)^1$	---	---	2.095	1.495	1.504	96
[16]aneN ₄	---	---	---	1.457	1.511	81

The angles of the macrocycle are similar to those of [16]aneN₄ (81) for the six-member rings except the C-N-C angles which are larger for [16]aneN₄, 114.4(3) compared to 107.8(11) for ClCr(L)²⁺. The C-N-C angles of the five-member ring compare with those of reported complexes containing ethylenediamine (93,95,96).

The nitrogens form a fair least-squares plane (92) defined by the following equation, $0.53169X + 0.56726Y + 0.62889Z = 6.41185$ with an average deviation of 0.04^oÅ. The chromium is slightly displaced (0.056^oÅ from the least-squares plane) toward the chlorine. The chelate ring conformation, CCTg², is the one predicted (97) to have the minimal conformational strain energy.

²T, twist; C, chair; g, gauche, where T and C refer to the six-member rings and g the five-member ring.

LITERATURE CITED

1. L. Y. Martin, L. J. DeHayes, L. J. Zompa and D. H. Busch, J. Amer. Chem. Soc., 96, 4046 (1974).
2. J. Sand and F. Singer, Annales, 190, 329 (1903).
3. G. M. Bennett and E. E. Turner, J. Chem. Soc., 105, 1057 (1914).
4. F. Hein, Chem. Ber., 195, 52 (1919).
5. W. Herwig and H. H. Zeiss, J. Amer. Chem. Soc., 79, 656 (1957).
6. W. Herwig and H. H. Zeiss, J. Amer. Chem. Soc., 81, 4798 (1959).
7. R. P. A. Sneed, "Organochromium Compounds", Academic Press, New York, N.Y., 1975.
8. F. Glocking, R. P. A. Sneed and H. H. Zeiss, J. Organometal. Chem., 2, 109 (1964).
9. F. Hein and K. Schmiedeknecht, J. Organometal. Chem., 5, 454; 6, 45 (1966).
10. K. Nishimura, H. Kuribayashi, A. Yamamoto and S. Ikeda, J. Organometal. Chem., 37, 317 (1972).
11. F. Hein and D. Tille, Z. Anorg. Allg. Chem., 329, 72 (1964).
12. W. Metlesics and H. H. Zeiss, J. Amer. Chem. Soc., 81, 4117 (1959).
13. F. Hein and H. P. Scharoer, Chem. Abstracts, 68, 39773h (1968); Monatsber. Deut. Akad. Wiss. Berlin, 9, 196 (1968).
14. F. A. L. Anet and E. LeBlanc, J. Amer. Chem. Soc., 79, 2649 (1957).
15. F. A. L. Anet, Can. J. Chem., 37, 58 (1959).
16. C. E. Castro and W. C. Kray, Jr., J. Amer. Chem. Soc., 85, 2768 (1963).

17. J. K. Kochi and D. Davis, J. Amer. Chem. Soc., 86, 5264 (1964).
18. J. K. Kochi and D. Buchanan, J. Amer. Chem. Soc., 87, 853 (1965).
19. A. R. Schmidt and T. W. Swaddle, J. Chem. Soc., A, 1927 (1970).
20. J. H. Espenson and J. P. Leslie, II, J. Amer. Chem. Soc., 96, 1954 (1974).
21. R. G. Coombes, M. D. Johnson, and N. Winterton, J. Chem. Soc., 7029 (1965); R. G. Coombes and M. D. Johnson, J. Chem. Soc. (A), 177 (1966).
22. R. S. Nohr and J. H. Espenson, J. Amer. Chem. Soc., 97, 3392 (1975).
23. D. Dodd and M. D. Johnson, J. Chem. Soc. (A), 34 (1968).
24. S. K. Malik, W. Schmidl and L. O. Speer, Inorg. Chem., 13, 2986 (1974).
25. P. Sevcik and D. Jakubcova, Collection Czechoslov. Chem. Commun., 42, 1767 (1977); 42, 1776 (1977).
26. W. Schmidt, J. H. Swinehart, and H. Taube, J. Amer. Chem. Soc., 93, 1117 (1971); M. Ardon, K. Woolmington and A. Pernick, Inorg. Chem., 10, 2812 (1971).
27. (a) J. H. Espenson and D. A. Williams, J. Amer. Chem. Soc., 96, 1008 (1974); (b) J. P. Leslie, II, and J. H. Espenson, J. Amer. Chem. Soc., 98, 4839 (1976).
28. M. R. Hyde and J. H. Espenson, J. Amer. Chem. Soc., 98, 4463 (1976).
29. W. Cohen and D. Meyerstein, Inorg. Chem., 13, 2434 (1974).
30. J. R. Hanson, Synthesis, 1 (1974).
31. J. K. Kochi and P. E. Mocadlo, J. Amer. Chem. Soc., 88, 4094 (1966).
32. J. K. Kochi and J. W. Fowers, J. Amer. Chem. Soc., 92, 137 (1970).

33. D. Lal, D. Griller, S. Husband, and K. U. Ingold, J. Amer. Chem. Soc., 96, 6355 (1974).
34. The value agrees quite well with the range of rates listed in ref. 28, $3.4 \times 10^7 - 3.5 \times 10^8 \text{ dm}^3 \text{ m}^{-1} \text{ s}^{-1}$.
35. C. T. Loo, L. Y. Goh, and S. H. Goh, J. Chem. Soc. (Dalton), 585 (1972).
36. (a) J. J. Daly, F. Sang, R. P. A. Sneeden and H. H. Zeiss, Chem. Comm., 243 (1971); (b) J. J. Daly and F. Sang, J. Chem. Soc. (Dalton), 2584 (1972); (c) R. P. A. Sneeden and H. H. Zeiss, J. Organometal. Chem., 47, 125 (1973); (d) J. J. Daly, F. Sang, R. P. A. Sneeden and H. H. Zeiss, J. Chem. Soc. (Dalton), 73 (1973); (e) J. J. Daly, F. Sang, R. P. A. Sneeden and H. H. Zeiss, Helv. Chim. Acta, 56, 503 (1973).
37. (a) A. M. van den Bergen, K. S. Murry, R. M. Sheahan, and B. O. West, J. Organometal. Chem., 90, 299 (1975); (b) A. L. Marchese, M. Scudder, A. M. van den Bergen, and B. O. West, J. Organometal. Chem., 121, 63 (1976).
38. D. Dodd and M. D. Johnson, J. Organometal. Chem., 52, 1 (1973).
39. J. Halpern and J. P. Maher, J. Amer. Chem. Soc., 87, 5361 (1965).
40. P. B. Chock and J. Halpern, J. Amer. Chem. Soc., 91, 582 (1969).
41. H. Cohen and D. Meyerstein, J. Chem. Soc. (Dalton), 2559 (1974).
42. J. Halpern and J. P. Maher, J. Amer. Chem. Soc., 86, 2311 (1964).
43. (a) J. Halpern and P. F. Phelan, J. Amer. Chem. Soc., 94, 1881 (1972); (b) L. G. Marzilli, P. A. Marzilli, and J. Halpern, J. Amer. Chem. Soc., 93, 1374 (1971); (c) P. W. Schneider, P. F. Phelan, and J. Halpern, J. Amer. Chem. Soc., 91, 77 (1969).
44. T. S. Roche and J. F. Endicott, Inorg. Chem., 13, 1575 (1974).
45. J. H. Espenson and A. H. Martin, J. Amer. Chem. Soc., 99, 5953 (1977).

46. The systematic name for the trivial ligand name is meso-5,7,7,12,14,14-hexamethyl-1,4,8,11-tetraazacyclotetradecane.
47. M. J. D'Aniello, Jr., and E. Kent Barefield, J. Amer. Chem. Soc., 98, 1610 (1976).
48. Inorganic Synthesis, Vol. 10, Earl L. Mutterties, Ed., McGraw-Hill, New York, N.Y., 1969, pp 26.
49. Inorganic Synthesis, Vol. 16, Fred Basolo, Ed., McGraw-Hill, New York, N.Y., 1975, pp 220.
50. (a) E. K. Barefield and F. Wagner, Inorg. Chem., 15, 1370 (1976); (b) Personal communications with Dr. Frank Wagner, Strem Chemicals Inc., Andover, Mass., October 1977.
51. R. B. Fisher and D. G. Peters, "Quantitative Chemical Analysis", 3rd ed., W. D. Saunders Co., Philadelphia, Pa., 1968, pp 384.
52. C. S. Garner and D. A. House, Transition Metal Chemistry, 6, 59 (1970).
53. B. A. Zabin and H. Taube, Inorg. Chem., 3, 963 (1964).
54. A. Ernshaw, L. F. Lackworthy, and K. C. Patel, J. Chem. Soc. (A), 1339 (1969).
55. A. Dei and F. Mani, Inorg. Chem., 15, 2574 (1976).
56. The formal nomenclature for the trivial names are as follows: $\text{Me}_2[14]\text{aneN}_4$; meso-5,12-dimethyl-1,4,8,11-tetraazacyclotetradecane and $\text{Me}_6[14]\text{aneN}_4$; meso-5,7,7,12,14,14-hexamethyl-1,4,8,11-tetraazacyclotetradecane.
57. K. D. Kopple, J. Amer. Chem. Soc., 84, 1586 (1961), and references in ref. 30.
58. J. Glerup and C. Schaffer, Inorg. Chem., 15, 1408 (1976).
59. J. Ferguson and M. L. Tobe, Inorg. Chim. Acta, 4, 109 (1970).
60. Methods of Organic Chemistry, Vol. 13/2b, Georg Thieme, Ed., Houben Weyl 4th Ed., Stuttgart, Germany, 1974.

61. Ionization Potentials, Appearance Potentials and Heats of Formation of Gaseous Positive Ions, U. S. Dept. of Commerce, NSRDS-NBS-26, ca. 1964.
62. C. E. Castro and W. C. Kray, Jr., J. Amer. Chem. Soc., 88, 4447 (1966).
63. W. Kirmse, "Carbene Chemistry", 2nd ed., Academic Press, New York, N.Y., 1971, pp 428.
64. R. S. Nohr and L. O. Speer, J. Amer. Chem. Soc., 96, 2618 (1974); R. S. Nohr and L. P. Speer, Inorg. Chem., 13, 1239 (1974); J. H. Espenson and J. P. Leslie, II, Inorg. Chem., 15, 1886 (1976).
65. "Free Radicals", Vol. II, J. K. Kochi, Ed., John Wiley and Sons, New York, N.Y., pp 123.
66. (a) M. H. Abraham in "Comprehensive Chemical Kinetics", Vol. 12, C. H. Bamford and C. F. H. Tipper, Ed., Elsevier, Amsterdam, 1973; (b) F. R. Jensen and B. Rickborn, "Electrophilic Substitution of Organomercurials", McGraw-Hill, New York, N.Y., 1968.
67. M. D. Johnson, Acc. Chem. Res., 11, 57 (1978) and references therein.
68. J. P. Leslie, II, Ph.D. thesis, Iowa State University, 1975.
69. E. S. Swinbourne, J. Chem. Soc., 2371 (1960).
70. R. G. Wilkins, "The Study of Kinetics and Mechanism of Reactions of Transition Metal Complexes", Allyn and Bacon, Inc., Boston, Mass., 1974, pp 100.
71. L. P. Hammett, "Physical Organic Chemistry", 2nd ed., McGraw-Hill, New York, N.Y., Chapter 12.
72. J. E. Leffler and E. Grunwald, "Rates and Equilibria of Organic Reactions", John Wiley and Sons, Inc., New York, N.Y., 1963.
73. M. H. Abraham and P. L. Grellier, J. Chem. Soc., Perkin II, 1132 (1973).
74. F. R. Jensen, V. Madan, and D. H. Buchanan, J. Amer. Chem. Soc., 93, 5283 (1971).

75. H. L. Fritz, J. H. Espenson, P. A. Williams, and G. A. Molander, J. Amer. Chem. Soc., 96, 2378 (1974); D. Dong, B. K. Hunter and M. C. Baird, Chem. Commun., 11 (1978).
76. I. D. Brown, Coord. Chem. Rev., 26, 161 (1978).
77. D. Webster, R. C. Edwards, and D. H. Busch, Inorg. Chem., 16, 1055 (1977).
78. C. J. Cooksey and M. L. Tobe, Inorg. Chem., 17, 1558 (1978); P. W. Mak and C. K. Poon, Inorg. Chem., 15, 1949 (1976).
79. J. F. Endicott, J. Lilie, J. M. Kuszaj, B. S. Ramaswamy, W. G. Schmonsees, M. G. Simic, M. D. Glick, and D. P. Rillema, J. Amer. Chem. Soc., 99, 429 (1977).
80. Y. Iitaka, M. Shina, and E. Kimura, Inorg. Chem., 13, 2886 (1974); F. Wagner, M. T. Mocella, A. H. J. Wang, and E. K. Barefield, J. Amer. Chem. Soc., 96, 2625 (1974), and others.
81. W. L. Smith, J. D. Ekstrand, and K. N. Raymond, J. Amer. Chem. Soc., 100, 3539 (1978).
82. This analysis was performed by Mr. Francis Laabs of the Ames Laboratory Analytical Services Group, Iowa State University, Ames, Iowa.
83. R. A. Jacobson, J. Appl. Cryst., 9, 115 (1976).
84. R. A. Jacobson, "An Algorithm for Automatic Indexing and Bravais Lattice Selection. The Programs BLIND and ALICE", U. S. Atomic Energy Commission Report IS-3469, Iowa State University and Institute for Atomic Research, Ames, Iowa (1974).
85. C. R. Hubbard, M. W. Babich, and R. A. Jacobson, "A PL/1 Program System for Generalized Patterson Superpositions", U. S. Energy Research and Development Administration Report IS-4106, Iowa State University and Ames Laboratory-ERDA.
86. W. R. Busing, K. O. Martin, and H. A. Levy, "ORFLS, A Fortran Crystallographic Least Squares Program", U. S. Atomic Energy Commission Report ORNL-TM-305, Oak Ridge National Laboratory, Oak Ridge, Tennessee, 1962.

87. C. A. Hubbard, C. O. Quicksall, and R. A. Jacobson, "The Fast Fourier Algorithm and the Programs ALFF, ALFFDP, ALFFPROJ, ALFFT, and FRIEDEL," U. S. Atomic Energy Commission Report IS-2625, Iowa State University and Institute for Atomic Research, Ames, Iowa, 1971.
88. H. P. Hanson, F. Herman, J. D. Lee, and S. Skillman, Acta Crystallogr., 17, 1040 (1960).
89. D. H. Templeton, in "International Tables for X-ray Crystallography," Vol. 111, Table 3.3.2c, The Kynoch Press, Birmingham, England, 1962, pp 215-216.
90. R. F. Stewart, E. R. Davidson, and W. T. Simpson, J. Chem. Phys., 42, 3175 (1965).
91. C. A. Johnson, "ORTEP-11: A Fortran Thermal-Ellipsoid Plot Program for Crystal Structure Illustrations", U. S. Atomic Energy Commission Report ORNL-3794 (Second Revision with Supplemental Instructions), Oak Ridge National Laboratory, Oak Ridge, Tennessee, 1971.
92. W. R. Busing, K. O. Martin, and H. A. Levy, "ORFFE: A Fortran Crystallographic Function and Error Program", U. S. Atomic Energy Commission Report ORNL-TM-306, Oak Ridge National Laboratory, Oak Ridge, Tennessee, 1964.
93. R. Stomberg and I. Larking, Acta Chemica Scand., 23, 343 (1969).
94. B. M. Foxman, Inorg. Chem., 17, 1932 (1978).
95. K. N. Raymond and J. A. Ibers, Inorg. Chem., 7, 2333 (1968).
96. R. C. Elder, L. R. Florian, R. E. Lake, and A. M. Yacynych, Inorg. Chem., 12, 2690 (1973).
97. Y. Hung, L. Y. Martin, S. C. Jackels, A. M. Tait, and D. H. Busch, J. Amer. Chem. Soc., 99, 4029 (1977).

ACKNOWLEDGEMENTS

Life is change,

How it differs from the rocks.

(Jefferson Airplane)

To thank everybody who has helped me would be impossible, yet there are those who deserve recognition. Dr. J. H. Espenson has helped me explore learning. He has shown great patience and understanding at my futile attempts but also shared the joy of discovery. Dr. R. A. Jacobson and his group have been very kind putting up with my incessant questions. Mrs. Sue Musselman did the typing and helped put this thesis into acceptable form. Finally, I thank my parents and loving wife, Joan, for their concern and support when I needed them.